EFFECT OF HIGH CONCENTRATION GRADIENTS ON HYDRODYNAMIC DISPERSION

by

Murat Savaş Sarıoğlu

B.A. in Chemistry, Boğaziçi University, 1999

M.S. in Environmental Science, Boğaziçi University, 2003

Submitted to the Institute of Environmental Sciences in partial fulfillment of

the requirements for the degree of

Doctor

of

Philosophy

in Environmental Sciences

Boğaziçi University

2011

ACKNOWLEDGEMENTS

I would like to express my deepest gratitude to my advisor, Prof. Dr. Nadim Copty, for sharing his knowledge and experience with me. Without his guidance and support this research would have been impossible.

I would also like to acknowledge my jury members; Assist. Prof. Orhan Gündüz, Assist. Prof. Başak Güven, Prof. Turgut Onay, Prof. Orhan Yenigün; for spending their valuable time to evaluate this thesis.

The financial support of this study, by TÜBİTAK (Project Number 109Y326), is gratefully acknowledged.

I would like to thank Mehmet Ali Küçüker for his invaluable assistance in the experimental component of the study. I also acknowledge Gülhan Özkösemen and Filiz Ayılmaz for their help in the laboratory experiments.

I would also like to thank those who have touched my life in various and innumerable ways, especially my parents and Deniz. I couldn't have done it without you.

ABSTRACT

The hydrodynamic dispersion of contaminants in the subsurface is commonly described by Fick's Law which expresses the dispersive mass flux as a linear function of the concentration gradient with a constant dispersion coefficient. However, recent research has shown that the relationship deviates from linearity under high concentration gradient conditions. Although, several modifications of Fick's Law have been proposed in order to account for this deviation under specific conditions, there is still not a broadly accepted tool for modeling the dispersion flux in real environmental applications.

This study investigates the effect of high concentration gradients on hydrodynamic dispersion for experimental conditions beyond those considered in the literature, namely, existence of multiple species and low velocity conditions similar to those commonly encountered in natural subsurface systems. In order to test alternative dispersion models and determine transport parameters for subsequent model applications, three sets of stable miscible displacement experiments were conducted in two different types of porous media: (i) tracer experiments, (ii) brine experiments with varying flow rates and concentration gradients, (iii) mixture experiments where brine was mixed with a low concentration contaminant. The laboratory experiments showed that dispersive behavior deviates from Fickian Theory when high density gradients exist, for all high and low concentration solute components in groundwater.

A numerical model was developed and validated using the experimental results. The model was then used to perform Monte-Carlo simulations of a transport problem where high concentration gradients exist along with heterogeneity in hydrogeological parameters. Simulation results suggested that non-Fickian behavior may significantly affect observations of transport, subsequent parameter estimations and potential effectiveness of groundwater remediation activities.

ÖZET

Yeraltında kirletici taşınmasında, hidrodinamik dispersiyon genellikle Fick Yasası ile tanımlanır. Fick Yasası, dispersiyona bağlı kütle akısını, derişim gradyanının sabit dispersiyon katsayılı, doğrusal bir işlevi olarak ifade eder. Öte yandan, yakın zamanlı araştırmalar, ilişkinin, derişim gradyanının büyük olduğu koşullarda doğrusallıktan saptığını ortaya koymuştur. Belli koşullarda bu sapmayı hesaba katabilmek amacıylaFick Yasası'nda değişiklikler yapılması önerilmiş olsa da, henüz, gerçek çevre uygulamalarında dispersiyon akısını modellemek için genel kabul görmüş araç bulunmamaktadır.

Bu çalışma, büyük derişim gradyanlarının hidrodinamik dispersiyona etkisini, mevcut yayınlarda incelenmiş deneysel koşulların ötesinde araştırmayı amaçlamıştır. Bu araştırma koşulları, birden fazla kirleticinin bir arada bulunması ve doğal yer altı sistemlerinde yaygın olarak gözlemlenen düşük akış hızlarıdır. Alternatif dispersiyon modellerini sınamak ve bunu takip eden model uygulamalarında kullanılacak taşınma parametrelerini belirlemek amacıyla, iki farklı gözenekli ortamda, üç tür dengeli karışabilir yer değiştirme deneyi yapılmıştır: (i) izleyici deneyleri, (ii) farklı derişimlerde ve hızlarda tuzlu su deneyleri, (iii) tuzlu suyun içine düşük derişimli bir kirleticinin eklendiği karışım deneyleri. Laboratuar deneyleri, büyük derişim gradyanları söz konusu olduğunda, hem yüksek derişimli hem de düşük derişimli kirleticilerin dispersiyon davranışlarının Fick Kuramı'ndan saptığını göstermiştir.

Deney sonuçlarına dayanarak sayısal bir model geliştirilmiştir. Sayısal model, hem hidrojeolojik parametrelerin heterojen dağılım gösterdiği hem de derişim gradyanlarının büyük olduğu taşınma problemlerinde Monte-Carlo benzetimleri yapılmasında kullanılmıştır. Benzetim sonuçları, Fick Yasası'ndan sapan dispersiyon davranışlarının yer altı suyunda kirletici taşınması gözlemlerini, onlara dayanılarak yapılacak parametre tahminlerini ve yer altı suyu iyileştirme etkinliklerinin etkililiğini önemli ölçüde etkileyebileceğini göstermiştir.

TABLE OF CONTENTS

LIST OF FIGURES

LIST OF TABLES

1. INTRODUCTION

The potential of a contaminant to be harmful for humans or the environment is not only a function of its intrinsic properties, such as toxicity or carcinogenicity, but also its tendency to reach receptors. The study of fate and transport of contaminants in the environment provides us with tools to predict the damages that a contamination will cause. Such a study requires the understanding of numerous processes that affect the fate and transport. However, understanding individual processes is not sufficient for making predictions because natural systems involve complex interactions of various processes. In order to make accurate predictions, scientists develop transport models that include several processes.

The main processes affecting the transport of dissolved contaminants in groundwater systems are advection and hydrodynamic dispersion. Advection is the displacement of contaminants by the movement of the water body in which they are dissolved, while hydrodynamic dispersion (or simply dispersion) is the spreading of contaminants from higher to lower concentration zones. Dispersion causes a leveling of contaminant concentrations in volumes of groundwater with different contamination degrees. The leveling results in dilution of the bulk of the contamination, and the contamination of portions of the groundwater that would otherwise remain pristine if the only transport process was advection.

In other words, at any location, some of the contaminant from a given contamination source will arrive earlier than the flow conditions of the field would suggest, while some of it will arrive later, due to dispersion. This variation of arrival times will result in observing an S-shaped breakthrough curve (plot of contaminant concentration vs. time at an observation point), rather than a sharp change from the background concentration to peak concentration, as it would result from a purely advective transport. Figure 1.1 shows theoretical breakthrough curves that would result from the observation of contaminant concentrations from transport systems with advection only and advection and dispersion together.

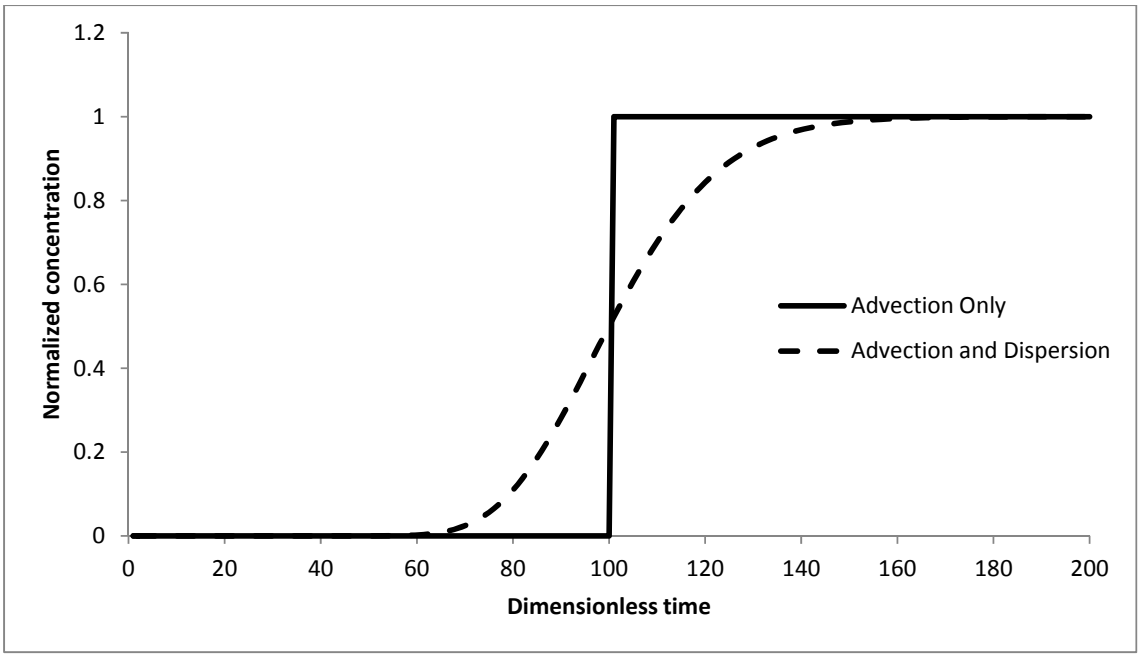

Figure 1.1. Comparison of breakthrough curves generated by an advection only transport model and an advective dispersive model.

The term hydrodynamic dispersion is generally used to include contaminant spreading due to both molecular diffusion and mechanical mixing. Molecular diffusion is the mass flux from regions of high concentration to regions of low concentration as a result of the Brownian motion of individual molecules, while mechanical mixing is the result of the non-uniform groundwater velocity distribution occurring at the pore and field scales. The non-uniformity of the flow field arises from the pore-scale velocity distributions, the irregular shapes of flow paths followed by dissolved particles around soil grains, and large-scale heterogeneities in aquifer properties. A schematic summarizing these processes is shown in Figure 1.2. One or more of these processes dominate in a particular groundwater contaminant transport problem, depending on the scale of porous medium in question, the velocity of groundwater and heterogeneity of hydrogeological parameters.

If it was possible to fully define the flow patterns in individual pores, transport of contaminants could be modeled in terms of advection and molecular diffusion only, without the need for the mechanical mixing contribution to hydrodynamic dispersion. However, such a model would require a massive amount of hydrogeological data to fully

define the flow and transport domain; moreover, simulations based on this model would require enormous simulation time and computational effort rendering such a modeling approach practically impossible. Therefore, macroscopic (empirical) dispersion models are being used to account for the phenomenon of mechanical mixing in practical applications.

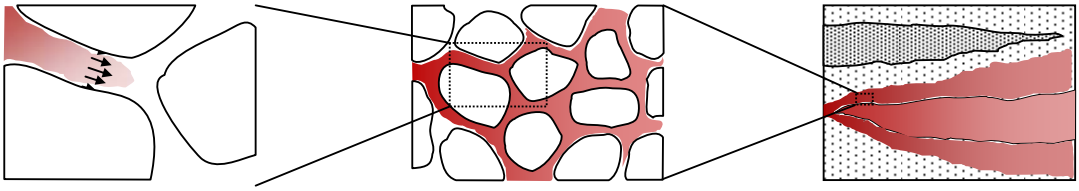

Figure 1.2. Processes that result in mechanical mixing: (a) pore scale velocity distribution, (b) irregularities of contaminant transport paths and (c) large-scale heterogeneities.

As presented in detail in the comprehensive history of the development of dispersion theories by Anderson (1984), early works on the hydrodynamic dispersion date back to early 20th Century. One of the earliest experimental studies on dispersion in porous media was performed by Slichter (1905). He successfully attributed the S-shaped breakthrough curves observed in the field and laboratory experiments to the shape of flow paths formed by interconnected pores and partly to molecular diffusion. The first theoretical work was performed by Taylor (1953). In the 1960's Taylor and others proposed that dispersion be defined with an expression similar to Fick's Law of diffusion, which was originally proposed by Adolf Fick, a German physiologist, in 1855 to define the diffusion of a gas across a fluid membrane. The adopted expression is given in Equation 1.1.

$$J=-D\nabla C \qquad (1.1)$$

where J is the dispersive mass flux, D is the hydrodynamic dispersion coefficient and C is the contaminant concentration and ∇C is the gradient of concentration in space. The hydrodynamic dispersion coefficient accounts for the effects of both mechanical mixing (spreading of contamination due to microscopic and macroscopic spatial variations of groundwater velocity) and molecular diffusion, and is usually determined indirectly by comparing observed breakthrough curves with transport model predictions.

The hydrodynamic dispersion coefficient is a function of the flow conditions the hydrogeological properties of the flow domain and the scale of the problem of interest. Under the same hydrogeological setting, and considering one dimensional flow conditions for simplicity, coefficients for different flow conditions can be calculated using Equation 1.2.

$$D=\alpha v+D^{*} \tag{1.2}$$

where α is the dispersivity constant, v is groundwater velocity and D^{*} is the effective diffusion coefficient in a porous medium. Dispersivity is thought to be dependent on the hydrogeological properties of the flow domain scale of the problem. The effective diffusion coefficient is relatively less important and unchanging in many hydrogeological settings. These parameters will be discussed in more details in the following sections. However, it is important to note that the classical dispersion theory assume that dispersion parameters are not dependent on absolute solute concentrations or concentration gradients, and as a consequence, dispersive flux is a linear function of the concentration gradient.

In this text, this linear relationship will be called the Fickian model or the Fick's Law. A Fickian model assigns a single dispersivity value to a given hydrogeological setting and accounts for the dispersive flux using this unique dispersivity value disregarding the spatial and temporal variations in flow rates and contaminant concentrations. Any representation which does not rely on a linear relationship between the dispersive flux and the concentration gradient will be called non-Fickian.

Although the Fickian representation of hydrodynamic dispersion has been used for many practical applications over the years, and it is still being commonly used, many researchers question the Fickian nature of hydrodynamic dispersion under certain conditions. One such example is dispersion near a contamination source (e.g. Fried, 1975; Gelhar et al., 1979; Dagan, 1982; Matheron and de Marsily, 1980; Gelhar and Axness, 1981; Smith and Schwartz, 1980). Gelhar et al. (1979) showed that the apparent dispersivity increases as the distance between the contamination source and observation point increases, and approaches an asymptotic value at some distance called the Taylor limit. These findings suggest that a dispersivity value obtained from a measurement at a

given site may not be appropriate for modeling the entire domain or a subset of the domain. On the other hand, if the Fickian model is to be used for making predictions of contaminant transport, a single dispersivity value should exist for a single hydrogeological setting. A satisfactory model, which is able to describe hydrodynamic dispersion given any set of possible hydrogeological settings, is not yet developed.

When salt domes and bedded salt formations were considered as long term repositories for high-level nuclear wastes, the need to understand the flow and transport in the vicinity of these formations emerged. The flow and transport near salt domes and bedded salt formations are characterized by the presence of sharp concentration fronts between the ambient groundwater and the high density groundwater, or brine. Although the density and viscosity of an aqueous solution are functions of both the solute concentration and the temperature, under common hydrogeological conditions the effect of temperature may be neglected because the ambient temperature tends to remain practically constant for time scales of groundwater applications. Henceforth, the terms solute concentration and density will be used interchangeably in the text.

Density differences between common groundwater and brine can be as high as 20%. At density variations about 5% or greater, the flow and transport processes are strongly coupled and as a consequence, the modeling and prediction are more complex than they are for dilute systems (Oldenburg and Pruess, 1995). The main coupling arises from the effect of density on the flow while the velocity occurs both in the advective term of the transport equation and in the definition of hydrodynamic dispersion coefficient. The resulting distribution of groundwater densities in turn adds to the coupling by affecting the velocity fields. In order to account for the coupling, generalized versions of the partial differential equations governing groundwater flow and contaminant transport are used as discussed in the Materials and Methods Chapter.

In addition to the problem of radioactive waste disposal, high concentration gradients may be observed in several other environmental problems including infiltration of landfill leachates having densities up to 3% higher than freshwater (Freeze and Cherry, 1979), deep injection of industrial wastewater containing high amounts of total dissolved solids, seawater/freshwater interfaces where density differences are typically equal to 3% or

higher (Pinder and Cooper, 1970), groundwater remediation involving the injection of surfactant and cosolvent solutions for the recovery of contaminants in the form of non-aqueous phase liquids (NAPLs), injection of brine in secondary petroleum recovery, dissolution and infiltration of salt used for de-icing of roads, and many other types of contamination in salt formations, such as discharge of industrial and municipal wastewaters near Tuz Gölü (e.g., Zeynel, 2002). However, the radioactive waste disposal drew the most attention due to its striking nature and, moreover, it induced more work on dispersion as it tends to be more dispersion dominated due to slower groundwater velocities in the vicinity of the formations chosen for disposal.

As presented by Kolditz et al (1998), numerous efforts have been made for modeling flow and transport under high concentration gradient conditions that are encountered in the vicinity of salt domes, starting in mid 1980's. However, most of these studies adopted Fickian models for hydrodynamic dispersion. Recently, it has been suggested that the dispersion of solutes is affected by the large concentration differences and the ensuing density contrasts that exist at groundwater-brine interfaces (e.g. Bouhroum, 1988 and 1989; Hassanizadeh et al., 1990). This understanding urged theoretical and experimental studies for defining hydrodynamic dispersion with a more general model than Fick's Law. More details of the studies on developing a generalized dispersion model will be described in the Literature Review Chapter of this dissertation.

Initial attempts to account for the effect of high concentration gradients on dispersive flux focused on defining the dispersion parameters as a function of density, the density difference, viscosity ratios, (mean) velocity, etc (e.g. Kempers and Haas, 1994). However, such models tend to be problem specific and do not mathematically explain the dependence of the dispersive flux on the concentration gradient. A theoretically-based, more generally applicable, non-linear form of Fick's Law was proposed by Hassanizadeh and Leijnse (1995). Subsequent experimental studies by the same group of researchers showed that, the proposed mathematical model was able to simulate experimental results, using a single set of initial dispersion parameters, namely dispersivity and a coefficient of dependence on high concentration gradient, for a limited range of flow and transport parameter values used in the experiments.

The primary means for investigating dispersive transport is to conduct miscible displacement experiments. A displacement experiment involves filling a physical model representing porous media with an initial fluid (resident fluid) and then inject a second fluid with different properties but still miscible the first one (displacing fluid) and monitoring the changes in concentration. More information on displacement experiments will be provided in Literature Review and Materials and Methods chapters. However it should be noted that, one important aspect of the transport under high concentration gradient conditions, that has to be considered when performing displacement experiments to investigate dispersive behavior, is the stability of the displacement front (interface between the two fluids) and resulting flow. As it will be described in Materials and Methods Chapter, the flow may be stable or unstable according to the direction of flow and relative positions of the resident and displacing fluids, and their relative densities and viscosities. The unstable case is further complicated by gravity induced flow and fingerings due to heterogeneity of the porous medium. As in most of published experimental studies, this study considers stable displacement cases only where the effect of high concentration gradients on dispersion can be better isolated.

This study evaluates the effect of high-concentration gradients on the dispersive flux for flow and transport conditions beyond those evaluated in previously published studies. In order to reach that goal, displacement experiments with (i) a low density solution (tracer) containing a single dissolved species; (ii) high density solutions (brines) containing a single dissolved species at a number of high concentrations; (iii) concentrated brine with multiple dissolved species (i.e., mixtures of salt at a high concentration and a contaminant at a low concentration) were used to displace the resident fluid vertically upward in homogeneous porous media at flow ranges including low velocity flow regimes where molecular diffusion is the dominant transport process were conducted. As part of this study a mathematical advection-dispersion model that accounts for the presence of high concentration gradients and a computer code based on it were developed and used for the interpretation of the experimental results as well as conducting Mote-Carlo simulations in order to investigate the effect of high concentration gradients on hydrodynamic dispersion in the presence of heterogeneity in flow parameters.

As part of this study a mathematical advection-dispersion model that accounts for the presence of high concentration gradients- including a non-Fickian expression for the dispersive flux- and a computer code based on it were developed and used for the interpretation of the experimental results as well as conducting Mote-Carlo simulations in order to investigate the effect of high concentration gradients on hydrodynamic dispersion in the presence of heterogeneity in flow parameters.

The rest of this thesis is organized as follows. The next chapter is review of the literature with the specific purpose of introducing notable advances that led to an improved understanding of hydrodynamic dispersion under high concentration gradient conditions. It reviews significant publications that contributed to the development of dispersion theories in porous media along with the experimental works on hydrodynamic dispersion under high concentration gradient conditions and attempts to represent the phenomenon mathematically. The third chapter states the purpose of this study and its significance as a scientific text.

The Materials and Methods Chapter explains how the experimental and computational components of the work were designed and conducted. It describes the experimental setup, the course of the experiments and establishes the mathematical basis for numerical model development efforts. The fifth chapter is on the verification and validation of the numerical models that were developed.

Chapters six through nine present the result from laboratory experiments and numerical simulations. Chapters on tracer experiments, brine experiments and contaminant mixtures describe in detail the laboratory findings of this study and then further test and improve the numerical models with experimental results. The Effect of Heterogeneity Chapter is an example application of the numerical models developed in preceding chapters. The main outcomes of experimental and modeling efforts and their implication to field applications are discussed in the Conclusions and Future Research Chapter.

2. LITERATURE REVIEW

2.1. Development of Dispersion Theories in Porous Media

The original Fick's Law was developed in 1855 by Adolf Eugen Fick to define the diffusion of a gas across a fluid membrane. It linearly related the diffusive mass flux to the concentration gradient through a coefficient of molecular diffusion (Fick, 1855). The diffusion coefficient or diffusivity was a function of the temperature and viscosity of the solution and the size of the solute particles. Although diffusion is a result of the random motion of individual particles, at a macroscopic scale it is perceived as a systematic movement from areas with high concentration to areas of low concentration. What Fick's First Law of molecular diffusion explained, was this macroscopic observation:

$$J_m = -D_m \nabla C \tag{2.1}$$

where J_m is the diffusive flux, D_m is the coefficient of molecular diffusion and C is the solute concentration. In the original Fick's Law the symbols J and D were used to represent the diffusive flux and the diffusivity, respectively, however the subscript m will be used to indicate the molecular diffusion related symbols throughout the text, to avoid confusion with hydrodynamic dispersion related symbols. In dilute aqueous solutions the coefficient of diffusion exhibits slight dependence on temperature. At room temperature it is in the range of 0.6×10^{-9} to 2×10^{-9} m^2/s depending on the type of molecule. Molecular diffusion generally decreases with increase in molecule size and its molecular weight however this effect is small except for macromolecules (Cussler, 2007). Similar to its contemporary Darcy's Law (Darcy, 1856) Fick's Law became one of the basic relationships in the field of hydrogeology.

Although Fick's Law in its original form was not intended to define the spreading behavior of solutes in porous media, following the theoretical work of Taylor (1921 and 1953), in the early 1960's, this form of equation was adopted to the subject of dispersive transport and developed then on (e.g., Bear, 1961a and 1961b). Over the years, many studies have focused on the factors controlling the hydrodynamic dispersion and

accordingly proposed modifications to the definition of the dispersion coefficient (e.g., Schwartz, 1977) however the form remained practically unchanged:

$$J=D\nabla C \tag{2.2}$$

where J is the dispersive flux, D is the coefficient of dispersion and C is the solute concentration.

Dispersion arises mainly from deviations of contaminant transport velocities from the average groundwater velocity due to irregularities of the flow field. By defining boundary conditions at the interface between the groundwater and individual soil particles, the transport of contaminants in porous media could be modeled using the Navier-Stokes equations and molecular diffusion. However, this would be an immensely time consuming task, even for an idealized porous medium, and therefore the S-shaped breakthrough curves commonly observed in field and experimental transport problems are instead explained using macroscopic-scale or continuum equations mentioned above, namely the Darcy's Law and Fick's Law.

The continuum equations comprise advective and dispersive terms. Advection is the displacement of solutes by the movement of groundwater in which they are dissolved, whereas dispersion is the spreading of contaminants due to molecular diffusion and to irregularities and heterogeneities in the subsurface flow conditions. The effect of molecular diffusion under field conditions is generally small except in regions of very low permeability. Other processes that may be present depending on hydrogeological conditions and type of the contaminant in question are retardation and biogeochemical reactions and transformations.

The initial attempts to define dispersion can be grouped into 3 main approaches. The first approach is to represent the porous media by simplified geometric shapes such as interconnected channels, and define the transport in the resulting system using exact mathematical models (e.g., Taylor, 1953). The second approach uses statistical techniques to relate the dispersion to the microscopic motion of water and solute particles (e.g., Scheidegger, 1954). The third approach consists of averaging the equations defining

microscopic flow patterns in pores, over a representative elemental volume (e.g., Bear, 1972).

As stated earlier, the dispersion coefficient combines the effect of molecular diffusion and mechanical mixing. Mechanical mixing is commonly represented as a function of medium properties and specific groundwater discharge, or average linear velocity (Nikolaevskii, 1959; de Jong and Bossen, 1961). For isotropic media, the dispersion coefficient is defined as a symmetrical tensor (Bear, 1961b; Scheidegger, 1960):

$$\mathbf{D}=\left(D_m^*+\alpha_T q\right)\mathbf{I}+\left(\alpha_L-\alpha_T\right)\mathbf{qq}/q \qquad (2.3)$$

where D^*_m is the effective molecular diffusion coefficient, α_T and α_L are transversal and longitudinal dispersivities respectively, **I** is the unit tensor, **q** is specific discharge vector and is q its magnitude. The effective molecular diffusion coefficient, D^*_m, is the reduced value of the molecular diffusion in a water body due to the obstruction resulting from the presence of the porous medium. Except in cases where groundwater velocity is relatively very small, the effect of mechanical dispersion dominates over the effect of molecular diffusion. For one-dimensional flow such as flow through a sand column, the hydrodynamic dispersion tensor reduces to:

$$D=D_m^*+\alpha v \qquad (2.4)$$

where D is the hydrodynamic dispersion coefficient, α is the dispersivity and v is the average linear groundwater velocity.

The dispersivity appearing in the above equation is a best-fit parameter that encompasses the effect of the porous medium properties. Dispersivity values cannot be measured directly but are determined empirically by matching observed breakthrough curves with model predictions. Field observations have shown that dispersivities generally increase with the increase in travel distance of the contamination in the porous medium (Sudicky and Cherry, 1979; Gelhar, 1993). At a distance which is specific to the medium, dispersivity becomes asymptotic to a certain value. This distance is sometimes called the Taylor Limit. This fact weakens the applicability of the Fickian Model, especially in the

vicinity of the contamination source or at early times. It has also been suggested that it is not valid at large concentration differences (e.g., Hassanizadeh, 1986a and 1986b), as will be discussed in the next section.

More recently, many researchers have focused on developing alternative dispersion theories through stochastic techniques for the definition of the dispersivity coefficient for heterogeneous porous media (see for example reviews by Gelhar, 1993; Dagan and Neumann, 1997). Gelhar and Axness (1983) derived expressions for the Taylor Limit in terms of the stochastic parameters of porous media, namely in terms of the hydraulic conductivity statistical spatial structure. Dagan (1984) proposed a similar theory that approaches Fickian representation at large times.

2.2. Experimental Works on Hydrodynamic Dispersion under HCG Conditions

Several experimental studies, by various researchers, have been made in order to determine the validity of dispersive transport models based on Fick's Law, under high concentration gradient conditions. In the field, dispersion parameters can be empirically determined by injecting a tracer (a non-reactive, non-absorbing, low concentration solute, whose concentration can be detected easily, by preferably a physical method) into the aquifer in question and monitoring the tracer concentration at an observation well. The observed breakthrough curves are then compared with curves generated by an advective-dispersive model in order to find the dispersivity that fits the observed curve the best.

A common procedure used in the study of hydrodynamic dispersion under high concentration gradient conditions in the laboratory is to conduct a displacement test. In a displacement test, a fluid that fills the pore volume of a physical model that represents a porous medium is displaced by a fluid having different properties, such as concentration, density, viscosity etc. The former is called the resident fluid and the latter is called the displacing fluid. The change in concentration with time is monitored along the flow path or at an outlet where the pore liquid is being discharged to obtain concentration profiles or breakthrough curves. Similar to a tracer test, the parameters are then determined by curve fitting.

However, it is important to note that, when analyzing the results of displacement experiments it must be considered whether the flow was stable or unstable. The stability of the flow depends on the viscosity and density differences of the resident and displacing fluids. Hill (1952) was the first to observe displacement of fluids with different viscosity and density and distinguished three flow configurations: inherently stable, inherently unstable and velocity dependent. Slobod and Howlett (1964) defined four configurations, as given in Table 2.1, depending on viscosity (μ) and density (ρ) differences of resident (subscript r) and displacing (subscript d) fluids, direction of flow, specific discharge (q) relative to some critical specific discharge, q_c:

Table 2.1. Stability configurations according to viscosity and density differences and flow conditions (Slobod and Howlett, 1964)

Configuration	**Direction of flow**	**Stability**
$\mu_r, \rho_r < \mu_d, \rho_d$	up	always stable
$\mu_r, \rho_r < \mu_d, \rho_d$	down	stable if $q < q_c$
$\mu_r, \rho_r > \mu_d, \rho_d$	up	always unstable
$\mu_r, \rho_r > \mu_d, \rho_d$	down	stable if $q > q_c$

In configurations deemed unstable, fingering of the concentration front is observed. Fingerings cause further variation of spatial distribution of concentration. Therefore, unstable displacement experiments are not appropriate for the testing of dispersion models. For stable displacement experiments, which are the focus of this study, it was observed in the literature that dispersion is influenced by density differences, in addition to parameters commonly used in the modeling of hydrodynamic dispersion.

During the 1960s many researchers conducted displacement experiments. Brigham et al., (1961) focused on the effect of viscosity only, while Slobod and Howlett, (1964); Ben Salah, (1965); Krupp and Elrick, (1969); and Starr and Parlange, (1976) explored the effects of both density and viscosity. The general conclusion from these studies is that although viscosity and density both influence the breakthrough curves, the influence of density differences are more pronounced. These studies led to questions regarding the validity of Darcy's Law and Fick's Law for high concentration gradient conditions.

When long term disposal of high level nuclear wastes in salt formations came into consideration, concerns about the transport of nuclides to the biosphere through groundwater were expressed (e.g., Sander and Herbert, 1985; Roxburg, 1987). Therefore a need for accurate modeling of groundwater transport in the vicinity of these repositories emerged. Although the density of groundwater in near-surface aquifers is generally constant, the presence of high concentrations significantly affects groundwater density. Density values as high as 1200 kg/m^3 are reported near salt domes and embedded salt formations (e.g., Stheeman, 1963; Visser, 1974; Frape et al., 1984). Moreover, these regions of the groundwater showed very steep concentration gradients. Boehme et al., (1985) reported that density increase from 1040 to 1180 kg/m^3 was observed over a 30 m distance in Gorleben, a salt dome in Germany.

The need for better understanding of transport processes and their modeling under high concentration gradient conditions invoked a new generation of experimental studies starting in the 1980s. Table 2.2 gives a summary of some key brine displacement experiments. The experiments and their main findings are also briefly described below.

In his displacement experiments, Bouhroum (1985) studied density and viscosity effects independent of each other. He observed that apparent dispersivities decreased with increase in density differences. However as in many of the previously cited studies, he concluded that density or viscosity effects on dispersion may be included by defining dispersion parameters as a function of density differences, viscosity ratios, and velocity (Bouhroum, 1988 and 1989).

Hassanizadeh et al. (1990) conducted stable displacement experiments in a vertical column packed with glass beads. Breakthrough curves were built up through measurements of electrical conductivity, which is linearly related to solute concentration for solutions containing a single solute. They made similar observations as Bouhroum (1985). However their experimental setup was not able to maintain a constant flow rate and they did not perform enough experiments to cover a large velocity range. Therefore no explicit statement was done on the effect of velocity on high concentration gradient dispersion.

Table 2.2. List of selected experimental studies on hydrodynamic dispersion under high concentration gradient conditions

Experiment	Stability	Heterogeneity	Fluids	Dimensions	CMT*	Main findings
Bouhroum (1985) analyzed in Bouhroum (1988, 1989)	Stable	Homogeneous	NaCl	1D, vertical flow, longitudinal dispersion	Electrical	Apparent longitudinal dispersivity decreases with increasing density differences
Hassanizadeh et al. (1990)	Stable	Homogeneous	NaCl	1D, vertical flow, longitudinal dispersion	Electrical	Linear Fick's Law was not suitable for modeling of dispersion under HCG conditions
Moser (1995) analyzed in Schotting et al (1999)	Stable	Homogeneous	NaCl	1D, vertical flow, longitudinal dispersion	Electrical	Dispersion is not affected by the densities of individual fluids but by the difference between them
Anderson (1997) analyzed in Watson et al (2002a and 2002b)	Stable	Homogeneous	NaCl	1D, vertical flow, longitudinal dispersion	Electrical	Darcy's Law remains valid even under high concentration gradient conditions
Oswald (1998) analyzed in Johannsen et al. (2002)	Stable	Homogeneous	NaCl	1D, horizontal flow, transverse dispersion	Outflow sampling	Apparent transverse vertical dispersivity decreases with increasing density differences
Jiao (2001) analyzed in Jiao and Hötzl (2004)	Both	Homogeneous	NaCl Glycerin	1D, vertical flow, longitudinal dispersion	Electrical	Dispersion can be modeled using Fick's Law
Kretz et al. (2003)	Both	Heterogeneous	Sugar Glycerin	1D, vertical flow, longitudinal dispersion	Acoustic	Dispersion is affected by heterogeneity

* Concentration measurement technique

Moser (1995) performed four series of experiments: (i) tracer experiments, where the displacing fluid's concentration was only slightly higher than the resident fluid's concentration; (ii) resident/displacing fluids with various large density differences, where the same flow rate was applied; (iii) resident/displacing fluids having the same large density difference, with various flow rates; and (iv) resident/displacing fluids with similar, high densities (but with small density difference). These experimental results were numerically analyzed further in Schotting et al (1999). The results of these experiments show the same tendency as in Hassanizadeh et al. (1990) and earlier experiments: Longitudinal dispersivity decreases with increasing density difference. It also confirmed observations by Slobod and Howlett (1964) and Krupp and Elrick (1969) that decrease in the dispersivity become less prominent with increasing flow rate. Another important conclusion was that when densities of both resident and displacing fluids are high, Darcy's Law and Fick's Law were valid. The deviation from the linear Fick's Law does not depend on absolute salt concentrations but only on gradients.

Anderson (1997) performed experiments in a column using homogeneous porous media with various grain sizes, where the flow could be regulated. These experiments were analyzed by Watson et al. (2002a and 2002b). The results are in agreement with previous observations, in other words that Fick's Law is subject to criticism when high concentration differences exist, while Darcy's Law is not.

Jiao and Hötzl (2004) analyzed experiments conducted by Jiao (2001) under both stable and unstable conditions and concluded, like Bouhroum (1988 and 1989) and Kempers and Haas (1994), that all breakthrough curves could be modeled with classical Fick's Law but using a variable dispersivity which is defined as a function of fluid properties as well as medium properties. However, the density gradients used in their experiments were not high enough to be expected to affect the dispersive transport and the absolute concentrations they used were in the tracer range.

Kretz et al. (2003) did both stable and unstable displacement experiments using glass beads with non-uniform size to mimic a heterogeneous porous medium, whereas all previous experiments used homogeneous media. They consider two distributions of the hydraulic conductivity with the same statistical parameters but different spatial

arrangements. Concentrations were measured using an acoustic technique. They concluded that for high groundwater velocity, the dispersivity is function of the porous medium's heterogeneity only, while for low velocity, the dispersivity is an exponential function of the flow rate, with opposite exponents for stable and unstable flow conditions.

Spitz (1985) and Leroy et al. (1992) investigated horizontal flow for the effect of density gradients (stable, horizontal density front) on transverse dispersion. They reported that mixing reduced with increasing density differences, especially at low velocities, and the gravity effect was larger for stratified media than for homogeneous materials.

Oswald (1998) performed laboratory experiments to assess the effect of concentration difference on transverse dispersivity (i.e., the dispersivity perpendicular to the flow) which were later analyzed by Johannsen et al. (2002). Their setup included stationary high density solution underneath flowing freshwater which results in a horizontal density interface. They found that the transverse dispersivity decreased as concentration differences between the two solutions increased.

2.3. Mathematical Representation of Dispersion under HCG Conditions

One approach to mathematically account for the effect of high concentration gradient on dispersion was to maintain a Fickian-type expression (i.e., $J=-DdC/dx$) but define the dispersion parameters as function of the flow and solution properties, specifically the viscosity and density. However, this approach does not allow the dispersion coefficients to be calculated a-priori. In most of the experimental studies mentioned above, dispersivities were calculated empirically for specific cases, using various parameter estimation techniques but no tool was provided for the determination for the dispersivity under the same hydrogeological settings but a different concentration gradient. This approach limits the use of the methods they propose for making future predictions for varying concentration and flow conditions.

An alternative approach was proposed by Hassanizadeh (1990) who suggested that the results of high concentration gradient experiments could be modeled with a non-linear dispersion theory, which allows for the use of a single dispersivity value for a given

hydrogeological setting, and proposed several extensions of Fick's Law. Hassanizadeh and Leijnse (1995) provided the theoretical background for the non-linear theory. Their mathematical derivation culminated into the following equation for the hydrodynamic dispersion:

$$(1+\beta J)\mathbf{J}=-\rho\mathbf{D}\cdot\nabla\omega \qquad (2.5)$$

where β is the coefficient of dependence on high concentration gradient, ρ is fluid density, and ω is the solute mass fraction, J is the magnitude of the dispersive flux, **J** is the dispersive mass flux vector and **D** is the dispersion tensor. It should be noted that this equation reduces to linear Fick's Law as concentration differences are small and the term βJ becomes negligible compared to one.

Results of experiments from Moser (1995) and Anderson (1997) were used to validate the proposed non-linear expression for dispersive flux. First, dispersivities for experimental columns were determined by curve fitting to breakthrough curves obtained from tracer experiments and then coefficients of dependence on high concentration gradient, β, were determined by comparing apparent dispersivities determined in experiments to dispersivities found in tracer tests. They managed to find a unique β value for each experimental setup that was later used to generate mathematical model results that satisfactorily matched experimental breakthrough curves with varying density differences for the considered flow conditions. Based on these experimental results, Schotting et al. (1999) give an empirically determined relationship for the non-linearity coefficient, β:

$$\beta = \frac{0.0125}{q^{1.76}} \qquad (2.6)$$

where q is the specific discharge in units of m/s. Note that β is not a function of the concentration differences. This model was validated for limited flow conditions, specifically for $9.0\text{x}10^{-5}$ m/s $< q <$ $3.0\text{x}10^{-3}$ m/s, in relatively homogeneous soils (low dispersivity values), for single non-reactive species and with a stable configuration. In order to develop a commonly acceptable generalized theory of hydrodynamic dispersion,

more experimental and modeling studies are needed to extend the verifiability of the theory.

Equation 2.6 suggests that Equation 2.5 reduces to Fick's Law at high velocities also, since β approaches zero as v approaches infinity. In other words, deviation from Fick's Law is expected at low to normal flow rates and when density differences are big, whereas at low concentrations or high velocities, dispersive behavior is expected to conform with the Fickian Theory.

3. PURPOSE

Based on the literature review presented in the previous section, there is clear evidence that Fick's law in its classical form is not valid for applications where high concentration gradients exist. Some researchers have proposed the use of a modified dispersion coefficient that is calculated from the solution properties such as density and viscosity (e.g. Kempers, 1991). However, this approach is restrictive, especially for two or three dimensional modeling purposes involving time and space variations of concentration gradients or multiple concentration fronts. Moreover, Schotting et al (1999) claimed that the effect of high concentration gradient on dispersive flux is dependent on the groundwater velocities.

Another approach proposed in the literature is a modified, non-linear version of Fick's Law (Hassanizadeh and Leijnse, 1995). This non-linear model allows the use of a single predetermined dispersivity value for a given porous medium but with the dispersive flux departing from the Fickian value, depending on the concentration gradient, by a non-linear coefficient expressed in terms of the flow rate. This non-linear theory has not yet fully validated with substantial experimental data for different flow conditions.

Despite the recent progress in this area of contaminant transport, several important questions remain. All of the cited literature assumed the presence of a single, non-reactive species, namely brine. However, in real contaminant transport applications brine is not the only solute of concern. The most popular and recent example is the transport of nuclides in the vicinity of salt domes and bedded salt formations, which are considered as long term repositories for high level nuclear wastes. In this case, the contaminant of concern, namely the radioactive waste, is not expected to reach concentrations high enough to cause deviations from the linear Fick's Law. A question that springs to mind is, whether the nuclides in the presence of brine would obey linear Fick's Law or not.

The majority of laboratory displacement experiments that have been performed to date were based on relatively homogenous soils and, hence, the dispersivity values tend to be relatively small. On the other hand, most natural groundwater systems are heterogeneous in

the distribution of the flow parameters. Another question that arises from these two facts is to find a way to account for the impact of heterogeneity on dispersion under high concentration gradients.

Most researchers agree that for stable flow, the impact of high concentration gradient on dispersion increases with decrease in groundwater velocities. However, the proposed modification of Fick's law has not been validated for low velocities, where β, the high concentration gradient coefficient of the non-linear model of Hassanizadeh and Leijnse (1995), approaches infinity. Hence, there is still a need for a dispersion model that covers slow groundwater flow rates that can be found, as an example, in the vicinity of salt formations that are considered as a final repository for high level radioactive wastes.

In order to address these problems, laboratory-scale stable displacement experiments were conducted. The experimental setup consists of a glass column filled with sand (or glass beads) and equipped with a pump to supply a constant flow rate, electrodes to make in situ concentration measurements and a fraction collector to take effluent samples to make ex situ concentration measurements. In all experiments conducted within the scope of this study, the high concentration fluid (brine with and without the contaminant) was injected from the bottom of the column in order to achieve a stable front. Experiments involving a range of brine concentrations were conducted, as well as experiments involving flow rates well above and below the common values of commonly encountered groundwater flow. Contaminant and brine concentrations were mostly monitored by taking timed samples from the outlet of the column. Samples were later analyzed using either an atomic absorption spectrophotometer or a set of ion selective electrodes or and conductivity probes.

The results of these experiments were used to assess the validity of Fick's Law under high concentration gradients. Since available general purpose computer models do not account for non-Fickian dispersion under high concentration gradient conditions, a new non-linear, coupled groundwater flow and solute transport computer model was developed to analyze the observed transport of contaminants with brine. However, the developed model was found insufficient for modeling cases of extremely low dispersivity. To extend the numerical analysis into low dispersivity settings and to create a tool for verifying the

results of the developed model, a general purpose variable density flow and contaminant transport model, SEAWAT (Langevin et al, 2003), was also modified to include the non-linear theory that was selected to model dispersive transport under high concentration gradient conditions.

The models were later validated and calibrated with the results of the column experiments and then used to simulate non-Fickian dispersion under heterogeneous flow conditions. These simulations involved a multitude of runs with the same set of model parameters, differing only in the distribution of hydraulic conductivities over the flow domain. The results were analyzed statistically to assess the combined effects of high concentration gradients and heterogeneity on hydrodynamic dispersion.

In summary, this study was conducted in order to gain further understanding and insight into dispersive flux under high concentration gradient situations and how it can be modeled mathematically. The experimental work provided data to assess the validity of Fick's law and to validate modifications of this law beyond the studies reported in the literature. Based on these experimental observations, a computer program was developed, validated and used to numerically evaluate combined effects of high concentration gradient and heterogeneity. This program can serve as a tool for the prediction of groundwater and contaminant transport under high concentration gradient conditions.

4. MATERIALS AND METHOD

4.1. Experimental Setup

Vertical displacement experiments were conducted in glass columns packed with well characterized silica sand or uniformly sized spherical glass beads. The columns were Cole-Parmer EW-34696-18 Chromaflex® standard chromatography columns, consisting of a borosilicate glass cylinder and two PTFE plastic lids fitted with screwable connectors for tubing. All materials are non-reactive and non-absorbing to avoid unwanted effects on such as decay or retardation that will complicate the interpretation of the breakthrough curves. Two identical columns were used for all experiments reported in this study. These two columns are 60 cm long with an internal diameter of 4.8 cm. The columns are leaktight up to 340 kPa and they were further sealed using silicone tape to ensure there was no leakage. Figure 4.1 presents a schematic of the column.

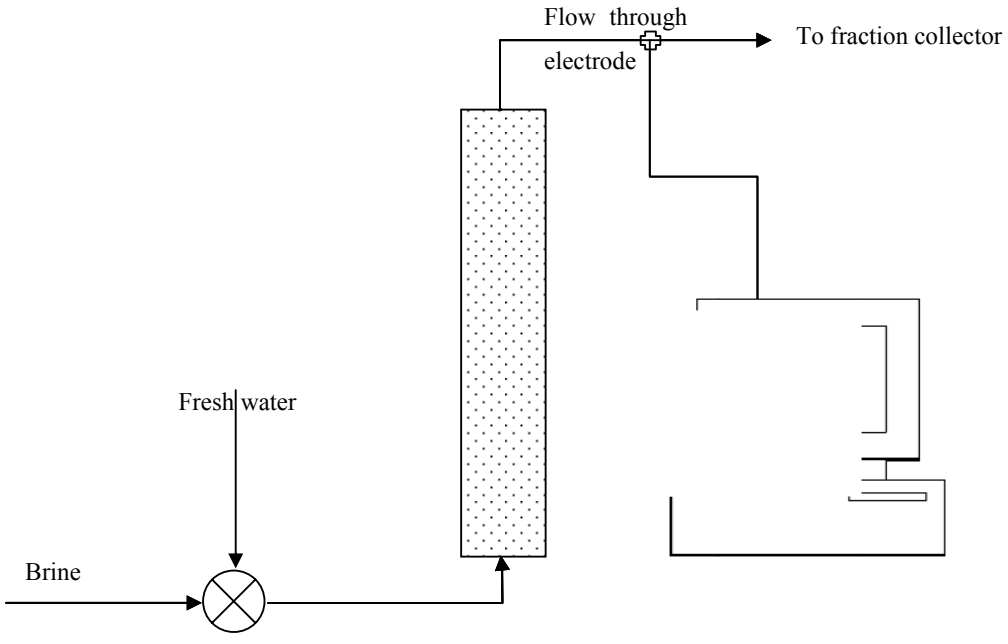

Figure 4.1. Schematic of the vertical column for stable displacement experiments

The sand that was used to fill the experimental columns was 60-70 AFS supplied from Siltaş. A complete analysis report of the sand is presented in Appendix A. The reported average particle size of the sand was 0.2 mm with 97.68% being between 0.355 mm and 0.125 mm. These statistical parameters correspond to a calculated porosity between 0.3395 and 0.3849 according to Sohn and Moreland (1968). The sand falls into fine sand size class according to Udden-Wentworth grain-size classification scheme (Wentworth, 1922) shown in Table 4.1 and the size distribution is uniform enough to be considered homogeneous. Uniform spheres, such as the glass beads used in this study may have porosities between 0.260 and 0.476 depending on their spatial arrangement (Lambe and Whitman, 1969). According to Wentworth scale, glass beads fall into the coarse sand range.

Table 4.1. Udden-Wentworth grain-size classification scheme (Wentworth, 1922)

Size range (mm)	Wentworth size class	Unconsolidated material	Consolidated material
>256	Boulder	Gravel	Conglomerate / Breccia
64-256	Cobble		
4-64	Pebble		
2-4	Granule		
1-2	Very coarse sand	Sand	Sandstone
0.5-1	Coarse sand		
0.25-0.5	Medium sand		
0.125-0.25	Fine sand		
0.0625-0.125	Very fine sand		
0.031-0.0625	Coarse silt	Silt	Siltstone
0.0156-0.031	Medium silt		
0.0078-0.0156	Fine silt		
0.0039-0.0078	Very fine silt		
0.00006-0.0039	Clay	Mud	Claystone

The filling of the column was done by repeatedly adding approximately 1 cm thick layers of sand or glass beads and compacting by a metal pestle. The same force was use to compact the sand in different columns to make the experimental setups as similar as

possible. This is the common practice for constructing dry packed soil columns as reported in the detailed review of experimental soil column designs by Lewis and Sjöstrom (2010). The column is then filled with distilled water by pumping water through the bottom lid slowly enough to avoid the formation of dry pockets (approximately 1 ml/min). The porosity of the column is determined from the difference between the dry and saturated weights. The relevant calculations are shown in the results section of this thesis, before each set of experimental results.

To attain a stable flow configuration in a displacement experiment, the more concentrated solution has to be pump through the lower connector and the upper one should serve as an outlet while the column is kept perpendicular to the ground. Plastic lids have matching screens that help prevent the sand from escaping into tubing and also distribute the flow over the cross sectional area of the column. Cole-Palmer Masterflex L/S variable speed peristaltic pump systems were used to inject solutions through the lower lid, at a the steady flow rate, to avoid any contact of the solutions with equipment except with the appropriate tubing. The constancy of the flow was monitored by collecting timed samples from the outlet and determining collected volume. The pumping rate can be adjusted using a knob on the controlling device connected to the pump. With existing pumps and tubing, flow rates from 0.2 to 200 ml/min can be supplied.

Several measurement techniques have been tested to monitor the concentrations at the outlet. It should be noted that, since the scope of this study involves experiments with more than one solute species, the measurement technique should be able to differentiate between them. The most appropriate technique was found to be sampling the effluent at timed intervals and then measuring concentrations ex situ. The details of tested techniques are discussed in following paragraphs.

The first technique was to use ion selective, flow through microelectrodes. These electrodes have the advantage of allowing continuous measuring of the effluent concentration in a rapid way without the need to collect samples. However, these electrodes proved to be non effective at lower concentrations since they produce uncertainty in the measurement, which reached significant percentages of the actual concentration, unless the concentration was relatively high. Although this set of

microelectrodes was used in the early experiments, they were not replaced as they completed their working lives. The results of preliminary tests for flow-thru microelectrodes are shown in Figure 4.2.

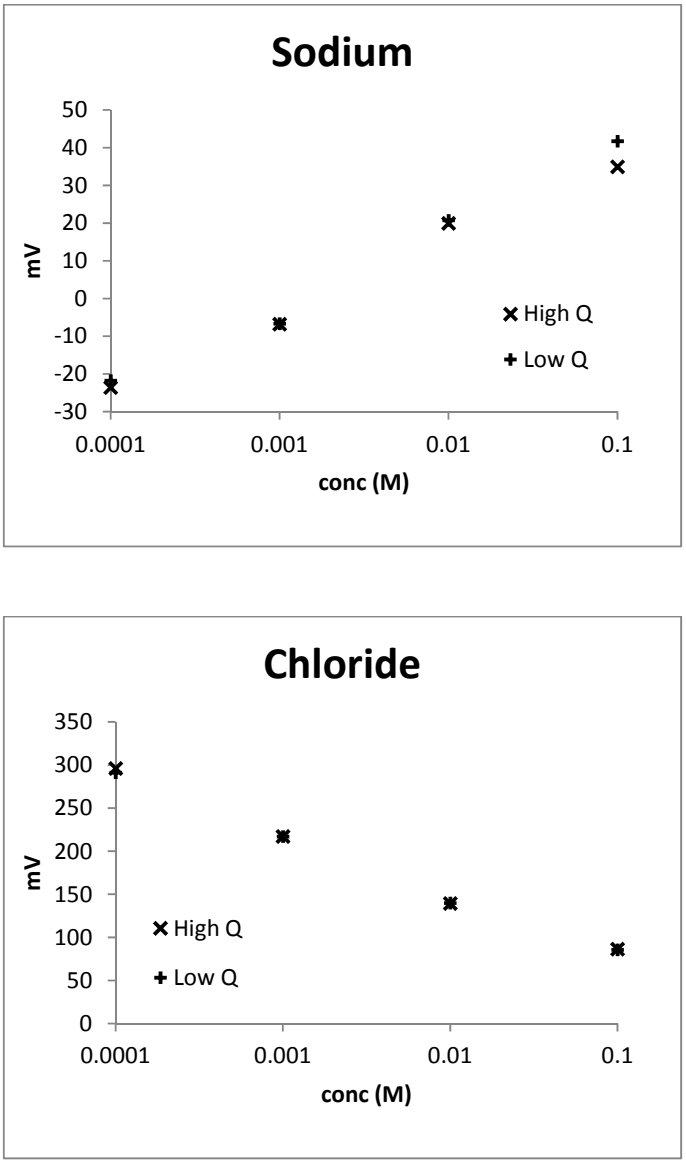

Figure 4.2. Calibration curves for flow-through micro ISEs under different flow conditions

As microelectrodes were not useful in measuring low concentrations, another technique should be used for tracer tests which involved relatively low concentrations such

as 10^{-3} M. As the in situ technique proved to be prone to errors which are unacceptably high for a dispersion study, the alternative should involve collecting samples from the outlet. In the early experiments, samples were collected by hand and later analyzed using atomic absorption spectrophotometer. Although accurate, this method was difficult to apply and time consuming because it required dilution of samples up to 100 times, especially for peak concentrations.

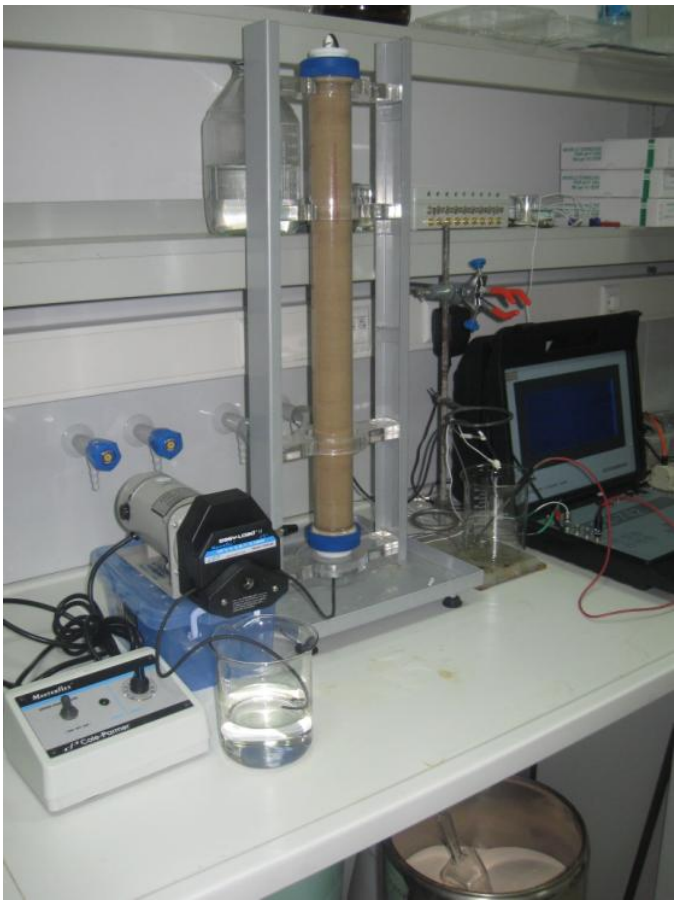

Figure 4.3. Experimental setup

The last method of concentration monitoring was sample collection followed by measurement with normal sized ion selective electrodes and conductivity probes. Since each breakthrough curve needed approximately 50 measurements, and hence collection of more than 50 samples, an automated fraction collector was used. The fraction collector is able to collect the effluent on the basis of either collection time or amount of collected

effluent. Although the flow rate was not changing during an experiment, a fixed collection time was chosen in order to obtain uniform sampling in time. The entire experimental setup can be seen on Figure 4.3.

At the beginning of each experiment, the column was filled with resident fluid (distilled water or a low concentration solution) until complete saturation, i.e. the pores contain only water, no air. To achieve complete saturation, a very low flow rate (0.5-1.0 ml/min) is chosen and distilled water is pumped from the bottom lid of the column for several hours, preferably overnight. Once the column is filled with the resident fluid, the flow rate is adjusted to the value determined for the displacement experiment. Flow rate is evaluated several times until a steady flow is observed and the influent reservoir was changed from resident fluid to displacing fluid.

Depending on the flow rate selected, salt water may need from around 15 minutes to around 15 hours to fill the pore volume of the column. If the transport was purely advective, the concentration monitored at the outlet would be that of the resident fluid until the pore volume is completely filled by the displacing fluid and that of the displacing fluid once the contamination reaches the outlet. However, hydrodynamic dispersion causes some portions of the contaminated water to arrive earlier than the bulk and some portions to arrive later. As a result, in order to capture the whole breakthrough curve, concentration measurement or sample collection has to start in advance and continue after the arrival time calculated using the pore volume of the column and the observed flow rate.

Since one of the aims of the study was investigating the dispersive behavior of low concentration contaminants in the presence of brine, the experimental procedure should be able to differentiate between all dissolved species. For experiments involving brine and a contaminant, ISE electrodes were used for analyzing the samples. In order to calibrate the electrodes and test for the effect of sorption on ion concentration measurements, batch experiments were designed. In batch experiments, porous material to be used for column packing, namely glass beads or sand, is soaked with a known solution for a contact time long enough to exceed the contact times in all column experiments, and concentrations are monitored in each batch before contact with porous material. Figure 4.4 shows the results

from batch experiments obtained with normal sized ISE electrodes used to determine contaminant concentrations in mixtures.

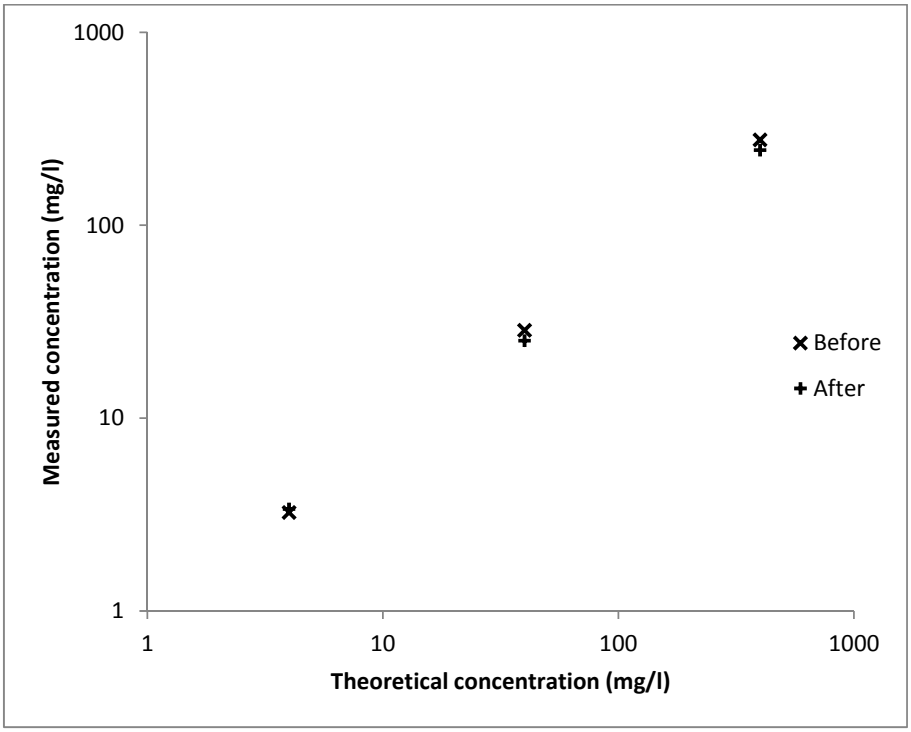

Figure 4.4. Batch experiments for the calibrating ISEs and testing sorption.

In all experiments, it was essential that the flow through the column remains steady. Variations in the flow would influence the interpreted dispersion coefficient and dispersivity values. For this purpose, the pump was allowed to operate for a long time with the resident fluid prior the injection of the displacing fluid to stabilize the flow. Moreover, the flow was monitored at different times during the injection of the displacing fluid. Experiments that exhibited any variation in the flow were discarded.

Another point to consider was that each experiment ended with a relatively high concentration solution (tracer, brine or a mixture) filling the pore volume. However, the next experiment should start with the column containing only the resident fluid (distilled water or 10^{-4} M NaCl solution). Between two consecutive experiments, the column was flushed with distilled water until the background concentration was observed at the outlet.

4.2. Experimental Procedure

The column was first used for tracer experiments, where the concentration of displacing fluid was slightly higher than that of resident fluid. The aim of tracer experiments is to determine the longitudinal dispersivity of the medium as well as testing the experimental procedure. In this set of experiments, several flow rates were applied keeping the concentration difference between displacing and resident fluids constant and relatively small. The Fickian Theory suggests that similar dispersivities be obtained from all experiments regardless of the flow rate applied. The results of tracer experiments will be discussed in detail in the first part of the Results section.

The same experimental procedure was then repeated with higher density differences, in order to investigate the validity of Fick's law under high concentration gradient. The first set of high concentration gradient experiments involved several flow rates while concentration difference between displacing and resident fluids was kept constant. In the second set, the concentrations were changed, keeping the flow rate constant. The dispersivity obtained from the tracer experiments, was then used to predict the results of the high concentration gradient experiments in order to assess the validity of the Fickian and modified dispersion models described in the next part of this section. Results of high concentration gradient experiments and comparison of models will be presented in the Results section.

Once the dispersion model was determined, a new set of experiments with both brine and a contaminant in the tracer concentration range was performed. Results of the third set were analyzed to investigate the dispersive behavior of low concentration contaminants in the presence of brine.

4.3. Mathematical Modeling of Solute Transport

4.3.1. Developed DENSTRAN Code

In groundwater contamination applications, the fate and transport of contaminants is represented in terms of a series of partial differential equations. These equations can be

solved analytically or through the use of various numerical methods. Analytical methods, although relatively simple to use, are only available for simplified problems, which may not fully represent real life cases. For more complex problems, a more realistic approach is using numerical models. In numerical modeling, governing differential equations are transformed into a system of algebraic equations. The chief disadvantage of this approach is the relatively large computational effort needed to solve these systems of equations and the large amount of data needed to fully define the problem.

Numerical methods used in solving mathematical models of groundwater flow and transport problems can be divided into two broad categories; (i) Eulerian methods and (ii) Lagrangian methods. In the Lagrangian method, the domain is divided into a grid and the transport of the solute is simulated by the motion of a large number of particles distributed within the flow domain. Each particle is associated with a concentration equal to the local concentration in the aquifer. Lagrangian Methods are suitable for the solution of advection dominated problems. However when dispersion is involved, as in the topic of this study, these methods become too complex to be efficient.

The two most common Eulerian methods are the finite difference and finite element methods which are inherently based on the principle of conservation of mass. These methods are characterized by the definition of a computational grid over the flow and transport domains. For finite difference method, the grid consists of rectangular cells, while for the finite element method; the grid can consist of triangular or rectangular elements. The differential terms in the governing equations are then expressed in terms of the dependent variables (head and concentration etc.) at the grid points. The result is a system of algebraic equations, which can be solved using various direct, such as Gauss-elimination, or iterative methods (Wang and Anderson, 1982).

The Lagrangian methods are numerically more stable. However, since they involve tracking a large number of particles representing each species included in the model, the computational effort required for the specific problem of this study, which is a multi-species system which may be dispersion or even diffusion dominated, would be significant. Another disadvantage of the Lagrangian methods is that they are not based on the principle of mass conservation. Since conservation of mass is a crucial parameter and a necessary

condition for the prediction of reliable and defensible predictions, the Eulerian method was selected in this thesis over the Lagrangian method. As will be discussed later, numerical constraints were used in conjunction with the Eulerian to reduce the numerical instability issues.

Both Lagrangian and Eulerian methods have been used in numerous groundwater flow and contaminant transport models, including some common models such as MODFLOW (Harbaugh et al, 2000), MT3D (Zheng and Wang, 1999), SEAWAT (Langevin et al, 2003) and SUTRA (Voss and Provost, 2003.). Between the two Eulerian methods mentioned above, the finite element scheme is to some extent more flexible than the finite difference scheme because of the irregular computational method that can be used in the finite element. The finite difference method on the other hand is simpler to apply. Both of these methods are based on the principle of mass conservation. However, some schemes are associated with numerical problems such as numerical dispersion and artificial oscillations. Numerical dispersion results from the approximations used for the differential terms in the governing equations. It manifests itself as an added non-physical spread in the contamination. Artificial oscillations appear as “over-shooting” and “under-shooting” of the concentration at sharp interfaces of the concentration.

For the development of the numerical model that was used to analyze the results obtained from displacement experiments, finite difference method was chosen for its relative simplicity and the fact that it is based on the principle of mass conservation. From a computational point of view other methods could have been used. However, the main purpose of this study is to evaluate the effect of high concentration gradients on hydrodynamic dispersion. For this purpose finite difference method was deemed adequate. The implementation of the finite difference method to the density dependent flow and multi-species transport problem is described in detail below.

The method of finite difference is based on considering the problem domain as a finite set of points on a Cartesian grid and defining input parameters at centers of cells. Each cell is defined by a pair of ordered integers, (i,j), and parameters defined at that point have this pair as subscripts, e.g. $h_{i,j}$ or $C_{i,j}$ for head or concentration at cell (i,j). Derivative terms in the governing partial differential equation may be then expressed as differences of

parameters defined at adjacent cells. If cell dimensions are Δx along x-axis and by Δy along y-axis, numerical solution approaches analytical solution as Δx and Δy approach zero. If there are *m* cells along the x-axis and *n* cells along the y-axis, then differential equations are converted into a set of m by n algebraic equations with m by n unknowns.

When the spatial variations in fluid density are small, mathematical modeling of the groundwater flow is relatively straightforward regardless of the actual density values. However, where spatial variations in fluid density are high, such as in coastal aquifers or in the vicinity of salt formations, investigations of ground-water flow are more complicated because the density variations can substantially affect rates and patterns of fluid flow. The advective-dispersive equation governing the transport of solutes in groundwater where density variations are too high to neglect is (e.g., Schotting et al., 1999):

$$n\frac{\partial \rho}{\partial t}+\nabla(\rho q)=0 \tag{4.1}$$

$$n\frac{\partial \rho\omega}{\partial t}+\nabla(\rho\omega q+J)=0 \tag{4.2}$$

where n is porosity, q is the specific discharge, ρ is fluid density, ω is the mass fraction of salt in groundwater, t is simulation time and J is the dispersive flux of salt.

If a contaminant A is also present, an additional equation representing the transport of the contaminant is needed:

$$n\frac{\partial \rho\omega_A}{\partial t}+\nabla(\rho\omega_A q+J_A)=0 \tag{4.3}$$

where ω_A is the mass fraction of contaminant A in groundwater, and J_A is the dispersive flux of contaminant A.

Hydrodynamic dispersion is classically represented by a Fickian term, analogous to Fick's Law of diffusion, which linearly relates the dispersive flux to the concentration gradient (Bear, 1972; Domenico and Schwartz, 1990):

$$\mathbf{J}=-\rho\mathbf{D}\nabla\omega \tag{4.4}$$

where J is the mass flux vector due to hydrodynamic dispersion, D is the hydrodynamic dispersion tensor, ρ is fluid density and ω is the solute mass fraction. The dispersion tensor is assumed to be a function of velocity, or specific discharge, and medium properties only (Scheidegger, 1960):

$$\mathbf{D}=\left(D_m^*+\alpha_T q\right)\mathbf{I}+\left(\alpha_L-\alpha_T\right)\mathbf{qq}/q \tag{4.5}$$

where D^*_m is the effective molecular diffusion coefficient, α_T and α_L are transversal and longitudinal dispersivities respectively, **q** is specific discharge vector and q is its magnitude, and **I** is the unit tensor. The effective diffusion coefficient is defined as the product of the diffusion coefficient of the solute in water, D_m, and the tortuosity, τ:

$$D_m^*=\tau D_m \tag{4.6}$$

where τ represents the obstructing effect of the porous medium and takes values between zero and one.

Dispersivity is classically defined as a function of the medium properties, independent of the fluid properties (Scheidegger, 1960; Bear, 1979) and determined empirically for any transport problem. In common groundwater contamination problems, mechanical mixing dominates over molecular diffusion. For all analytical and numerical estimations of dispersive transport, in this study, the effective molecular diffusion coefficient is assumed constant and $D^*_m=10^{-9}$.

However, the assumption that the dispersivity is independent of the fluid properties is only valid for low concentrations (Hassanizadeh, 1986b). For high concentration gradient conditions, it may be needed to modify the dispersive flux appearing in Equation 4.4. For brines consisting of water and NaCl, Hassanizadeh and Leijnse (1995) proposed a non linear theory, which is an extension of the linear Fick's Law to cover the cases where large concentration differences exist:

$$(1+\beta J)\mathbf{J}=-\rho\mathbf{D}\cdot\nabla\omega \qquad (4.7)$$

where β is dependency factor on concentration gradient, ρ is fluid and ω is the mass fraction of salt.

Hydrodynamic dispersion acts in order to level down the sharp concentration fronts that exist between the two fluids, resulting in S-shaped breakthrough curves. Parameters, such as dispersivity and high concentration gradient coefficient, that cannot be calculated a-priori starting from known physical quantities, should be determined by fitting model result to observed breakthrough curves.

Under simplifying assumptions, i.e. simple flow domains with steady and spatially uniform flow that is not affected by transport and where dispersion obeys Fick's Law, the system of differential equations governing groundwater flow and transport can be solved analytically. However, for more complex problems, models necessitate more flexibility in the definition of transport processes, i.e. advection, dispersion, retardation, reactions if present etc. And because of the complexity of such a system, a numerical model should be developed. To keep the model simple, non-adsorbing medium and non-reactive solutes will be used in the experiments and subsequently in modeling.

For tracer tests, where concentrations are low enough for avoiding coupling between flow and transport and assuming dispersion is Fickian, an analytical solution (e.g. Ogata-Banks, 1961) can be used in fitting the experimental curves. However, the dispersivities thus obtained cannot be used in modeling the dispersion under high concentration gradients using the same analytical solution, even though the hydrogeological setting is the same, and hence the dispersivity is expected to be the same. For the latter case, a numerical model should be used to make predictions or to find the dispersion parameters (α and β) by fitting the curves obtained from the experiments.

A finite-difference scheme was used for solving the system of differential equations given in Equations 4.1-4.3. A Crank-Nicholson approximation was used for the time derivative, while three options were considered for the space derivative: (i) upstream weighting (ii) central in space weighting and (iii) total variation diminishing (TVD)

scheme. The one-dimensional Crank-Nicholson finite-difference approximations for flow and transport equations are given in equations 4.9 and 4.10.

$$n\frac{\rho_i^n-\rho_i^{n-1}}{\Delta t}-\frac{\rho^n_{i+\frac{1}{2}}K_{i+\frac{1}{2}}\frac{h^n_{i+1}-h^n_i}{\Delta z}-\rho^n_{i-\frac{1}{2}}K_{i-\frac{1}{2}}\frac{h^n_i-h^n_{i-1}}{\Delta z}}{2\Delta z}-\frac{\rho^{n-1}_{i+\frac{1}{2}}K_{i+\frac{1}{2}}\frac{h^{n-1}_{i+1}-h^{n-1}_i}{\Delta z}-\rho^n_{i-\frac{1}{2}}K_{i-\frac{1}{2}}\frac{h^{n-1}_i-h^{n-1}_{i-1}}{\Delta z}}{2\Delta z}=0 \qquad (4.9)$$

$$\frac{C_i^n-C\rho_i^{n-1}}{\Delta t}+\frac{C^n_{i+\frac{1}{2}}q^n_{i+\frac{1}{2}}-C^n_{i-\frac{1}{2}}q^n_{i-\frac{1}{2}}}{2n\Delta z}+\frac{J^n_{i+\frac{1}{2}}-J^n_{i-\frac{1}{2}}}{2n\Delta z}+\frac{C^{n-1}_{i+\frac{1}{2}}q^{n-1}_{i+\frac{1}{2}}-C^{n-1}_{i-\frac{1}{2}}q^{n-1}_{i-\frac{1}{2}}}{2n\Delta z}+\frac{J^{n-1}_{i+\frac{1}{2}}-J^{n-1}_{i-\frac{1}{2}}}{2n\Delta z}=0 \qquad (4.10)$$

Hydrodynamic parameters such as head, flow rate, density, hydraulic conductivity, are defined at the centers of cells. Depending on the selected spatial discretization scheme, the variables at the cell interfaces (denoted by the indices i+1/2 and i-1/2 in the above equations) are calculated from values at the centers of adjacent cells.

In order to solve differential equations, boundary and initial conditions must be specified. There are basically three types of boundary conditions (i) Dirichlet type, where the head or concentration of the boundary cell is specified (not necessarily constant in time or space, but a certain value is imposed at each timestep rather than calculating one from other hydrogeological variables); (ii) Neumann type, where the flux at the boundary cell is specified and (iii) Cauchy type, where both the value and the flux are specified at a boundary cell. Any type of boundary conditions can be included into the developed code (DENSTRAN). The details of boundary and initial conditions will be given for each simulation in the chapters presenting results of experimental and modeling components.

When the groundwater density is variable, the system of differential equations is highly coupled (i.e., the variables are highly dependent on each other). Furthermore, if a modified non-linear version of Fick's law is to be incorporated into these equations, the coupled system of equations will become highly non-linear. In order to solve this coupled non-linear system, an iterative algorithm was adopted and coded using standard Fortran 77 programming language. The code iterates between flow and transport solvers at each timestep while it also iterates within each solver. This algorithm is illustrated in Figure 4.5.

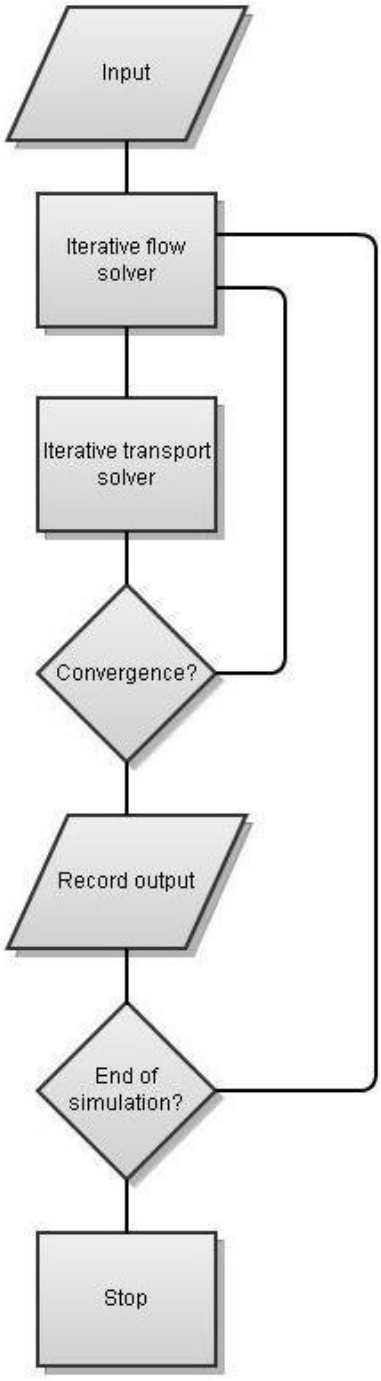

Figure 4.5. Flowchart of the developed code

4.3.2. Modified SEAWAT

SEAWAT-2000 is the latest release of SEAWAT, which is a generic, public domain, open code computer program for simulation of three-dimensional, variable-density, transient ground-water flow in porous media. It was designed by combining a modified version of MODFLOW-2000 -a groundwater flow model- and MT3DMS -a solute transport model- into a single computer program (Langevin et al, 2003). As a result, it combines the reliabilities of these two classic programs and has the advantage of using their standard data formats. Another advantage of SEAWAT is its flexible, modular structure. This structure allows adding more capabilities into SEAWAT by making only minor modifications in the code.

MODFLOW is a constant density groundwater flow program and hence, modifications were done to its code when init was incorporated into SEAWAT, in order to solve for the variable density flow. To keep modifications simple, SEAWAT employs the "equivalent freshwater head" concept. Guo and Langevin (2002) present detailed descriptions of modifications and the equivalent freshwater head concept. The modifications can be summarized as (i) addition of relative density difference terms; (ii) addition of solute mass accumulation terms; (iii) conservation of mass rather than volume; (iv) use of head instead of equivalent freshwater head in conversions between confined and unconfined conditions; (v) addition of variable-density correction terms for unsaturated conditions; and (vi) addition of variable-density correction terms for the water-table case.

The SEAWAT code relies on some basic assumptions, such as (i) Darcy's law is valid (laminar flow); (ii) the standard expression for specific storage in a confined aquifer is applicable; (iii) Fick's Law is valid (Fickian dispersive transport); (iv) heat and temperature distribution is uniform (isothermal conditions); (v) the porous medium is fully saturated with water and (vi) a single, fully miscible liquid phase of very small compressibility fills the pores. None of these assumptions contradicts with the main purpose of this study, which is to investigate the effect of high concentration gradients on hydrodynamic dispersion, except the validity of the Fick's Law.

As a consequence, the dispersion module of SEAWAT code was modified in order to incorporate the non-linear dispersion expression. Unlike the DENSTRAN code that was developed, the modified SEAWAT code employed a constant β value that was calculated a priori, from the specific discharge rate that corresponds to the flow rate applied but disregarding local variations of the specific discharge due to temporal changes in the density distribution. Another difference between the developed DENSTRAN code and the modified SEAWAT code was the explicit scheme used in modified SEAWAT whereas DENSTRAN solved dispersion equation implicitly. However, comparison between simulation results showed that, under the conditions of the simulations intended for this study, and the conditions of the column experiments as well, the differences between the outcomes of the two codes was negligible. Both codes can be readily modified to incorporate other expressions for non-Fickian transport or to implement other numerical schemes.

SEAWAT has several options for the solution scheme, such as Finite Differences (FD), Total Variation Diminishing (TVD) and Method of Characteristics (MOC), as MT3DMS does. The TVD method was chosen in order to avoid artificial oscillations without creating unacceptable numerical dispersion. Although the TVD method is computationally more time consuming, compared to implicit finite-difference method as an example, the short simulation times planned for this study allow for the choice of accuracy over efficiency. The modification of SEAWAT involves the dispersion module only.

5. MODEL VALIDATION

This study involves both experimental and numerical components. The experimental component consists of building a physical model representing a porous medium to investigate dispersive behavior under high concentration gradient conditions whereas the numerical component intends to evaluate mathematical models for describing this behavior. The experimental results will be discussed in detail, in the next three chapters. This chapter explains how the numerical models developed for simulating transport under high concentration gradient conditions were validated.

As previously stated, analytical solutions to differential equations governing contaminant transport exist only for idealized hydrogeological settings. However, these idealized solutions are generally inadequate for simulating real life cases where more processes or complexities have to be incorporated into the model in order to create realistic predictions. Models involving more complexity can be solved numerically. A discussion of the hydrodynamic dispersion theories, and a numerical analysis methodology were presented in the Literature Review Chapter.

There is no commonly approved and available software that simulates dispersive transport under high concentration gradient conditions. Therefore, in order to evaluate possible mathematical models, a complete transport simulator was coded using FORTRAN programming language and, additionally, the SEAWAT code was changed to incorporate the desired dispersion model. Details of numerical modeling efforts were discussed in detail in the Materials and Methods Chapter of this thesis.

A newly developed computational model has to be verified and validated in order to be used for making reliable predictions. Verification ensures that the mathematical model and the algorithms implemented for solving it, are coded free of errors, whereas validation is a measure of how successful a model is in making predictions. It is not possible to fully validate a computational model for all possible settings. The purpose of validating a model is to provide more statistical confidence in its capabilities.

5.1. Verification of the Codes against Analytical Solution

In order to verify and validate the developed DENSTRAN code and the modified SEAWAT code, their results under simplifying assumptions were compared to an analytical solution. One dimensional advective-dispersive transport, where flow is not affected by transport and dispersion obeys Fick's Law, can be modeled using Ogata-Banks (1961) analytical solution assuming steady state flow and non-reactive transport in a homogeneous medium:

$$C(x,t)=\frac{C_0}{2}\left[\operatorname{erfc}\left(\frac{x-vt}{2\sqrt{Dt}}\right)+e^{\left(\frac{vx}{D}\right)}\operatorname{erfc}\left(\frac{x+vt}{2\sqrt{Dt}}\right)\right] \qquad (5.1)$$

where C_0 is the initial concentration at the contamination source, x is distance from the contamination source, v is groundwater velocity, t is simulation time, D is dispersion coefficient, e is the base of the natural logarithm and erfc is the complementary error function. Such a model is broadly accepted to accurately represent experiments in a non-adsorbing medium, using non-reactive solutes having concentrations low enough to avoid coupling between flow and transport.

Although this equation is not intended for simulating density dependent flow with or without alternative dispersion models, it can be used to calculate the "apparent" dispersion coefficient and the "apparent" dispersivity from a breakthrough curve. However, it should be kept in mind that the dispersivities thus obtained cannot be used in modeling the dispersion under high concentration gradients using the same equation, even though the hydrogeological setting is the same, and hence the dispersivity is expected to be the same because the Ogata-Banks analytical solution does not account for high concentration gradient effect. For the latter case, numerical models should be used. On the other hand, under simplifying assumptions used in the analytical solution, all models are expected to produce the same results.

The developed codes were used to simulate transport in a hypothetical column similar to the one described in the Methodology chapter. In analogy to tracer experiments, the column is initially filled with freshwater and then diluted salt solution is injected from the

bottom layer of the column at a constant flow rate, starting at the beginning of the simulation. Unlike the actual column experiments described in the following chapter, the changes in salt concentration can be monitored not only at the outlet of the column which is situated at the upper end but also in all cells at a given time. Hydrogeological parameters used in numerical tracer test simulations are listed in Table 5.1.

Table 5.1. List of tracer test simulations

No	Velocity (m/s)	Resident conc. (g/l)	Displacing conc. (g/l)	Numerical Model	Dispersivity
1	2.12×10^{-3}	0	10^{-3}	DENSTRAN	1.00×10^{-3}
2	2.12×10^{-3}	0	10^{-3}	DENSTRAN	1.00×10^{-2}
3	2.12×10^{-3}	0	10^{-3}	DENSTRAN	5.00×10^{-2}
4	2.12×10^{-3}	0	10^{-3}	SEAWAT	1.00×10^{-3}
5	2.12×10^{-3}	0	10^{-3}	SEAWAT	1.00×10^{-2}
6	2.12×10^{-3}	0	10^{-3}	SEAWAT	5.00×10^{-2}

In all of the simulations using both numerical codes, boundary conditions were set as follows: (i) constant head and constant concentration boundary at the bottom row; (ii) no flow and no mass flux boundaries at the left and right sides of the columns and (iii) constant head and no mass flux boundary for DENSTRAN and no flow and no mass flux boundary for SEAWAT at the top row. The difference in the definition of the upper boundary between the two numerical codes arises from the techniques they utilize for solving the flow equation. The length of the column however was taken to be adequately long such that practically no contamination reaches the column exit over the duration of the simulation, rendering the simulated concentration independent of the imposed boundary conditions at the top end of the domain.

Tracer experiment using a single flow rate, a single salt concentration which is low enough to allow for the Fickian representation of dispersion and to avoid coupling of flow and transport but using a range of dispersivity values were simulated. Figure 5.1 through Figure 5.3 show numerical model results obtained with the three discretization options: central in space, upstream weighting and TVD, respectively. For central in space weighting, the developed DENSTRAN code showed good agreement with the analytical

solution (Ogata-Banks Equation) at relatively higher and medium dispersivities. However, at low dispersivities artificial oscillations were observed, as expected from the central-in-space weighing scheme being used (Ataie-Ashtiani and Hosseini, 2005). The upstream weighing scheme (Figure 5.2) showed no artificial oscillations but in return created numerical dispersion at an unacceptable rate. The TVD scheme (Figure 5.3) produced the best agreement with the analytical solution.

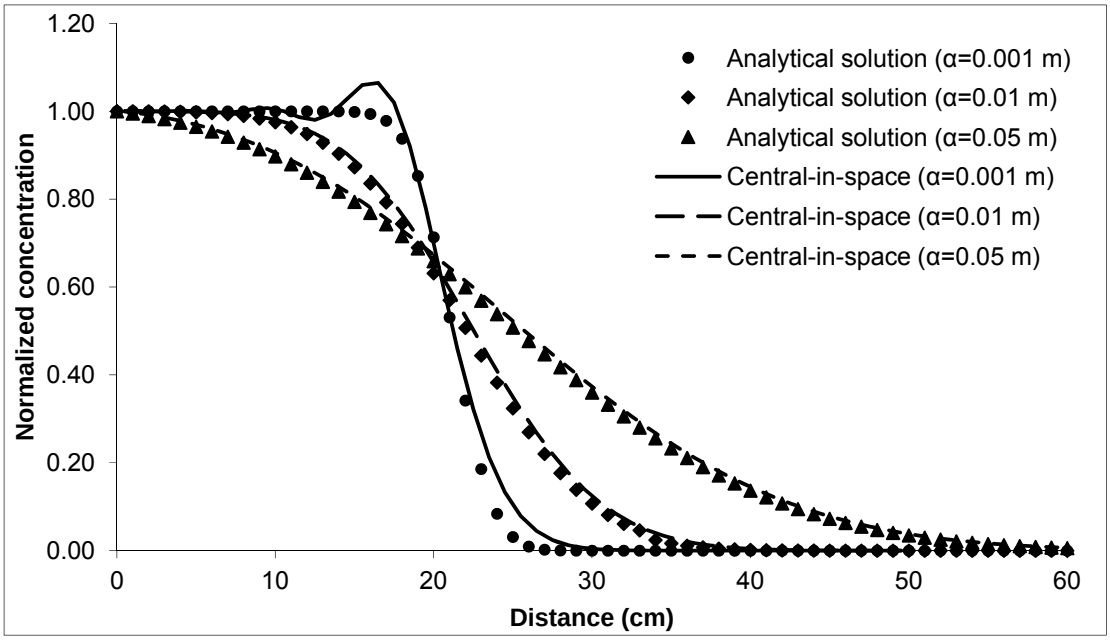

Figure 5.1. Comparison of numerical results of the DENSTRAN code using a central in space weighing scheme to analytical solution

The same procedure was employed to verify SEAWAT code. As a matter of fact, the original SEAWAT code was already verified and validated against a number of benchmark problems including box problems, Henry problem, Elder problem and HYDROCOIN problem (Langevin et al, 2003). However, the source code was modified in order to incorporate non-Fickian dispersion theories and compiled again. In order to test that no error was done in the modification and that no compatibility issues arose from the compilation, verification was deemed necessary.

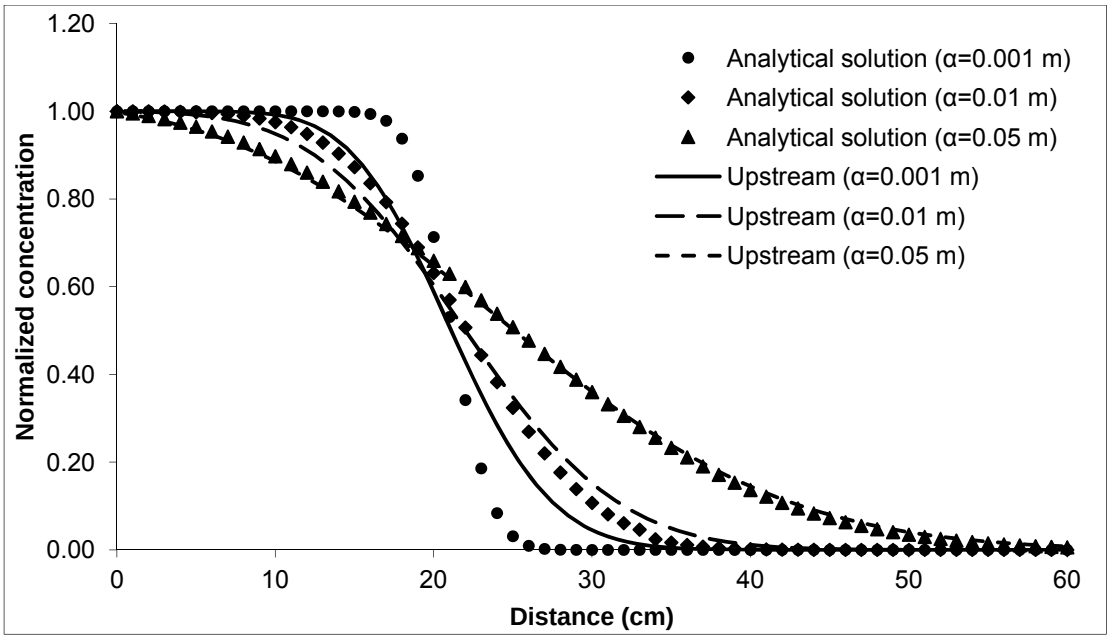

Figure 5.2. Comparison of numerical results of the DENSTRAN code using an upstream weighing scheme to analytical solution

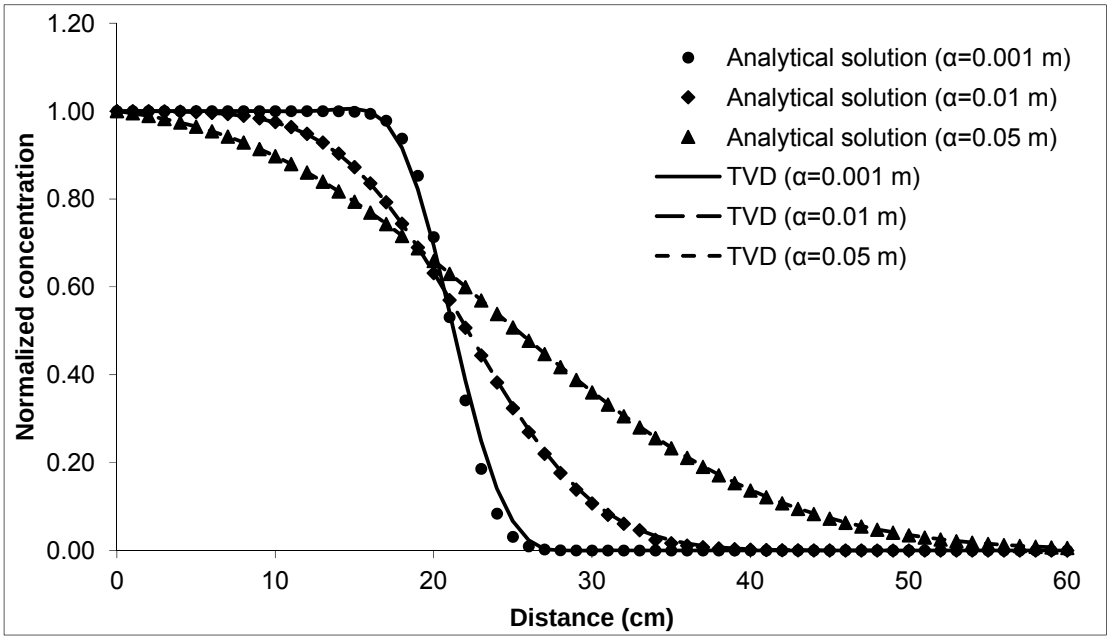

Figure 5.3. Comparison of numerical results of the DENSTRAN code using the TVD scheme to analytical solution

Figure 5.4 compare the results of simulations 4 through 6 with the analytical solution. SEAWAT results show good agreement with both DENSTRAN-TVD results and the analytical solution. The fact that both models produced results similar to analytical solution suggests that they were error free in terms of the implementation of the governing equations.

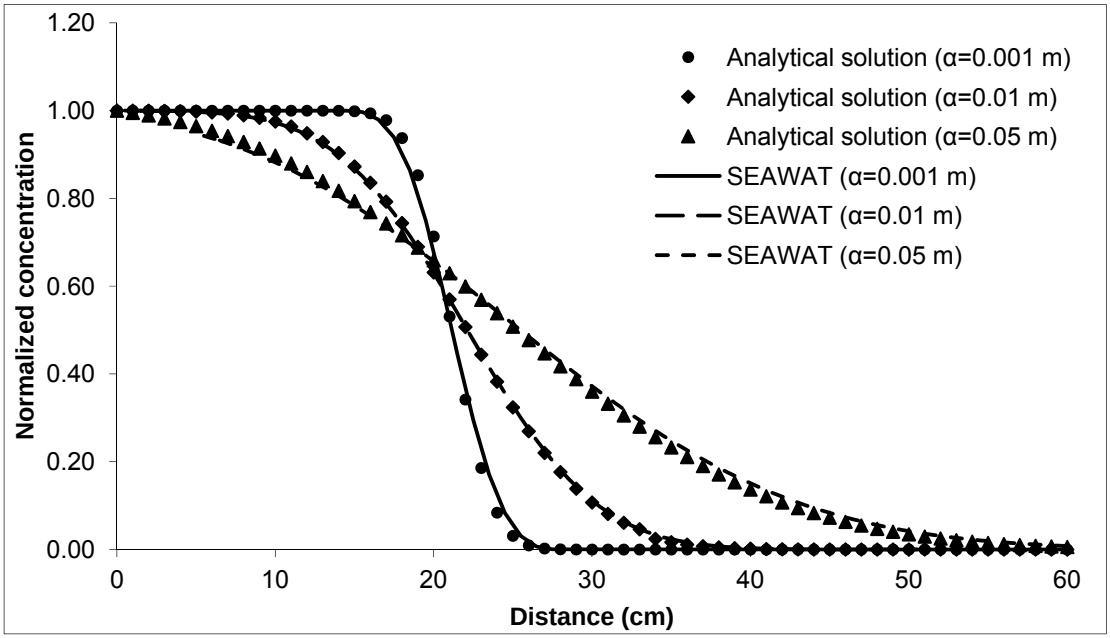

Figure 5.4. Comparison of numerical results from SEAWAT code using the TVD option to analytical solution

The agreement between the two models is important because tracer test simulations are the only step in the validation of the numerical models, where the results can be compared to an analytical solution. With the addition of the coupling between the flow and transport (higher spatial variation in the distribution of concentrations), and the non-Fickian dispersion models, the numerical codes will become too complex to be matched with an analytical solution and the only means for validation will be comparing the two codes to each other. However, some checks can be made such that the contaminant mass in the column is equal to the injected mass. It should be noted that a match between the results of two numerical models does not mean that the two model are working free of any errors. However it adds to the confidence we can place on both models.

Further validation of the models can be made by comparing model results to laboratory or field data. Laboratory tests have the advantage of being controlled and reproducible. Although scaling is still an important problem for the instrumentality of laboratory findings in field applications, results of laboratory experiments can be useful in testing the basic relationships. Comparison of numerical model results with laboratory findings will be presented in following chapters.

5.2. Sensitivity of the Model to Concentration

To quantify the effect of spatial variations in the density distribution and the magnitude of the density differences on the flow and transport, a new set of simulations were done using both numerical models. A list of hydrogeological parameters used in these simulations is given in Table 5.2. All simulations had the same set of flow and transport parameters, such as the average linear velocity and the dispersivity, except displacing fluid concentrations and dispersion models.

Table 5.2. List of variable density flow simulations

No	Linear velocity (m/s)	Resident conc. (M)	Displacing conc. (M)	Dispersion Model	Dispersivity (m)
7	1.28×10^{-4}	0	10^{-3}	Fickian	1.00×10^{-2}
8	1.28×10^{-4}	0	1	Fickian	1.00×10^{-2}
9	1.28×10^{-4}	0	2	Fickian	1.00×10^{-2}
10	1.28×10^{-4}	0	10^{-3}	Non-Fickian	1.00×10^{-2}
11	1.28×10^{-4}	0	1	Non-Fickian	1.00×10^{-2}
12	1.28×10^{-4}	0	2	Non-Fickian	1.00×10^{-2}

Figure 5.5 shows numerical simulation results obtained from simulations 7 through 9. At the conditions of the simulations, the effect of spatial concentration variations is negligible. In other words, brine experiment simulations produce the same results as the tracer experiment simulations when variable density flow is accounted for but a Fickian dispersion model is used. The concentrations used in simulations cover a very wide range from very low (0.01 g/l) to three times as high as seawater (100 g/l), therefore, the

similarity of the breakthrough curves can not be explained by the insignificance of density differences between simulations.

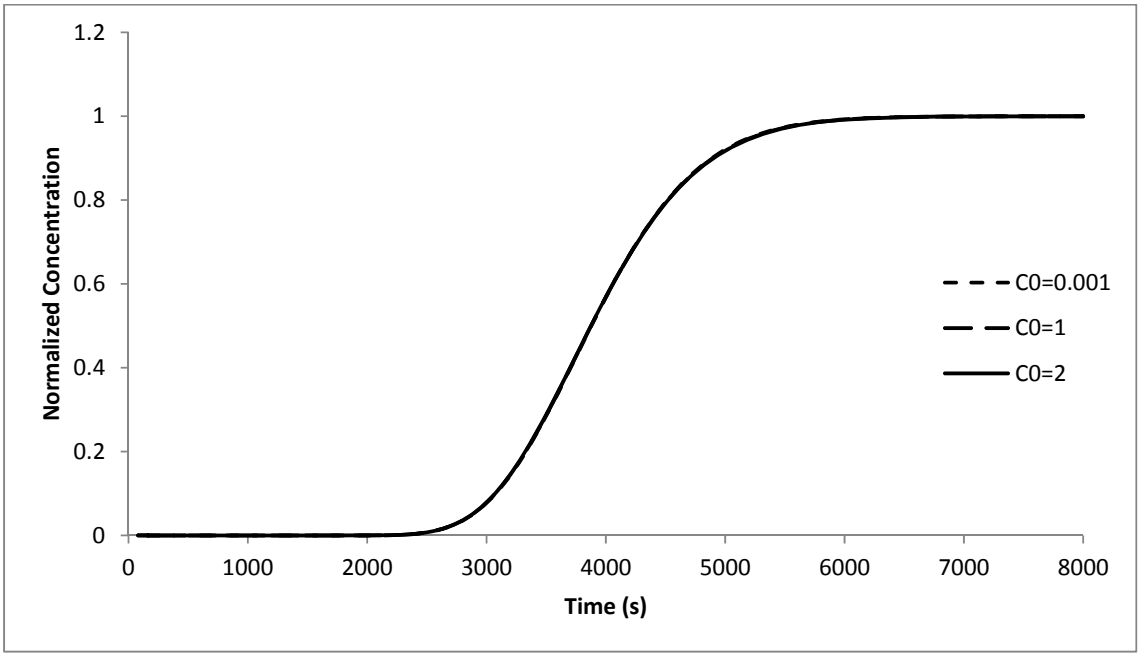

Figure 5.5. Comparison of numerical results of variable density flow and Fickian dispersion model with different displacing fluid concentrations

Figure 5.6 shows numerical simulation results obtained from simulations 10 through 12. Although there is evidence of an effect of density difference on dispersion, the effect appears to be small. The reason for the effect to be small is the one dimensional nature of the problem with the heavier displacing fluid being underneath the lighter resident fluid. Density effects are generally most pronounced in two- or three-dimensional problems such as the Henry problem and the salt water intrusion problem where gravity is the primary factor influencing the flow field. However it should be noted that, velocities used in these simulations were outside the range of velocities defined for the high concentration gradient coefficient relationship proposed by Schotting et al (1999).

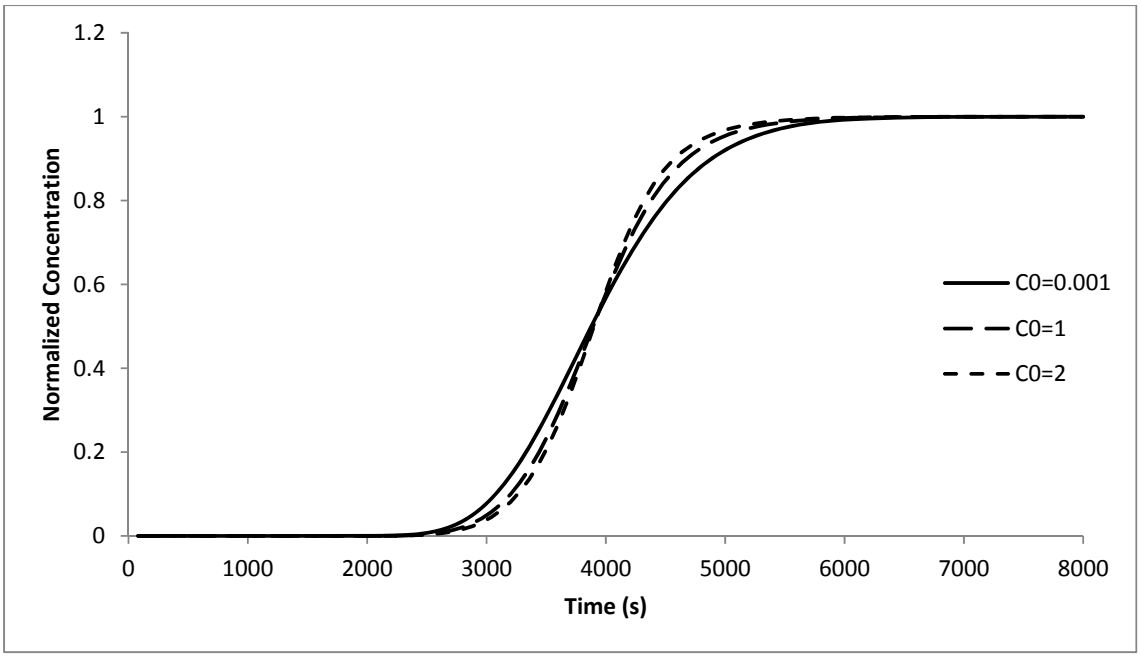

Figure 5.6. Comparison of numerical results of variable density flow and non-Fickian dispersion model with different displacing fluid concentrations

Preliminary analysis showed that the non-Fickian model predicts reduced dispersion as suggested by the experimental evidence. More discussion on the adaptability of the non-Fickian dispersion model and the supplied relationship between the coefficient of high concentration gradient effect, β, and specific discharge, q, on actual observations of hydrodynamic dispersion under high concentration gradient conditions will be provided in experimental sections that will follow.

6. TRACER EXPERIMENTS

6.1. Displacement Experiments

The common method for investigating the effect of high concentration gradients on dispersion is to conduct stable upward displacement experiments as described in the Literature Review Chapter. A displacement experiment consists of introducing some dense liquid (displacing fluid) into a laboratory column, representative of actual porous media, whose pore volume is initially filled with some less dense liquid (resident fluid). As explained in detail in the Materials and Methods Chapter, the denser fluid is introduced from the bottom of the column to achieve a stable upward flow configuration.

Both the displacing and resident fluids, used in the study were aqueous solutions of alkali halides or distilled water. This choice of material was justified by the facts that these compounds have very low reactivities; very low tendencies to absorb on the porous media, the column and the tubing material; and very high solubilities in water. They are also non-toxic, non-volatile and easy to detect by simple experimental techniques. Moreover, these compounds are the main components of groundwater in the vicinity of salt domes, consideration of which for waste repository contributed significantly to the interest on the transport of contaminants under high concentration gradients.

Experiments conducted during the course of the study can be classified in one of the following categories: (i) tracer experiments, where the concentration difference between the resident and displacing fluids is low and both solutions have low absolute concentrations; (ii) brine transport experiments (or brine experiments), where a low concentration resident fluid is displaced by a solution of a single solute with high concentration; (iii) contaminant mixture transport experiments (or mixture experiments), where a low concentration resident fluid is displaced by a solution containing two different solutes with one having a high concentration (brine range) and the second having a lower concentration (tracer range). Each group of experiments will be discussed in detail in the following sections, under the appropriate heading.

The first set of laboratory experiments is the tracer experiments that were conducted to determine the dispersivity of the column and to verify the operation of the experimental setup. Tracer tests are expected to obey both Darcy's Law and Fick's Law they allow for comparison with numerous published data as well as simple analytical solutions of the governing differential equations.

The first step in conducting displacement experiments is the preparation of the sand column. The properties of the materials and the details of the procedure used in the preparation of the column were described in the Materials and Methods Chapter. Once it is totally packed with sand or glass beads and sealed for leak tightness, the column was placed on a metal support that keeps it in an upright position and was connected to the peristaltic pump to start the introduction of freshwater. A very low flow rate is chosen to avoid forming of dry pockets that will interfere with the saturation of the column that will later affect the flow.

During the saturation, water from the outlet of the column was recycled into a reservoir and the change in the volume of water was determined. No water was lost due to evaporation because the reservoir was kept closed to the atmosphere at all times. The amount of water retained in the tubing and column lids is negligible and temperature remained constant. Under these conditions, the total pore volume and porosity of the column can be calculated from the change in the volume of water in the reservoir before and after the saturation. The porosity of the sand was found as n=0.38. The porosity for glass beads is also calculated the same way and found to be about n=0.33. The porosity calculated from the amount of water used in filling the pore space for each material was in accordance with the value calculated from the size and geometry data in the Materials and Methods Chapter. The average "apparent" porosity - calculated from curve fitting in tracer experiments - for the sand filled column was approximately 0.42 whereas the average apparent porosity of the glass bead filled column was 0.33. The difference between the apparent and calculated porosities of the sand filled column was attributed to retardation.

The saturated column is kept on its support in a vertical position in the course of all experiments conducted for this study. Although the column was leak tight, when it was kept for long periods between experiments in an upright position, it lost some of the water

through backflow and evaporation. To replace this lost amount and ensure saturation and uniform flow, the column was saturated with the selected resident fluid, until a steady flow at the desired rate was observed, before each experiment.

A tracer experiment starts when the inflow reservoir is changed from resident fluid to the displacing fluid after the complete saturation of the column is observed and a steady flow at the rate chosen for the experiment is reached. However, the monitoring of the effluent concentration does not start when injection of the displacing fluid starts because the contamination needs some time to reach the outlet, depending on the flow rate. It should be noted that, the arrival time to the outlet cannot be calculated from the groundwater velocity and the length of the column because the actual velocities of water and dissolved species are not identical according to Fick's Law. As a result, some contamination would come earlier than the bulk of the contamination whereas some would be delayed, referred to as tailing of the breakthrough curve.

A list of tracer experiments conducted and their experimental parameters are given in Table 6.1. For each experiment, the time dependent concentration values were normalized with the readings obtained from the stock solutions of resident and displacing fluids. Normalizing permits comparison of experimental results to each other by eliminating the effects of the measurement technique and the initial concentration.

First six experiments are conducted using sand as packing material. In experiments 9 through 13, glass beads were used for packing. Average linear velocities corresponding to selected values of pumping rates fall mostly in the range of natural values. Although much higher than typical values, 25 ml/min was included to match the values reported in the literature. However, at that flow rate, corresponding to an average linear velocity of 6.396×10^{-4}, an irregular shape of the breakthrough curve was observed and it was decided that flow was not constant throughout the experiment and the results were discarded.

Table 6.1. List of tracer experiments

No	Flow rate (ml/min)	Linear velocity (m/s)	Resident fluid	Displacing fluid	Packing material	Concentration monitoring
1	0.5	1.21×10^{-5}	Distilled water	10^{-3} M aq. NaCl	Sand	Sampling + A. A. S.*
2	1	2.42×10^{-5}	Distilled water	10^{-3} M aq. NaCl	Sand	Sampling + A. A. S.
3	2	4.85×10^{-5}	Distilled water	10^{-3} M aq. NaCl	Sand	Sampling + A. A. S.
4	5	1.21×10^{-4}	Distilled water	10^{-3} M aq. NaCl	Sand	Sampling + A. A. S.
5	10	2.42×10^{-4}	Distilled water	10^{-3} M aq. NaCl	Sand	Sampling + A. A. S.
6	25	6.06×10^{-4}	Distilled water	10^{-3} M aq. NaCl	Sand	Sampling + A. A. S.
9	1	2.42×10^{-5}	Distilled water	10^{-2} M aq. NaCl	Glass beads	Sampling + conductivity
10	2	4.85×10^{-5}	Distilled water	10^{-2} M aq. NaCl	Glass beads	Sampling + conductivity
11	5	1.21×10^{-4}	Distilled water	10^{-2} M aq. NaCl	Glass beads	Sampling + conductivity
12	10	2.42×10^{-4}	Distilled water	10^{-2} M aq. NaCl	Glass beads	Sampling + conductivity
13	25	6.06×10^{-4}	Distilled water	10^{-2} M aq. NaCl	Glass beads	Sampling + conductivity

* Atomic absorption spectrophotometry

6.2. Tracer Experiments in Sand Filled Column

The experimental breakthrough curves are fitted with Ogata-Banks analytical solutions to determine apparent dispersivities, using a least squares method that minimizes the sum of differences squared between the simulated and observed concentrations. Ogata-Banks solution is a one-dimensional, non-reactive, Fickian solution to the differential equations governing the groundwater transport that assumes homogeneous porous medium and a steady uniform flow field independent of the concentration distribution. Figure 6.1 through Figure 6.6 show that experimental curves can be successfully fitted using the analytical solution and hence the experimental setup is appropriate for the purpose. However, the classical hydrodynamic theory suggests that the dispersive flux is linearly related to the concentration gradient through a hydrodynamic dispersion coefficient which is in turn a linear function of the groundwater velocity and an empirical dispersivity factor which is representative of the medium properties only, as suggested by the equations $J = D\nabla C$ and $D = D_m^* + \alpha v$.

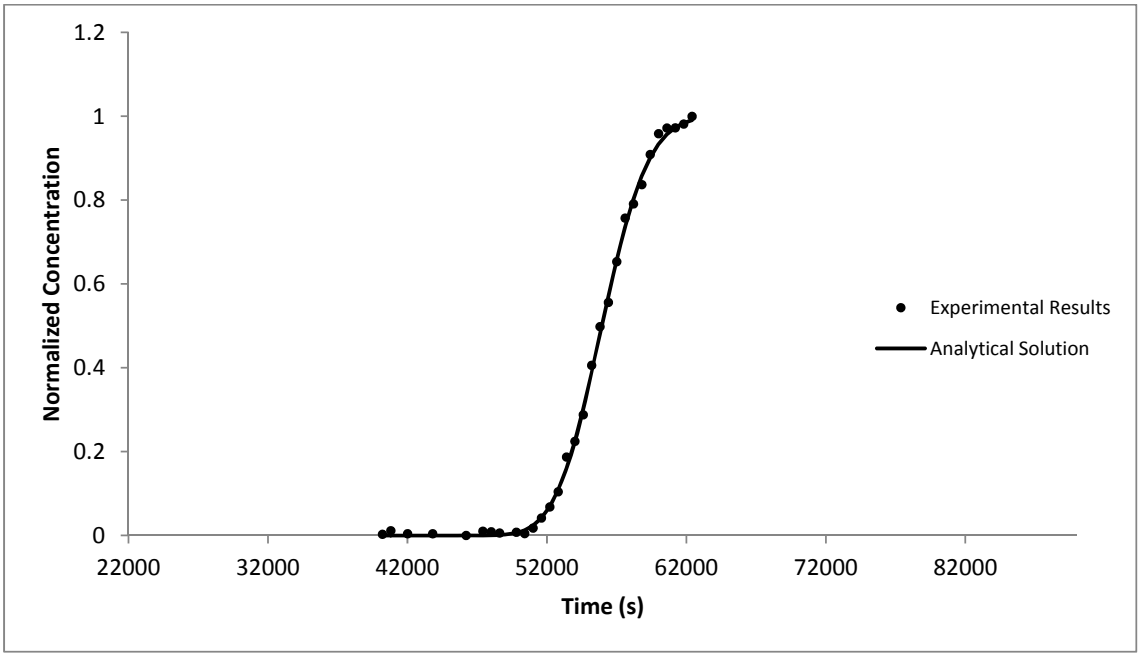

Figure 6.1. Comparison of the breakthrough curve from the sand tracer Experiment 1 with the analytical solution (Q=0.5 ml/min)

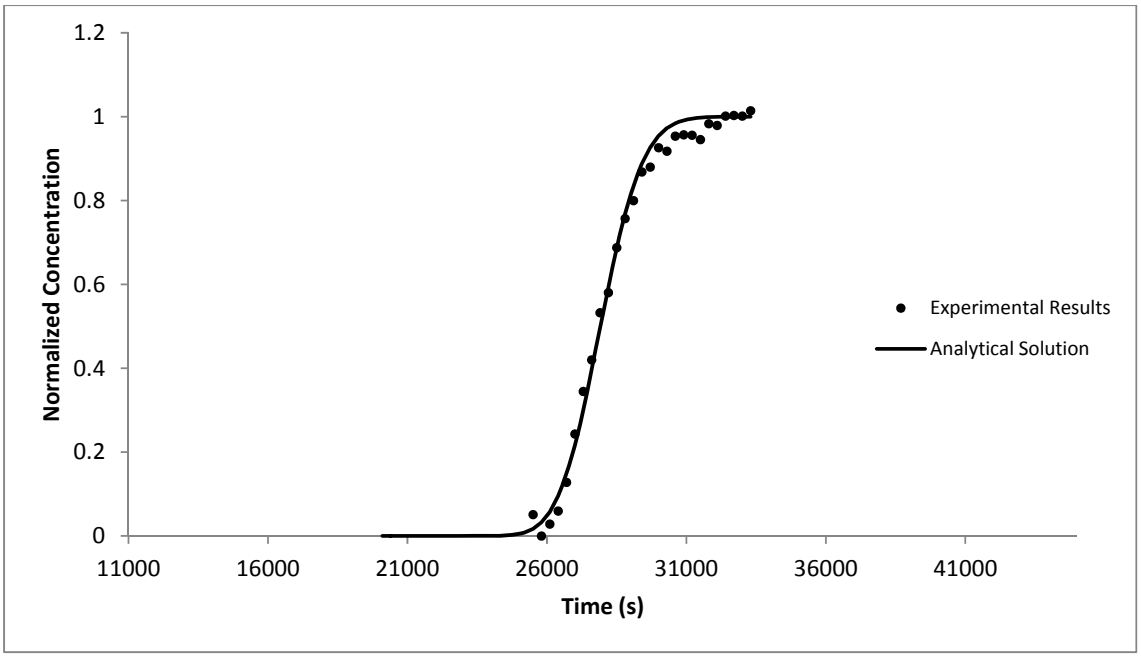

Figure 6.2. Comparison of the breakthrough curve from the sand tracer Experiment 2 with the analytical solution (Q=1 ml/min)

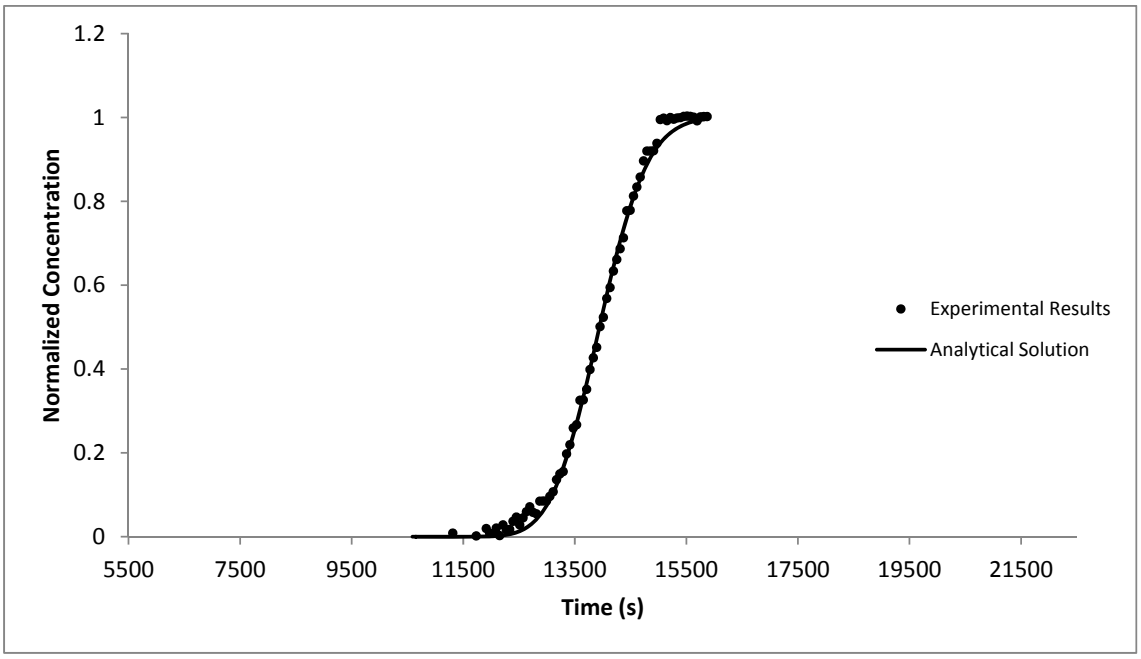

Figure 6.3. Comparison of the breakthrough curve from the sand tracer Experiment 3 with the analytical solution (Q=2 ml/min)

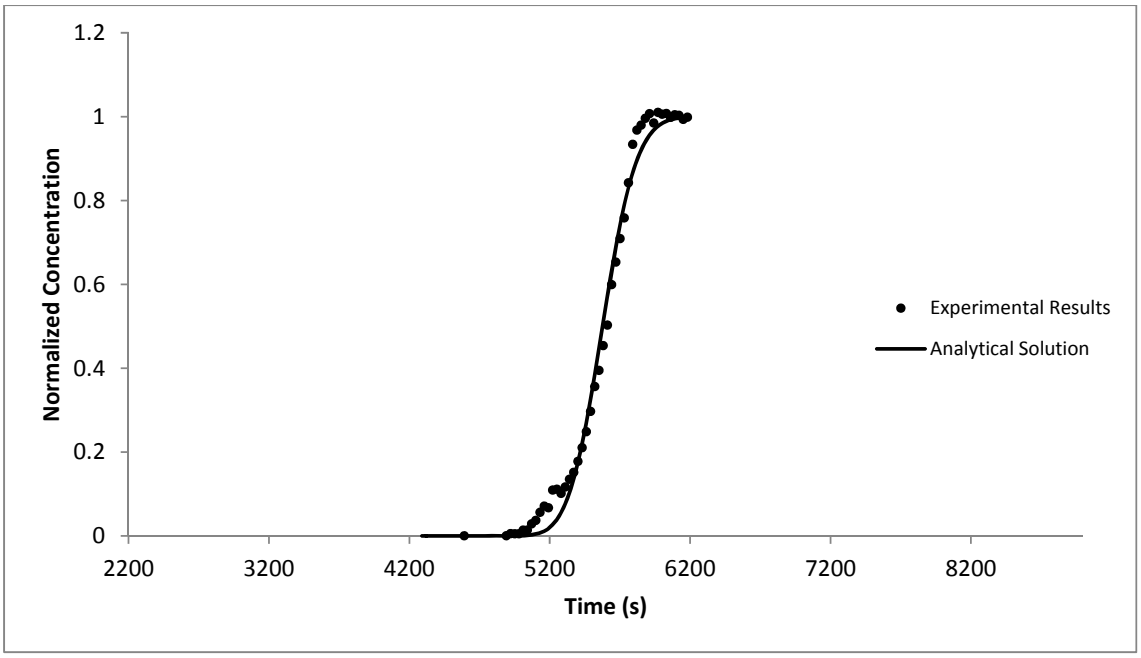

Figure 6.4. Comparison of the breakthrough curve from the sand tracer Experiment 4 with the analytical solution (Q=5 ml/min)

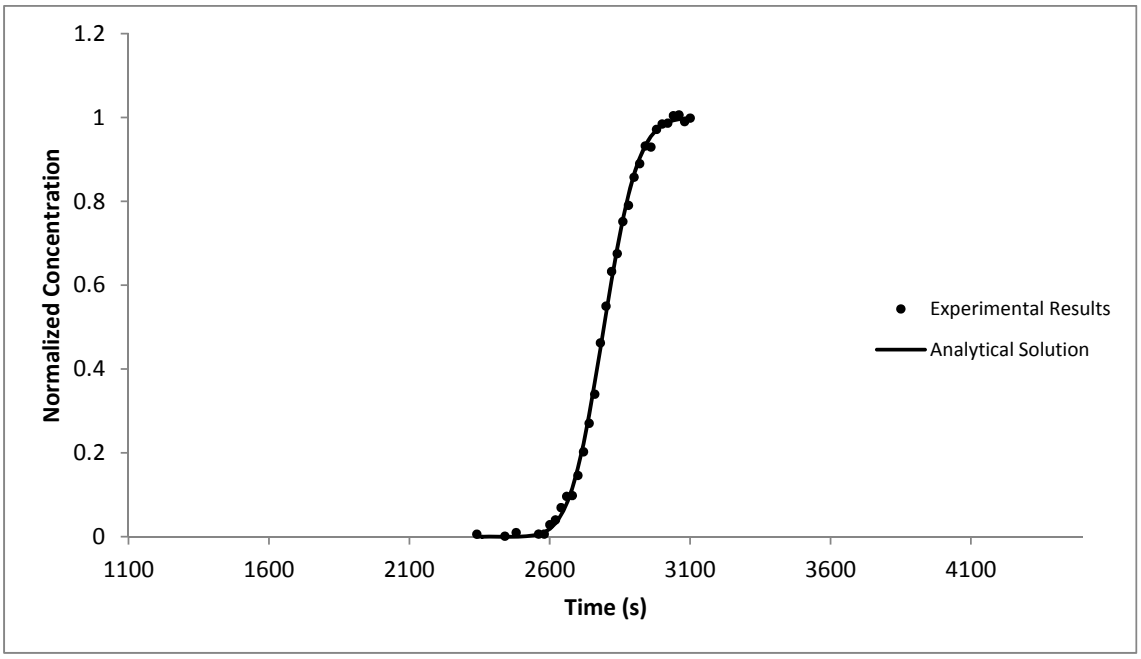

Figure 6.5. Comparison of the breakthrough curve from the sand tracer Experiment 5 with the analytical solution (Q=10 ml/min)

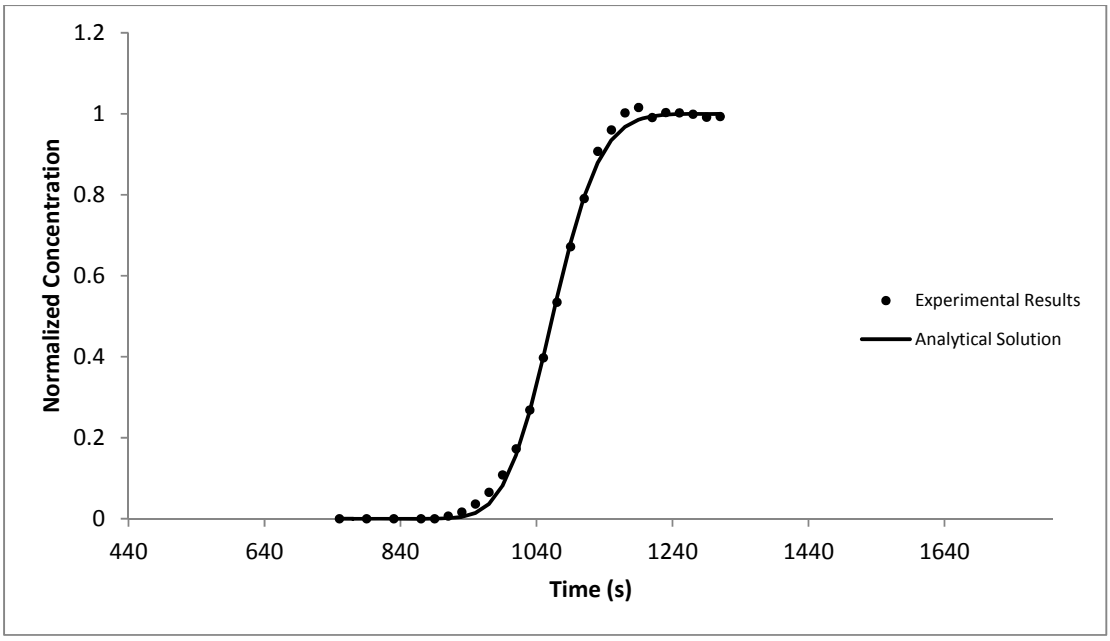

Figure 6.6. Comparison of the breakthrough curve from the sand tracer Experiment 6 with the analytical solution (Q=25 ml/min)

Thus apparent dispersivities are expected to be the same for all experiments, disregarding the diversity in flow rates or concentrations of resident and displacing fluids. If Fick's Law is valid for all transport problems, the dispersivity values obtained from the tracer experiment sets should also be useful for fitting analytical solutions to breakthrough curves obtained from displacement experiments with high concentration gradients, or brine experiments.

Figure 6.7 shows dispersivities obtained from tracer experiments in sand packing on a scatter plot versus average linear velocities. Figure 6.7 suggests that the dispersivities show a slight dependence on the velocity. The spread observed in the dispersivity estimates is similar to that reported in previous studies (e.g., Pfannkuch, 1963; Schotting et al., 1999). Bear (1972) also suggests that the dispersion coefficient can be expressed as a function of Pe^m where $1<m<1.2$, suggesting that the dispersivity is slightly dependent on velocity. However in most practical applications, dispersivity is taken to be independent of the velocity.

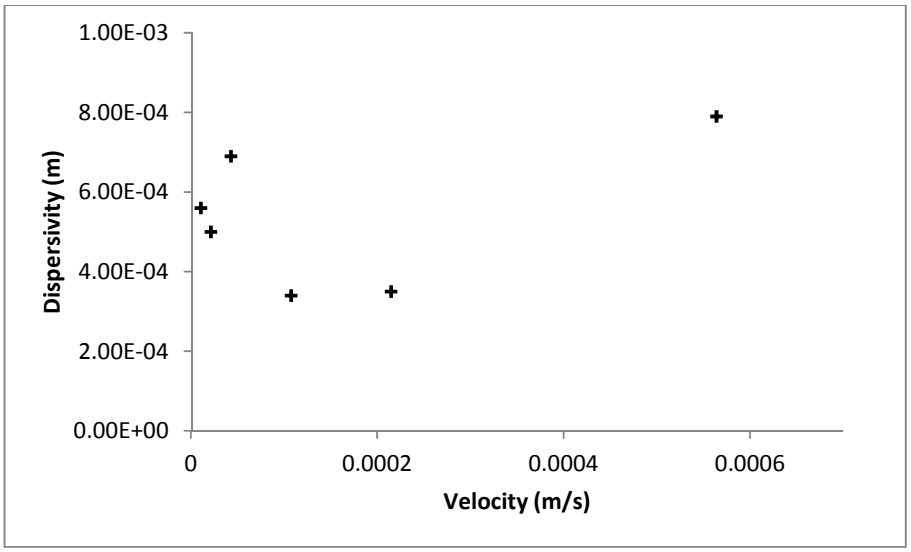

Figure 6.7. Scatter plot of apparent dispersivities vs average linear velocities from sand tracer experiments ($C_{displacing}=10^{-3}$ M)

Figure 6.8 presents dispersion coefficients used in fitting analytical solutions to breakthrough curves obtained in tracer experiments with sand packing as a function of average linear velocities. Dispersion coefficients show an increasing trend with increase in velocity. This observation is in agreement with statement made about dispersivities. Figure 6.9 compares results of the sand tracer experiments to values from the literature (Mannhardt and Nasreldin, 1994). Although the sand falls into fine sand classification according to particle size, the D/D_m vs P_e plot matches with coarse sand plot from Mannhardt and Nasreldin (1994) due to differences in experimental procedure and interpretation methods; such as column dimensions, uniformity of particle size, curve fitting procedure etc. However, the slopes match acceptably suggesting that the experimental procedure can reproduce previous results.

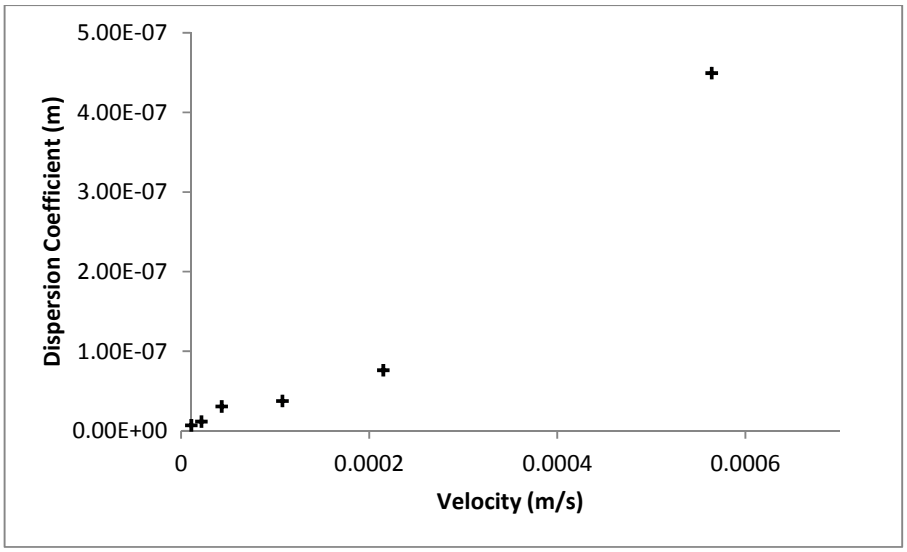

Figure 6.8. Scatter plot of dispersion coefficients vs average linear velocities from sand tracer experiments ($C_{displacing}=10^{-3}$ M)

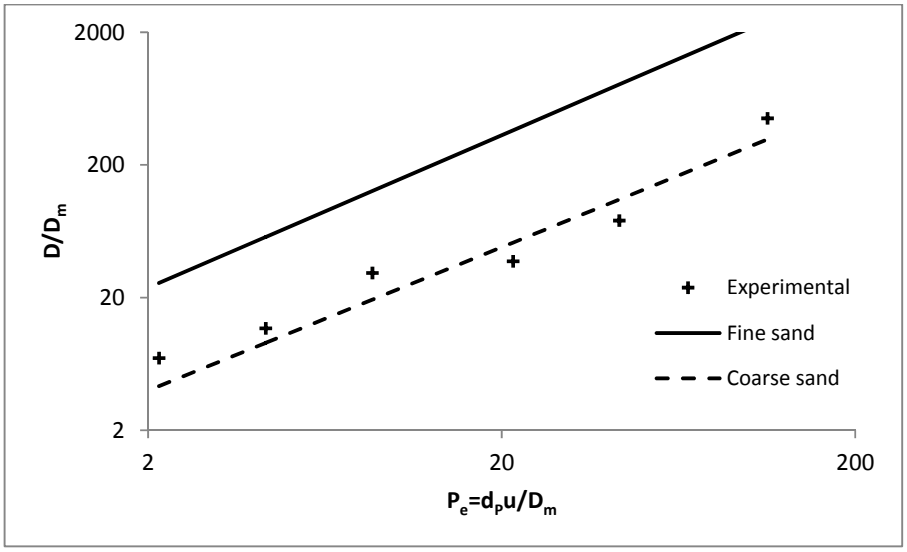

Figure 6.9. Comparison of normalized results from sand tracer experiments with data from literature (Mannhardt and Nasreldin, 1994)

6.3. Tracer Experiments in Glass Bead Filled Column

To further investigate the validity of Fick's Law under low concentration conditions, a second set of tracer experiments was designed with a different packing material and a slightly higher concentration difference ($C_{displacing}$=0.01 M instead of 0.001 M). Except the increased displacing concentration, the experimental procedure was exactly the same. However, since the packing material was changed, dispersivity of the medium was not expected to be the same as the sand tracer set. On the other hand, the result are expected to be consistent with Fickian Theory since the density difference between the resident and the displacing fluids is not high enough to cause deviation from Fickian behavior.

The glass bead tracer set includes experiments 9 to 13 in Table 6.1. Figure 6.10 through Figure 6.14 present breakthrough curves obtained in this set of experiments along with their best fitting analytical solutions.

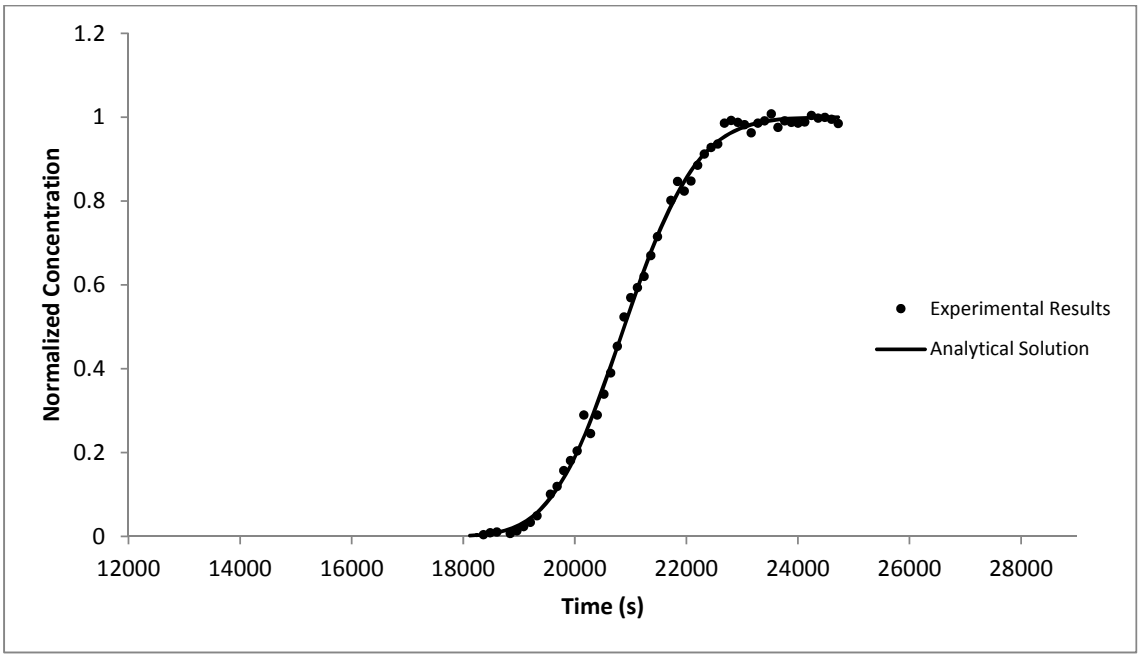

Figure 6.10. Comparison of the breakthrough curve from the glass bead tracer Experiment 9 with the analytical solution (Q=1 ml/min)

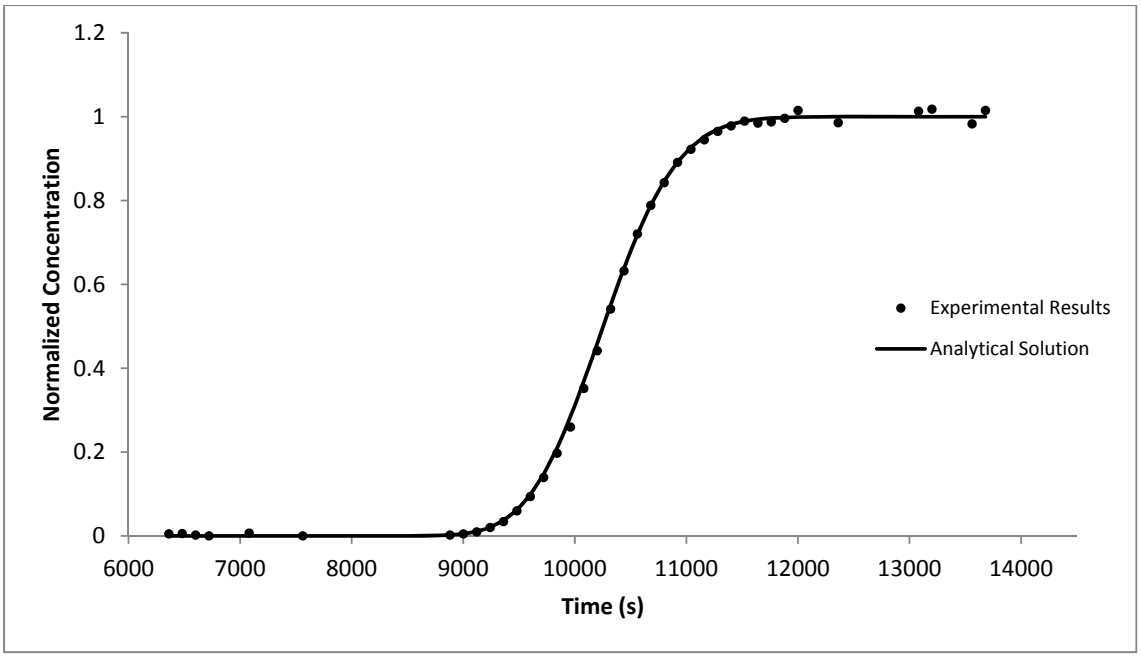

Figure 6.11. Comparison of the breakthrough curve from the glass bead tracer Experiment 10 with the analytical solution (Q=2 ml/min)

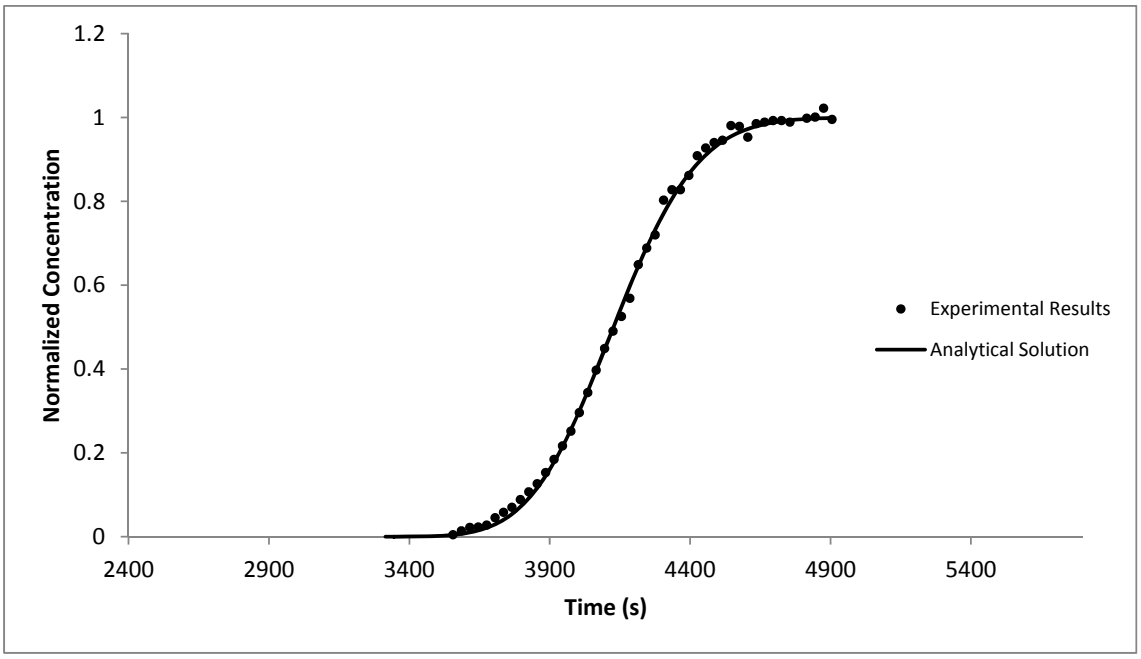

Figure 6.12. Comparison of the breakthrough curve from the glass bead tracer Experiment 11 with the analytical solution (Q=5 ml/min)

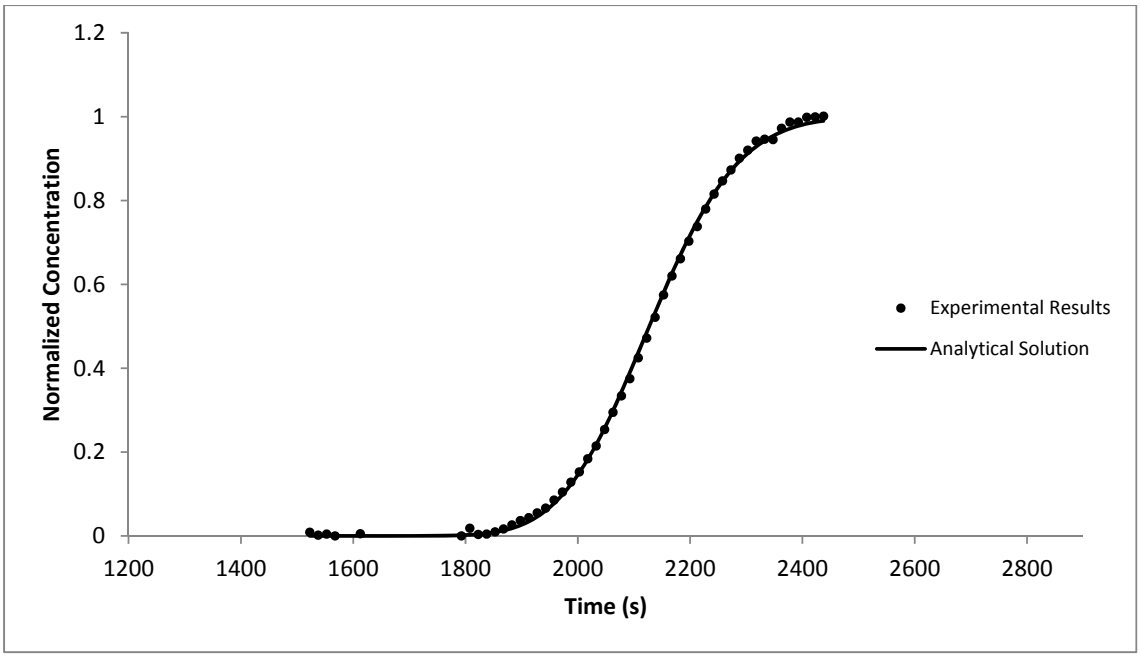

Figure 6.13. Comparison of the breakthrough curve from the glass bead tracer Experiment 12 with the analytical solution (Q=10 ml/min)

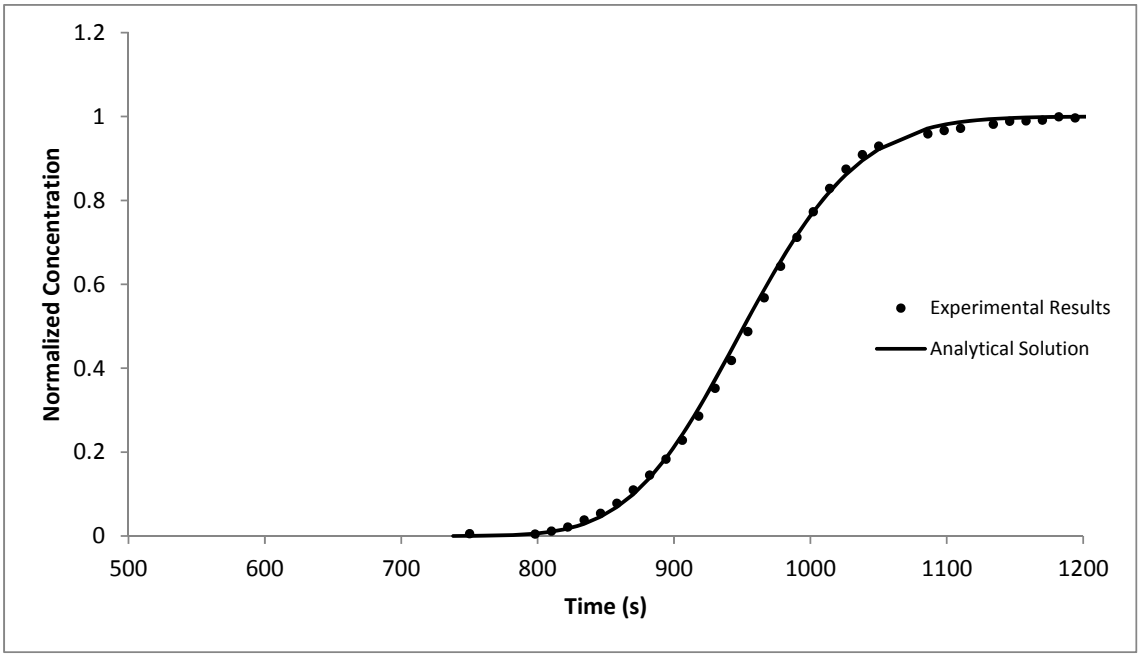

Figure 6.14. Comparison of the breakthrough curve from the glass bead tracer Experiment 13 with the analytical solution (Q=25 ml/min)

The best-fit dispersivities obtained from fitting analytical solutions to breakthrough curves obtained from tracer experiments with glass bead packing are shown in Figure 6.15. Figure 6.16 presents the best fit dispersion coefficient values obtained from fitting analytical solutions to breakthrough curves obtained in tracer experiments with glass beads packing. As with the sand packing set (experiments 1-8), dispersion coefficients show an increasing trend with increase in velocity. This observation, further justifies Fick's Law under the experimental conditions of tracer experiments. Figure 6.17 compares results of the sand tracer experiments to values from the literature (Mannhardt and Nasreldin, 1994). In accordance with size classification of the packing material, the D/D_m vs P_e plot falls below coarse sand plot from Mannhardt and Nasreldin (1994) and matches its slope.

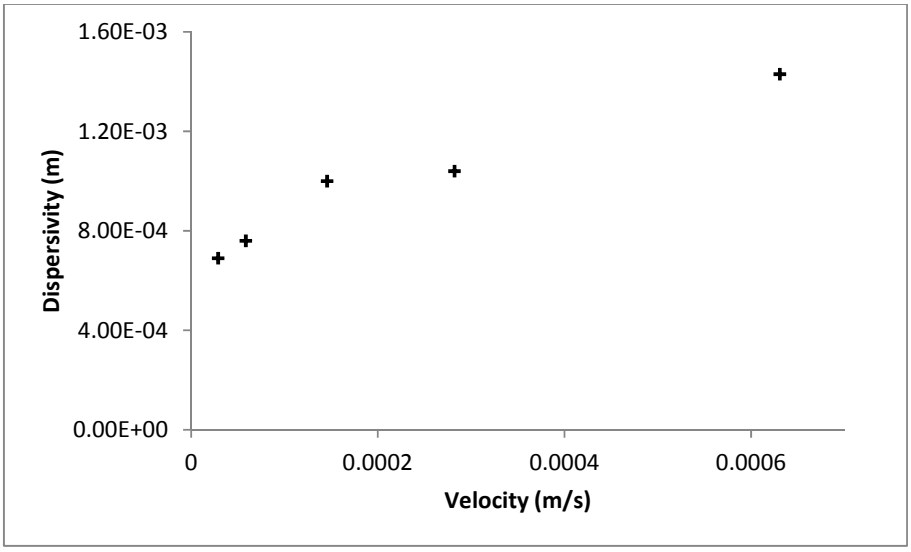

Figure 6.15. Best-fit dispersivities vs average linear velocities obtained from tracer experiments with glass bead packing

Comparing Figure 6.9 with Figure 6.17, it can be seen that better fit was obtained in glass bead experiments. This observation was attributed to the differences in displacing solution concentrations, particle geometry and measurement techniques between the two set. Higher concentrations used in glass bead set resulted in relatively less interference from sorption of solutes on particles. Relatively higher uniformity of shapes and sizes of glass beads provided a more uniform velocity distribution. Use of ex-situ electrical

conductivity meter instead of in-situ ion selective electrodes resulted in increased accuracy of concentration determination.

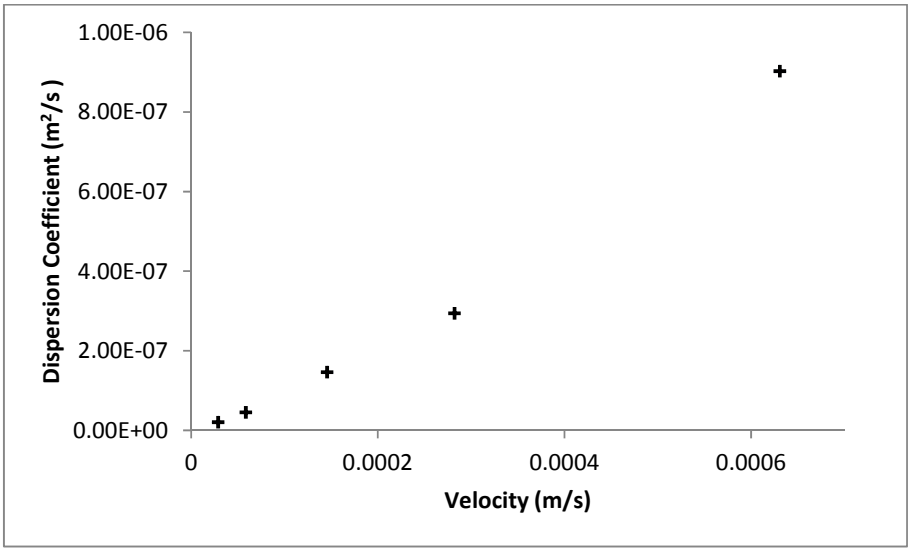

Figure 6.16. Best-fit dispersion coefficients vs average linear velocities obtained from tracer experiments with glass bead packing

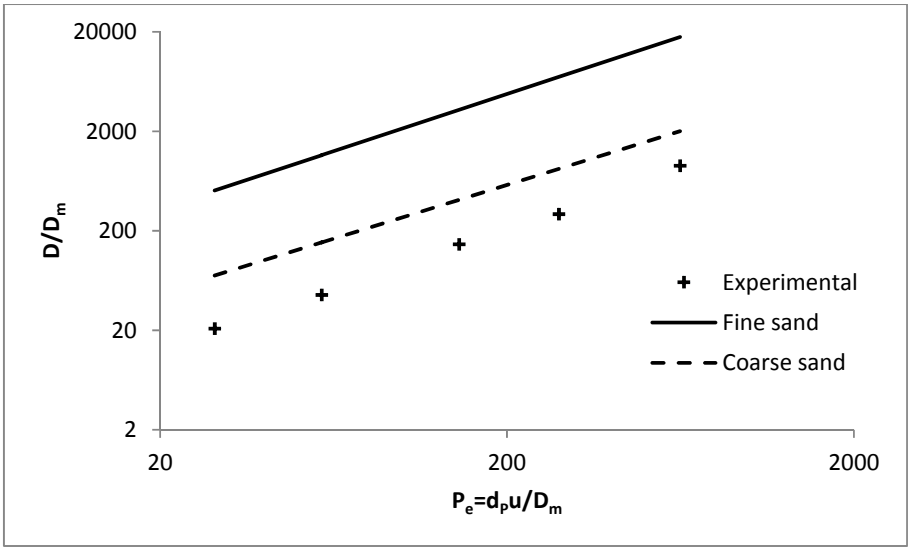

Figure 6.17. Comparison of normalized results from glass bead tracer experiments with data from literature (Mannhardt and Nasreldin, 1994)

7. BRINE EXPERIMENTS

The second part of the experimental component, involves experiments designed for testing the validity of Fick's Law under high concentration gradient conditions, namely brine experiments. Published literature suggests that brine displacement obeys Darcy's Law but not the Fick's Law. However, no commonly accepted model was proposed for defining dispersive transport under high concentration gradient. It is also reported that the dispersive flux for high-concentration gradients conditions may also be dependent on the velocity (Hassanizadeh and Leijnse, 1995; Schotting et al., 1999). A summary of dispersion theories along with modeling efforts is provided in the Literature Review Chapter.

Brine experiments consist of two sets; one with a single flow rate but different displacing fluid densities, and another with different flow rates but a single concentration difference. The same experimental setup as in the tracer experiments was used for brine experiments. Before every experiment, the column was soaked with resident fluid at a very low pumping rate until complete saturation is reached. When it is deemed that the column is fully saturated and the flow is steady at the rate of the experiment in question, the inflow reservoir is changed from freshwater to brine at the desired concentration.

Table 7.1 lists the parameters used in the brine displacement experiments. Experiments 14 through 17 have the same flow rate but a different displacing fluid concentration was used in each. The aim of this set of experiments is to reveal the dependence of the dispersive behavior on density differences while the hydrogeological parameters and flow conditions are kept the same. In experiments 18 through 27 flow rates over a large range were used whereas the concentration difference was kept the same. The purpose of this set was to investigate the effect of groundwater velocity on the dispersive transport under high concentration gradient conditions.

Table 7.1. List of brine experiments

No	Flow rate (ml/min)	Linear velocity (m/s)	Resident fluid	Displacing fluid	Packing material	Concentration monitoring
14	5	1.21×10^{-4}	Distilled water	10-3 M aq. NaCl	Sand	Sampling + A. A. S.
15	5	1.21×10^{-4}	Distilled water	10-2 M aq. NaCl	Sand	Sampling + A. A. S.
16	5	1.21×10^{-4}	10-4 M aq. NaCl	10-1 M aq. NaCl	Sand	Flow-through ISE*
17	5	1.21×10^{-4}	10-4 M aq. NaCl	1 M aq. NaCl	Sand	Flow-through ISE
18	0.5	1.21×10^{-5}	10-4 M aq. NaCl	1 M aq. NaCl	Sand	Flow-through ISE
19	1	2.42×10^{-5}	10-4 M aq. NaCl	1 M aq. NaCl	Sand	Flow-through ISE
20	3	7.27×10^{-5}	10-4 M aq. NaCl	1 M aq. NaCl	Sand	Flow-through ISE
21	4	9.70×10^{-5}	10-4 M aq. NaCl	1 M aq. NaCl	Sand	Flow-through ISE
22	5	1.21×10^{-4}	10-4 M aq. NaCl	1 M aq. NaCl	Sand	Flow-through ISE
23	6	1.45×10^{-4}	10-4 M aq. NaCl	1 M aq. NaCl	Sand	Flow-through ISE
24	7	1.70×10^{-4}	10-4 M aq. NaCl	1 M aq. NaCl	Sand	Flow-through ISE
25	10	2.42×10^{-4}	10-4 M aq. NaCl	1 M aq. NaCl	Sand	Flow-through ISE
26	15	3.64×10^{-4}	10-4 M aq. NaCl	1 M aq. NaCl	Sand	Flow-through ISE
27	25	6.06×10^{-4}	10-4 M aq. NaCl	1 M aq. NaCl	Sand	Flow-through ISE

* Ion selective electrode

The packing of the column was not changed in order to keep the medium effects on the dispersivity unchanged. Thus, according to Fick's Law, it is valid to expect that the dispersivity value obtained from the tracer experiments should be successful in fitting experimental brine breakthrough curves.

7.1. Impact of the Magnitude of the Density Differences on Dispersion

As shown in Figure 7.1 through Figure 7.4, it is possible to generate breakthrough curves that fit the experimental curves, using the Ogata-Banks analytical solution, which does not account for the density effect on flow and transport. However, the analytical solution was only used for qualitatively evaluating any trends in the "apparent" dispersivities. It should be noted that, the Fickian Theory states that the dispersivity is dependent on the medium properties only and the dispersion coefficient is a linear function of the dispersivity and groundwater velocity. If this theory was valid under high concentration gradient conditions it should be possible to find a unique dispersivity value to fit all breakthrough curves obtained from the same experimental column (Q=5 ml/min).

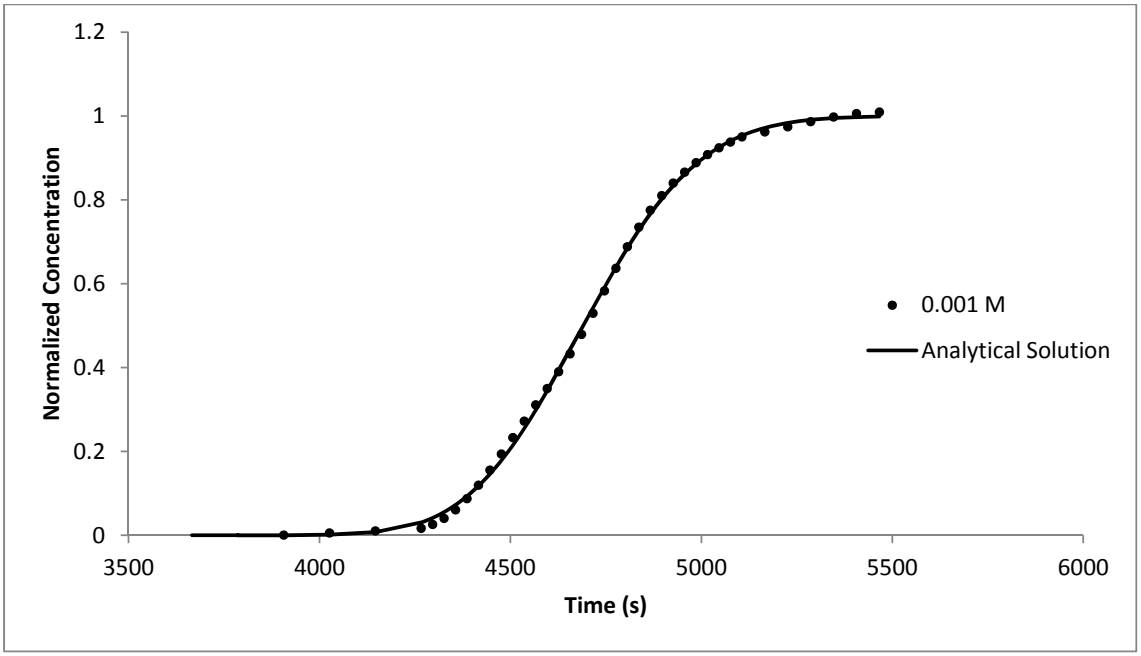

Figure 7.1. Comparison of the breakthrough curve from the variable density Experiment 14 with the analytical solution ($C_{displacing}=10^{-3}$ M, $\alpha_{as}=0.74$ mm)

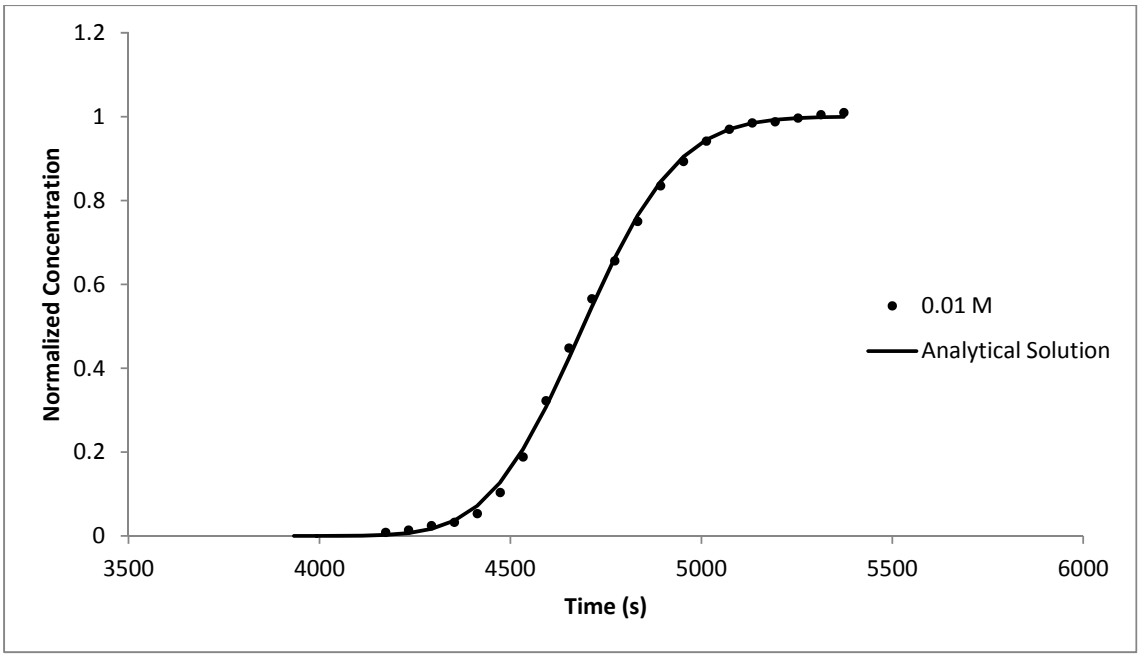

Figure 7.2. Comparison of the breakthrough curve from the variable density Experiment 15 with the analytical solution ($C_{displacing}=10^{-2}$ M, $\alpha_{as}=0.49$ mm)

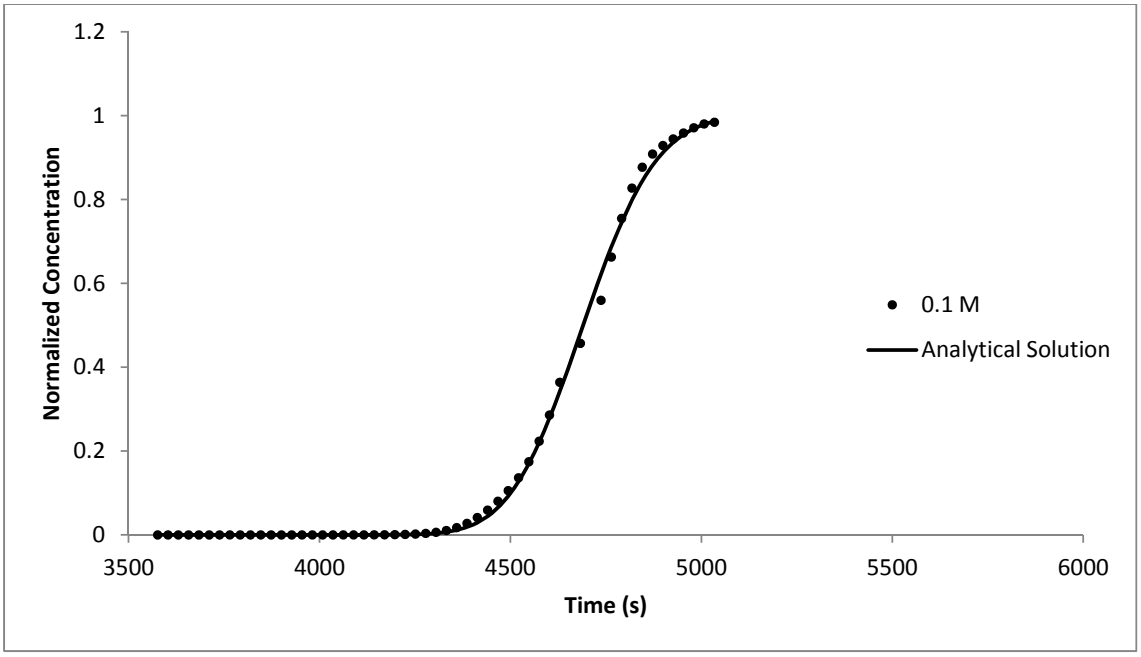

Figure 7.3. Comparison of the breakthrough curve from the variable density Experiment 16 with the analytical solution ($C_{displacing}=10^{-1}$ M, $\alpha_{as}=0.28$ mm)

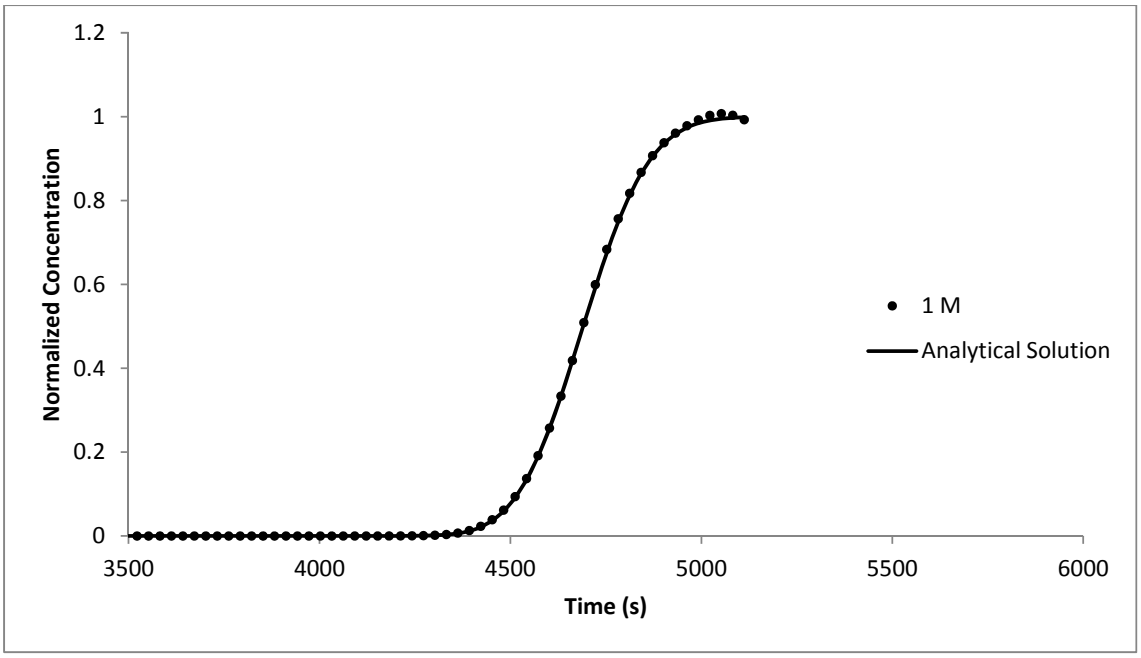

Figure 7.4. Comparison of the breakthrough curve from the variable density Experiment 17 with the analytical solution ($C_{displacing}$=1 M, α_{as}=0.22 mm)

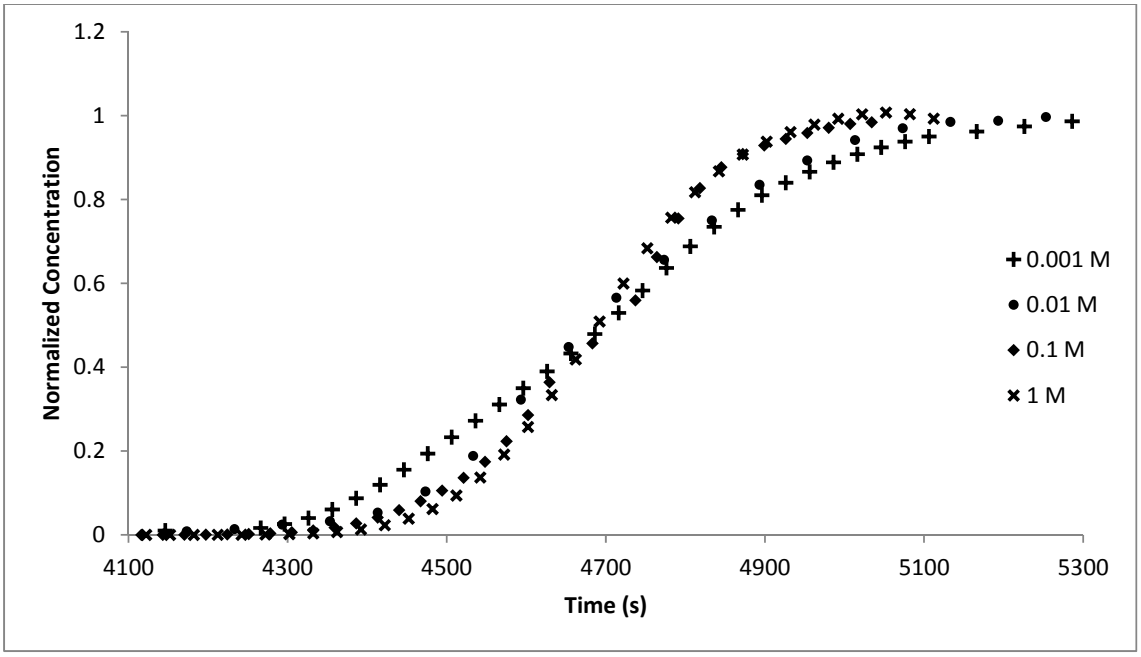

Figure 7.5. Comparison of the breakthrough curves obtained in the variable density experiments 14 through 17 with each other (Q=5 ml/min)

Figure 7.1 through Figure 7.4 show that, as the concentration difference between resident and displacing fluids increases, the extent of the mixing zone decreases. A similar trend can be seen in Figure 7.5, which shows all four breakthrough curves plotted together. Breakthrough curve from Experiment 14, which has the smallest concentration difference between resident and displacing fluids, or, in other words, is closest to tracer experiments, was the least steep whereas that of Experiment 17, which has the highest difference, was the sharpest.

Figure 7.6 compares the dispersivities used in fitting the experimental breakthrough curves obtained from brine experiments with constant flow rate and different brine concentrations. It can be seen that observed dispersivities decrease with increase in concentration differences. This observation is in accordance with the findings of researchers mentioned in the Literature Review section (e.g., Bouhroum, 1985; Hassanizadeh, 1990; Moser, 1995). The fact that the apparent dispersivities observed in the experiments conducted in the same sand column were not the same contradicts with the linear Fick's Law which states that the dispersive flux is linearly related to concentration gradients and velocities.

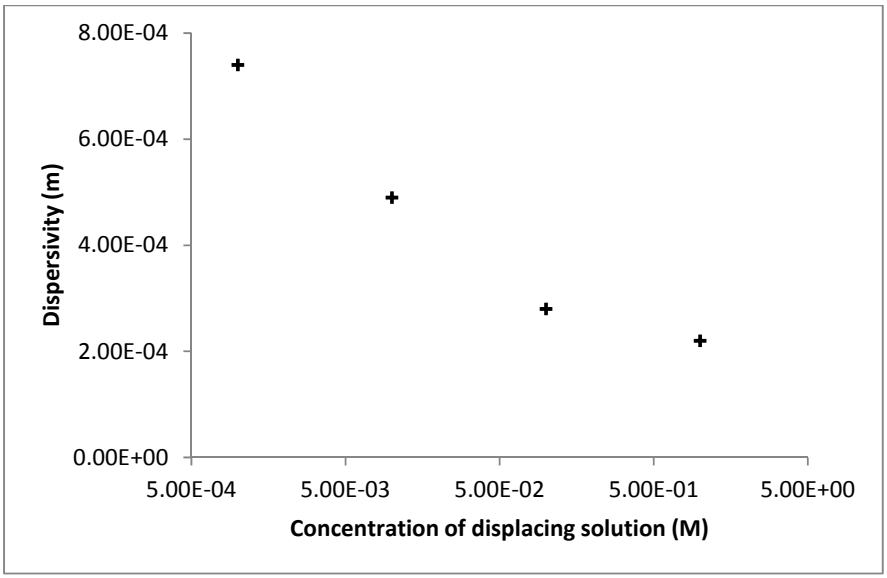

Figure 7.6. Apparent dispersivities observed in the variable density experiments vs displacing fluid concentrations (Q=5 ml/min)

Since the apparent dispersivities were different for each experiment, dispersion coefficients also showed a decrease with increase in concentration differences as shown in Figure 7.7.

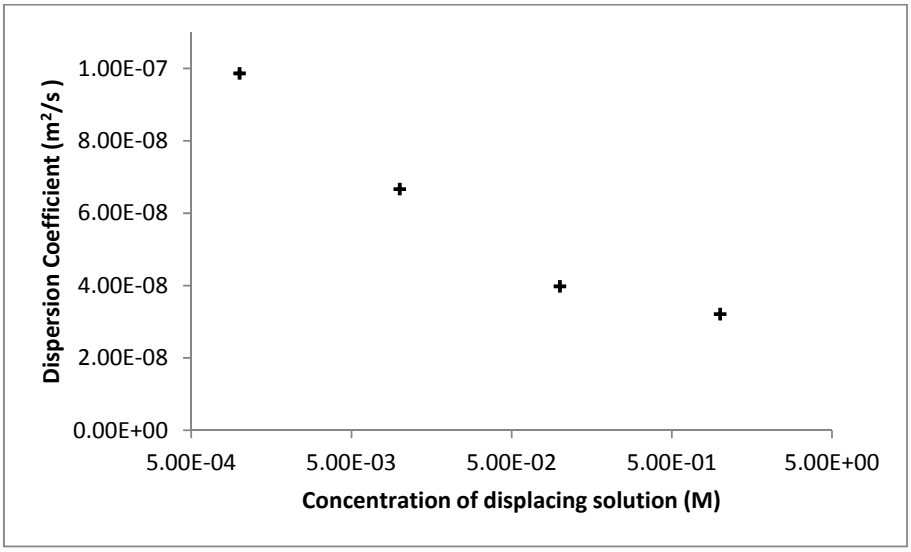

Figure 7.7. Dispersion Coefficients determined in the variable density experiments vs displacing fluid concentrations (Q=5 ml/min)

7.2. Comparison of Model Results with Experimental Results

In order to test the non-Fickian Model, the apparent dispersivity (from best fit analytical solution) of the experiment with the smallest density difference ($C_{displacing}=10^{-3}$ M) was selected and non-Fickian numerical simulations were done with the parameters of the first four brine experiments (Table 7.1). In other words, numerical simulations of stable, vertical, upward displacement experiments were performed, using the parameters of experiments 14 through 17 in the Table 7.1 and the highest dispersivity value in Figure 7.7. Similar to the column experiments, the porous medium in the simulations was homogeneous and the concentration was monitored at an observation point located at 60 cm from the point of injection. Figure 7.8 through Figure 7.11 show the comparison of the numerical solutions to experimental results. For all numerical simulations α_{ns}=0. 74 mm, Q=5 ml/min and $\beta=10^9$ sm^2/kg.

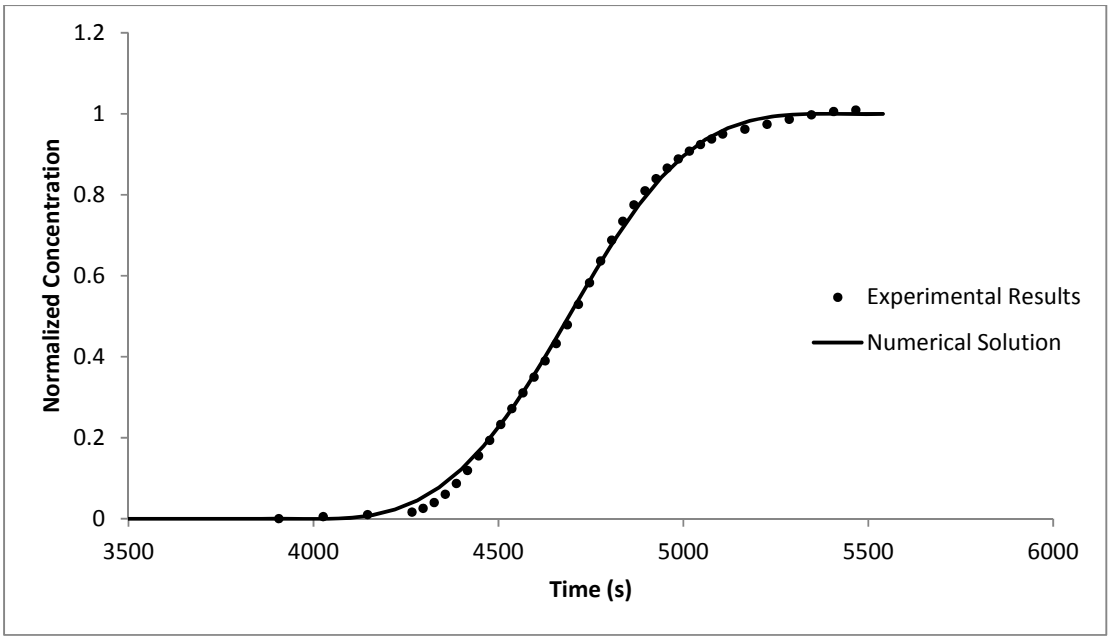

Figure 7.8. Comparison of the breakthrough curve from the variable density Experiment 14 with the numerical solution ($C_{displacing}=10^{-3}$ M)

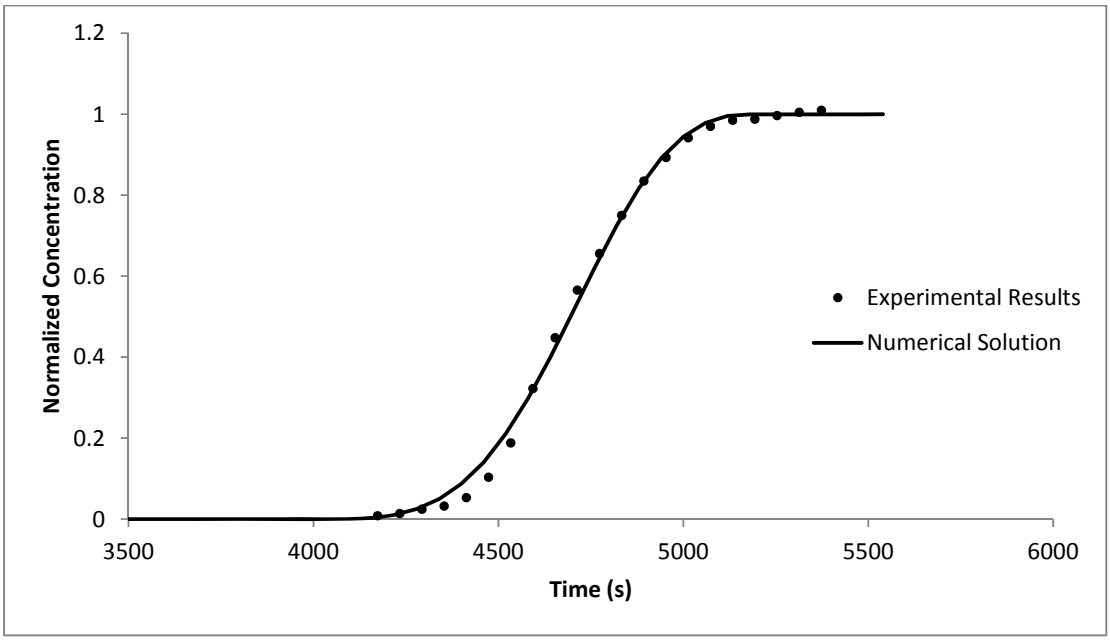

Figure 7.9. Comparison of the breakthrough curve from the variable density Experiment 15 with the numerical solution ($C_{displacing}=10^{-2}$ M)

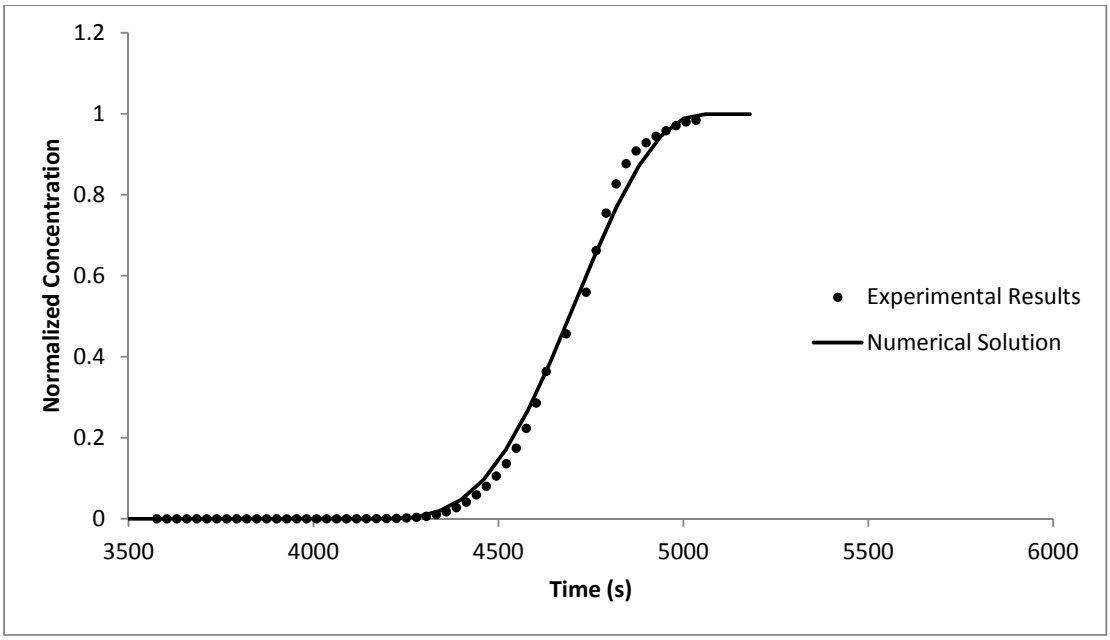

Figure 7.10. Comparison of the breakthrough curve from the variable density Experiment 16 with the numerical solution ($C_{displacing}=10^{-1}$ M)

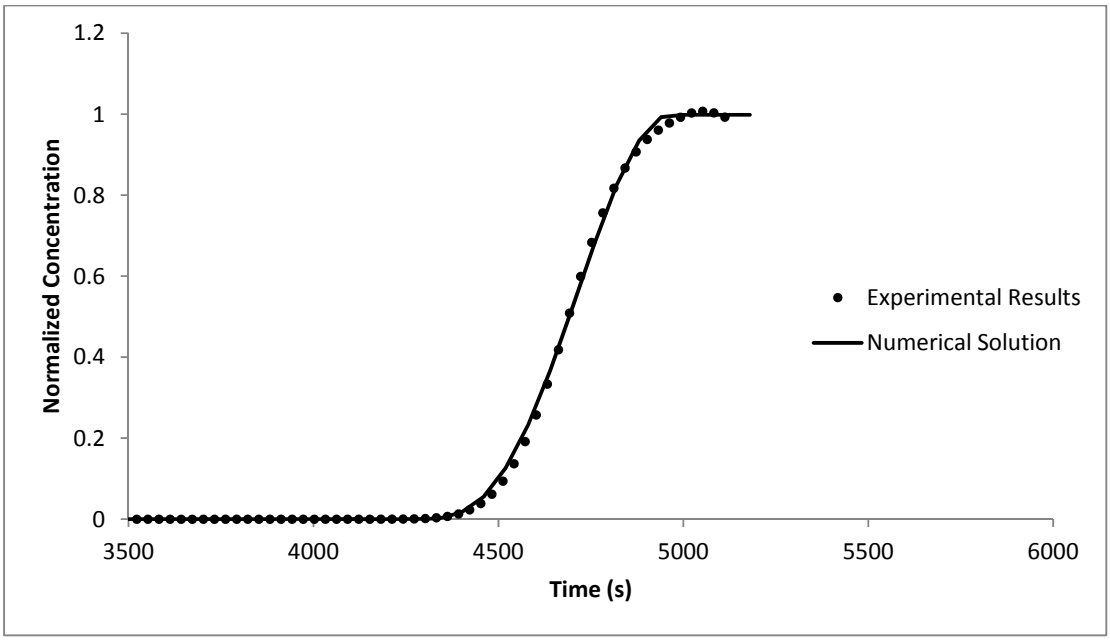

Figure 7.11. Comparison of the breakthrough curve from the variable density Experiment 17 with the numerical solution ($C_{displacing}=1$ M)

7.3. Impact of Velocity on Brine Dispersion

The second brine experiment set involved a single concentration difference while a range of different flow rates were employed. The experimental procedure was the same as in the first part. As in the first part, a single dispersivity value that fits all the breakthrough curves is expected to be found according to linear Fick's Law because the porous medium is still the same.

Figure 7.12 through Figure 7.21 compare the breakthrough curves obtained in the second part of brine experiments ($C_{displacing}$=1 M) to the analytical solution. Contradicting with Fick's Law, it was not possible to fit all curves using the same dispersivity value. This suggests that groundwater velocity affects the way the hydrodynamic dispersion depends on the concentration difference. This observation is consistent with the findings of Schotting et al. (1999) that was mentioned in the Literature Review section.

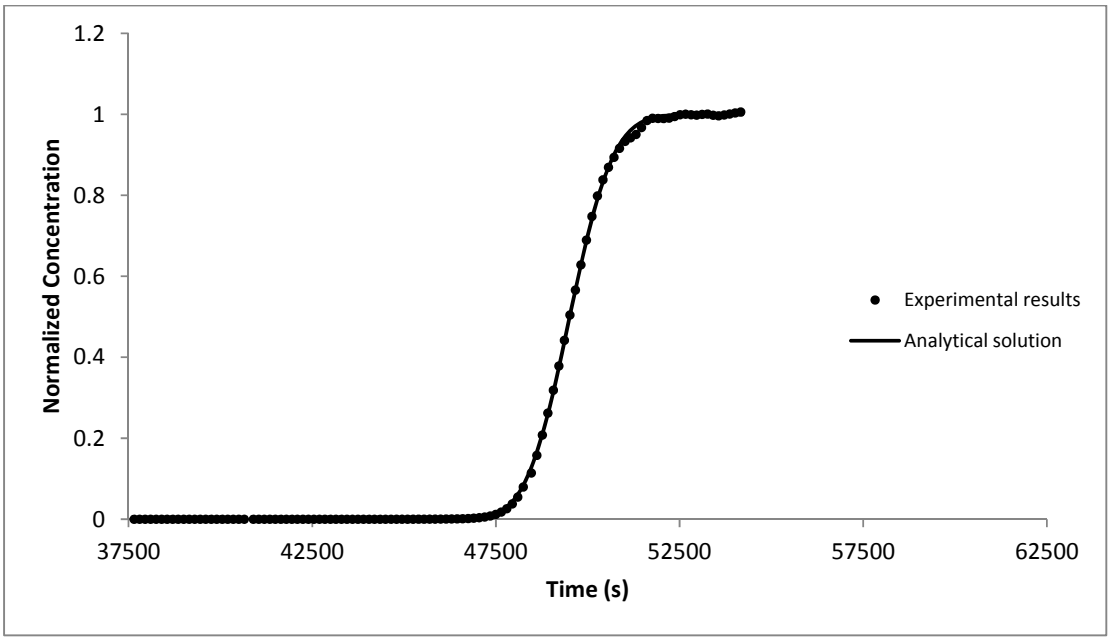

Figure 7.12. Comparison of the breakthrough curve from the sand brine Experiment 18 with the analytical solution (Q=0.5 ml/min, α_{as}=0.023 mm)

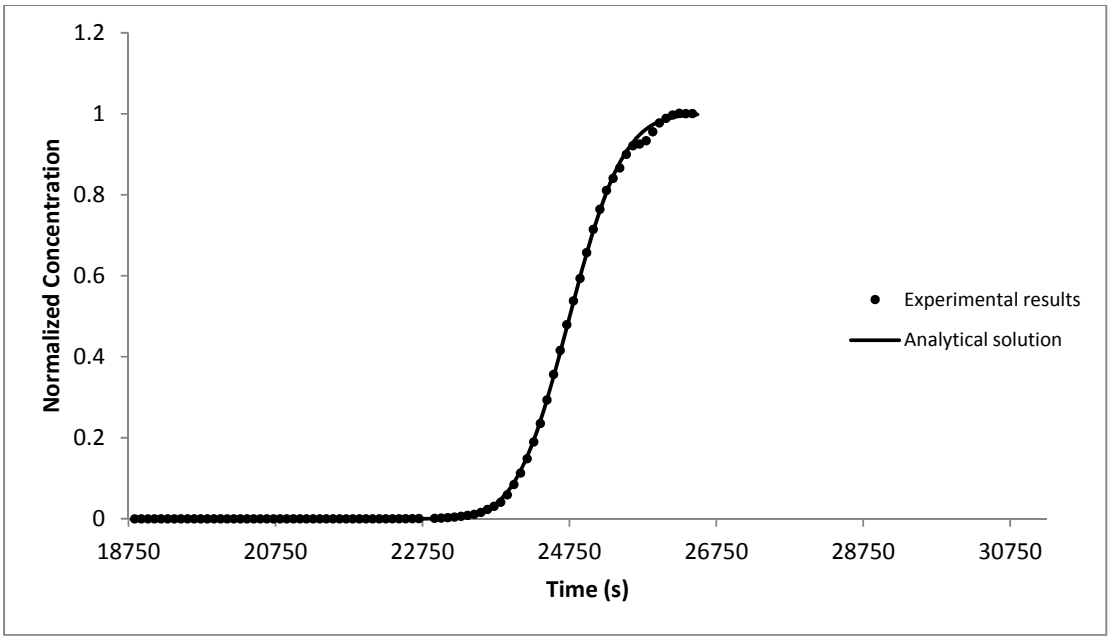

Figure 7.13. Comparison of the breakthrough curve from the sand brine Experiment 19 with the analytical solution (Q=1 ml/min, α_{as}=0.12 mm)

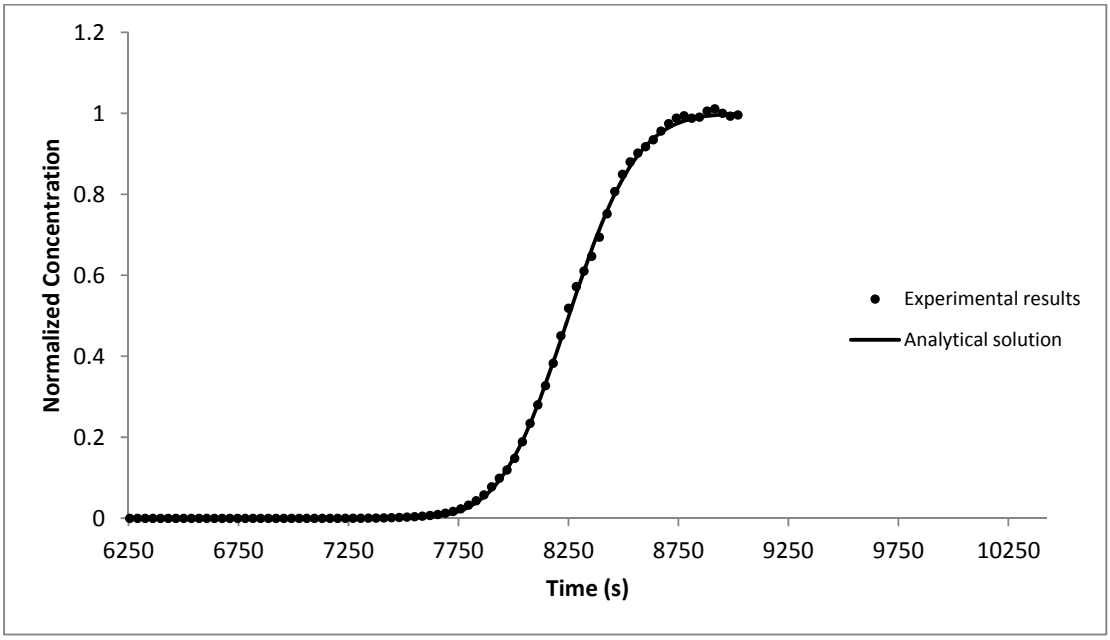

Figure 7.14. Comparison of the breakthrough curve from the sand brine Experiment 20 with the analytical solution (Q=3 ml/min, α_{as}=0.25 mm)

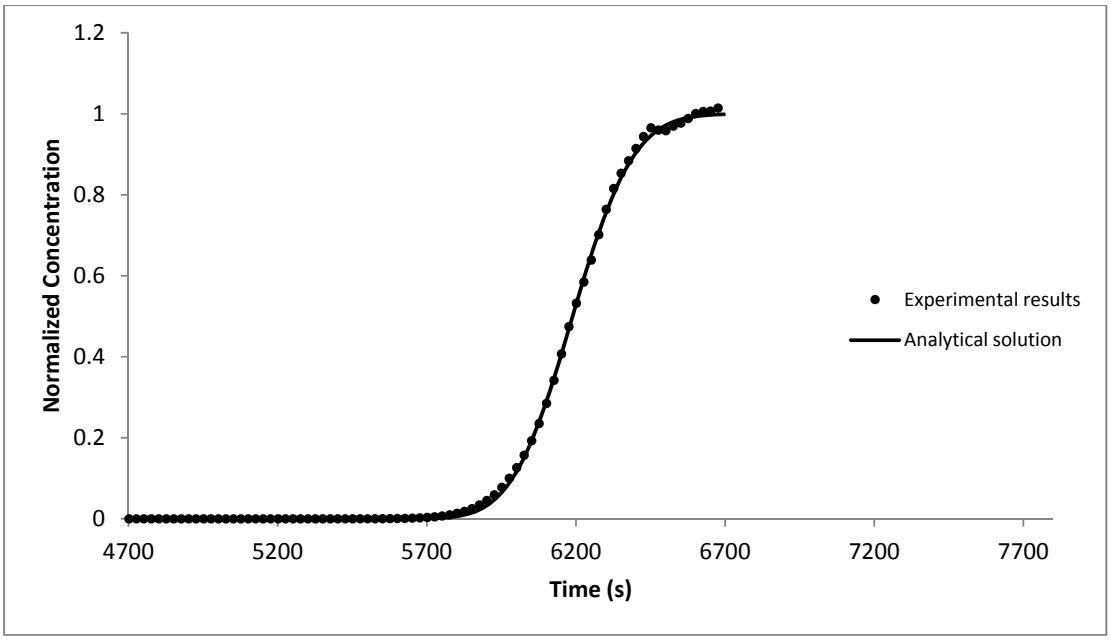

Figure 7.15. Comparison of the breakthrough curve from the sand brine Experiment 21 with the analytical solution (Q=4 ml/min, α_{as}=0.19 mm)

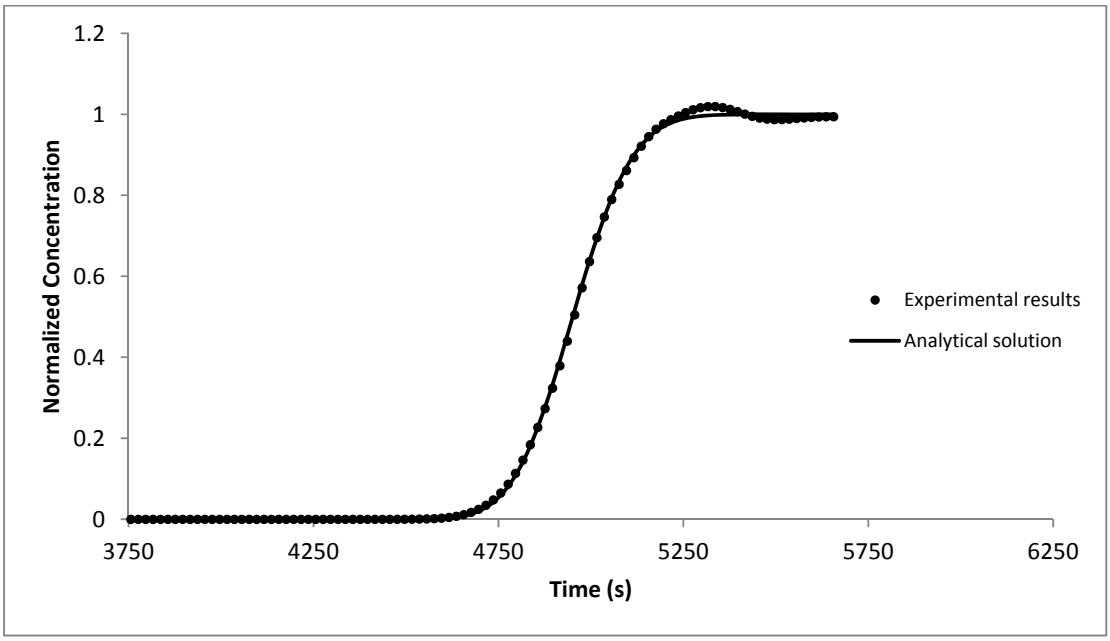

Figure 7.16. Comparison of the breakthrough curve from the sand brine Experiment 22 with the analytical solution (Q=5 ml/min, α_{as}=0.19 mm)

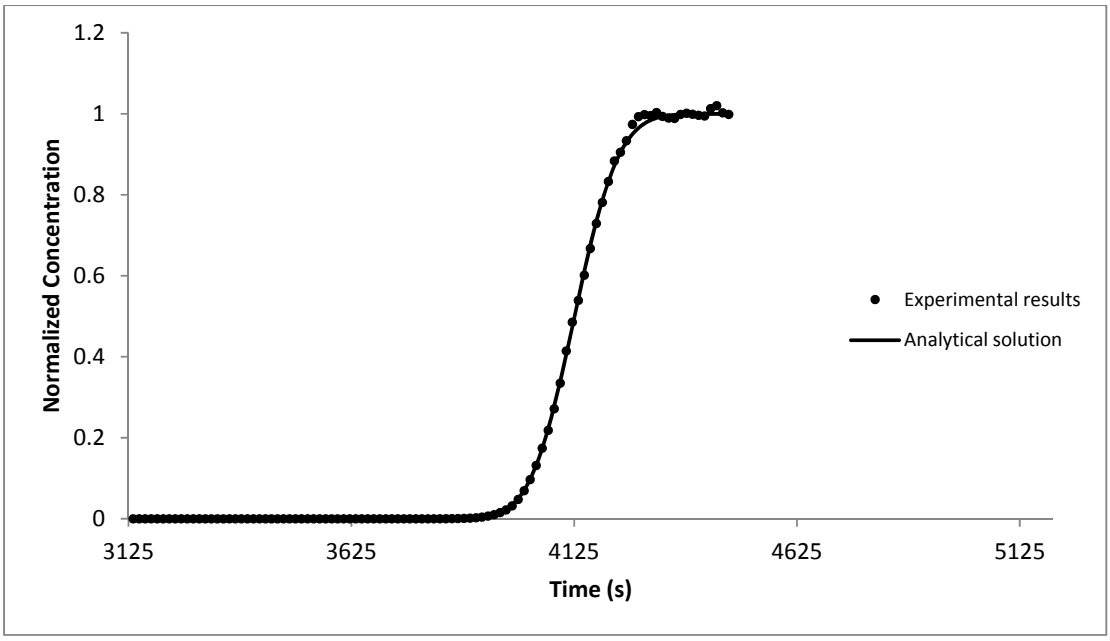

Figure 7.17. Comparison of the breakthrough curve from the sand brine Experiment 23 with the analytical solution (Q=6 ml/min, α_{as}=0.10 mm)

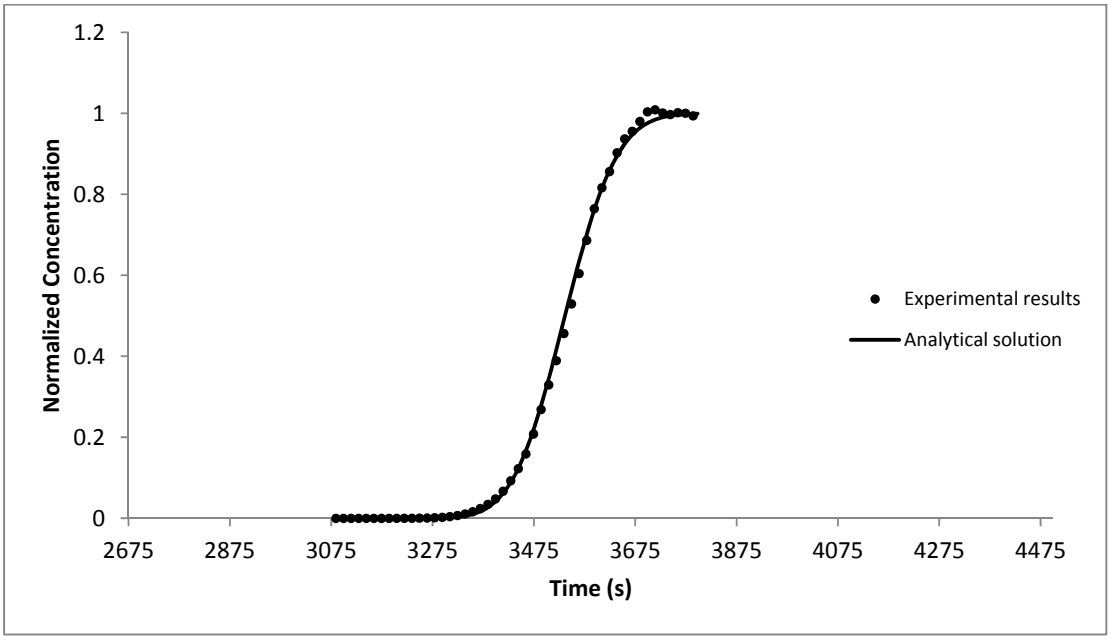

Figure 7.18. Comparison of the breakthrough curve from the sand brine Experiment 24 with the analytical solution (Q=7 ml/min, α_{as}=0.15 mm)

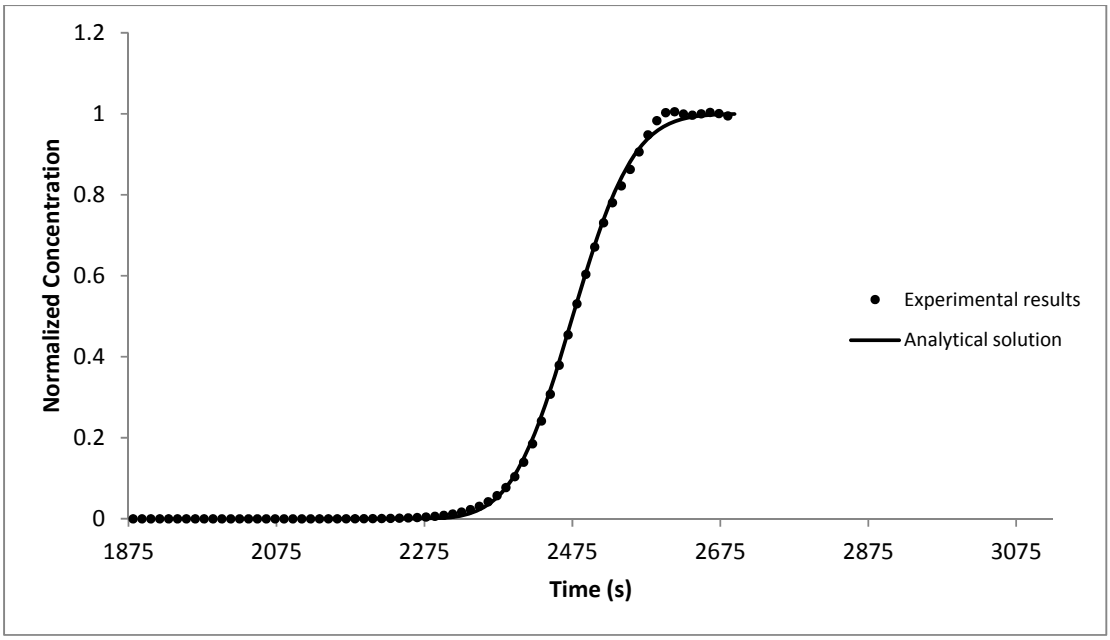

Figure 7.19. Comparison of the breakthrough curve from the sand brine Experiment 25 with the analytical solution (Q=10 ml/min, α_{as}=0.20 mm)

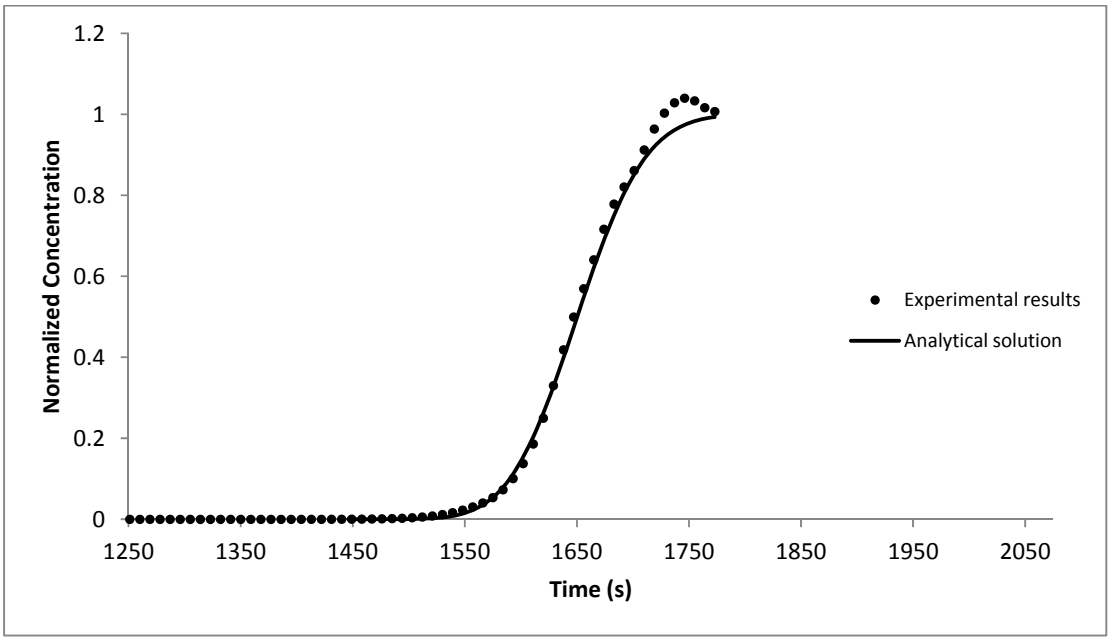

Figure 7.20. Comparison of the breakthrough curve from the sand brine Experiment 26 with the analytical solution (Q=15 ml/min, α_{as}=0.25 mm)

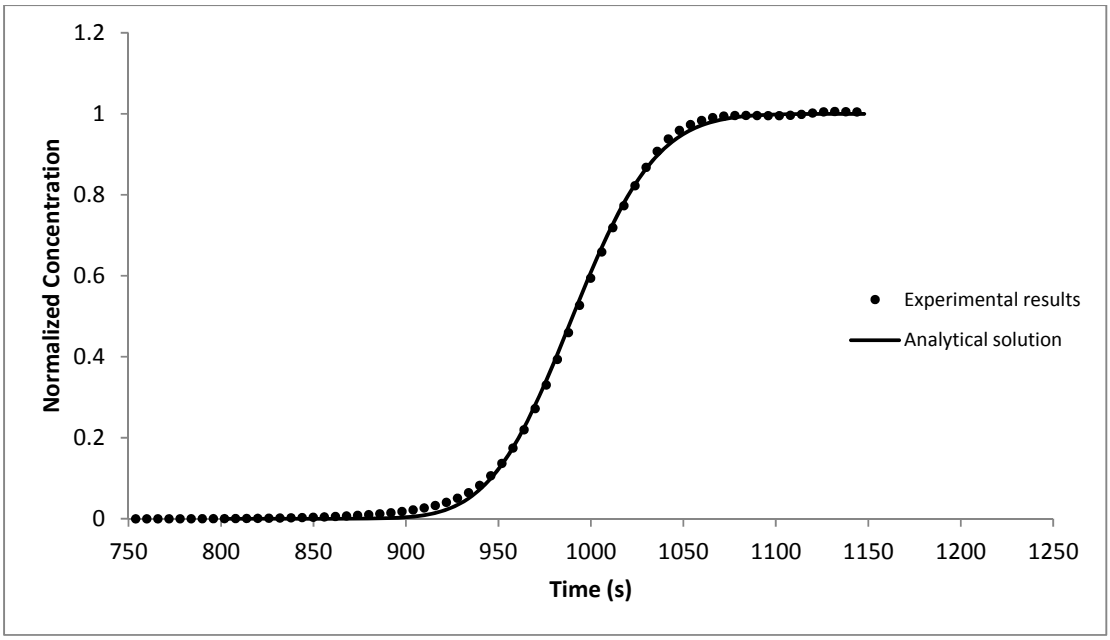

Figure 7.21. Comparison of the breakthrough curve from the sand brine Experiment 27 with the analytical solution (Q=25 ml/min, α_{as}=0.38 mm)

Figure 7.22 presents a scatter plot of apparent dispersivities observed in brine experiments 18 through 27 versus average linear velocity. The plot shows a trend of increase in apparent dispersivities with increase in flow rate. The experimental results support the argument that hydrodynamic dispersion deviates from the Fickian Theory under high concentration gradient conditions. On the other hand, the fact that the difference between the brine and the tracer dispersivities gets reduced as the velocity increases shows that the deviation from Fickian behavior is insignificant at relatively high flow rates.

This observation can be explained by the differences in exposure times. Since the length of the column or in other words the travel length is fixed, the travel time is only controlled by the velocity. Since the area and the porosity are also not changing, the travel time is a function of the flow rate applied. When the travel time is short, there is less time for the high concentration gradients to take their effects.

This reasoning supports the theory that proposes that the reduction in hydrodynamic dispersion is caused by the leveling of neighboring zones of different concentrations (e. g. Schotting et al, 1999). At low velocities, for each unit length of the porous medium, the contaminant plume have more time to level the differences in concentrations between neighboring zones.

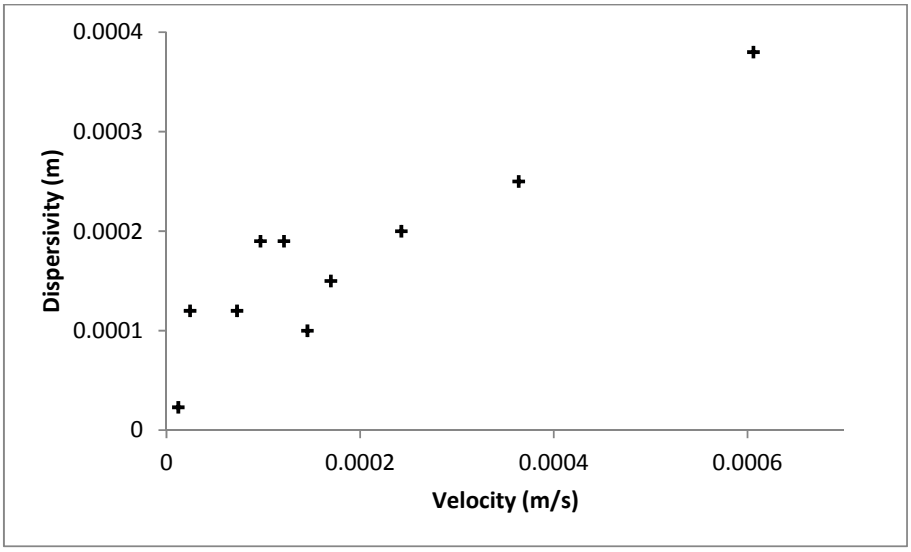

Figure 7.22. Apparent dispersivities observed in the sand brine experiments vs average linear velocity ($C_{displacing}$=1 M)

Figure 7.23 presents a scatter plot of dispersion coefficients observed in brine experiments 18 through 27 versus average linear velocity. Although dispersion is dominated by mechanical mixing, the plot shows a non-linear trend of increase in dispersion coefficients with increase in flow rate.

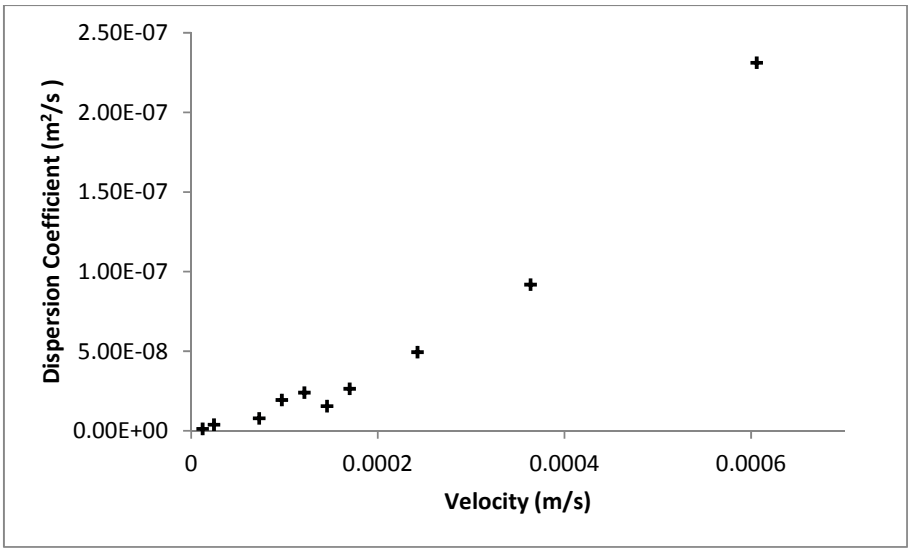

Figure 7.23. Dispersion coefficients determined in the sand brine experiments vs average linear velocity ($C_{displacing}$=1 M)

Figure 7.24 compares dispersion coefficients observed in brine experiments in sand packing to those observed in tracer experiments in sand packing as a function of average linear velocity.

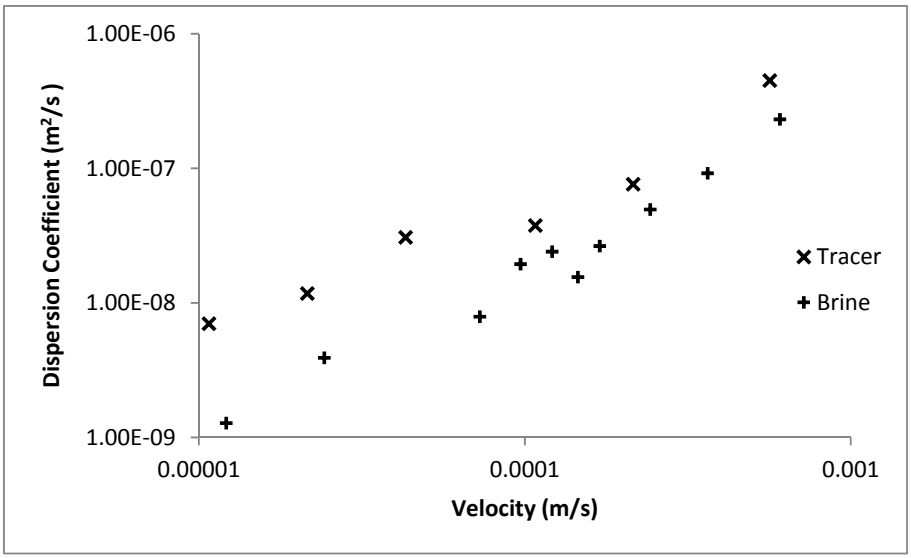

Figure 7.24. Comparison of dispersion coefficients observed in tracer and brine experiments conducted in the sand column

8. MIXTURE EXPERIMENTS

8.1. Contaminant Mixtures

Experimental evidence from the literature and the results of the experiments conducted in this study thus far show that a Fickian Model for dispersive flux is not valid for the high concentration solutes in groundwater, when brine is separated from the ambient groundwater with sharp concentration fronts and high density differences. An alternative dispersion model from the literature was evaluated by comparison to experimental results in preceding chapters and a computer program for the simulation of transport was developed using the model parameters with the highest accordance with the experimental results.

Another important question is how a second, dilute contaminant would behave under high concentration gradient conditions? A dilute solute is expected to obey the Fick's Law when it is the only contaminant in the groundwater or the total concentration of all contaminants does not add up to a value that would create density differences high enough to cause coupling between flow and transport and deviation from Fick's Law. However there is no experimental evidence or direct mathematical inference to estimate the dispersive behavior of a dilute contaminant mixed with brine.

The occurrence of a contaminant at low concentration in the presence of another contaminant at much higher concentration is not unlikely in natural settings. In the problem of radioactive waste disposal in salt formations, the high concentration gradients are mainly caused by sodium chloride, which is not indeed the contaminant of concern. The radioactive compounds are not expected to reach concentrations similar to that of sodium chloride because they are introduced into the system in much smaller quantities compared to salt, and their water solubilities are much lower than that of sodium chloride. There are no mathematical or experimental studies reported in the literature, investigating the dispersive behavior of dilute contaminants in the presence of brine or other high concentration contaminants, although an understanding of this behavior is the key to fully understand the transport of radioactive contaminants in the vicinity of salt formations.

Other examples of groundwater contaminant mixtures with both concentrated and dilute components include flushing of NAPL plumes with surfactants and cosolvents, where the actual contaminant is expected to remain at relatively lower concentrations whereas the remedial fluid will be in abundance, landfill leachates with low concentrations of hazardous compounds, concentrated brine from deicing of roads contaminated with compounds like lead or hydrocarbons from automobile exhaust. All of these examples require a model that incorporates effects of high concentration gradient on the transport of both high and low concentration contaminants.

In order to investigate dispersive behavior of low concentration contaminants mixed with brine, contaminant mixture (or mixture) experiments were conducted. A mixture experiment is basically similar to a brine experiment, differing only by the presence of a second, low concentration contaminant in the stock solution. As the second contaminant, Potassium Bromide was selected and added to brine with 2 M NaCl concentration at a concentration of 10^{-2} M. The justification for choosing Potassium Bromide as the second contaminant is provided in the Materials and Methods Chapter.

Table 8.1 lists the different mixture experiments conducted. Each experiment involves two dissolved species in the displacing fluid, and hence two breakthrough curves, two apparent dispersivities, two apparent dispersion coefficients etc. In order to distinguish between the two components of the displacing solution, their corresponding observations will be labeled by the chemical formula of the dissolved species.

It should be noted that brine components of mixture experiments are expected to give similar results with brine experiments because they only differ from brine experiments by the presence of a second contaminant at a relatively low concentration, specifically only 0.5% of the sodium chloride concentration by moles. Such a small interference is not expected to affect the dispersive behavior of the brine. This anticipation was also justified by comparing NaCl results of experiments 28 through 32 to the results of the brine experiments. However, KBr results of experiments 28 through 32 are unique in the sense that they have concentration in the tracer range whereas total concentrations and fluid densities are in the brine range.

Table 8.1. List of mixture experiments

No	Flow rate (ml/min)	Linear velocity (m/s)	Resident fluid	Displacing fluid	Packing material	Concentration monitoring
28	1	2.42×10^{-05}	Distilled water	2 M aq. NaCl+ 10-2 M aq. KBr	Glass beads	Sampling + conductivity Sampling + ISE*
29	2	4.85×10^{-05}	Distilled water	2 M aq. NaCl+ 10-2 M aq. KBr	Glass beads	Sampling + conductivity Sampling + ISE
30	5	1.21×10^{-04}	Distilled water	2 M aq. NaCl+ 10-2 M aq. KBr	Glass beads	Sampling + conductivity Sampling + ISE
31	10	2.42×10^{-04}	Distilled water	2 M aq. NaCl+ 10-2 M aq. KBr	Glass beads	Sampling + conductivity Sampling + ISE
32	25	6.06×10^{-04}	Distilled water	2 M aq. NaCl+ 10-2 M aq. KBr	Glass beads	Sampling + conductivity Sampling + ISE

* Conductivity measurements were used for the determination of NaCl concentrations whereas KBr concentrations were determined using ion selective electrodes

8.2. High Concentration Component

Figure 8.1 through Figure 8.5 compare NaCl breakthrough curves of experiments 28 through 32 ($C_{displacing}$=2 M) with the analytical solution. As already mentioned, these breakthrough curves are expected to be similar to those observed in experiments 18 through 27, or sand brine experiments, in the sense that they should deviate from Fickian behavior due to the density differences between resident and displacing fluids. However, there were several differences between the two sets. These differences are the NaCl concentration of displacing solution, presence of a second contaminant, method of concentration monitoring and the size and shape of the particles used in column packing. Since both the classical and the modified dispersion theories relate dispersive flux to the characteristics of the porous medium, apparent dispersion parameters of the two sets are not expected to be similar although both are expected to deviate from Fickian behavior. Figure 8.2 shows that the mixing zone was not fully captured. However the experiment was not discarded since the curve fitting results were found to be consistent with the theory and the results of other experiments.

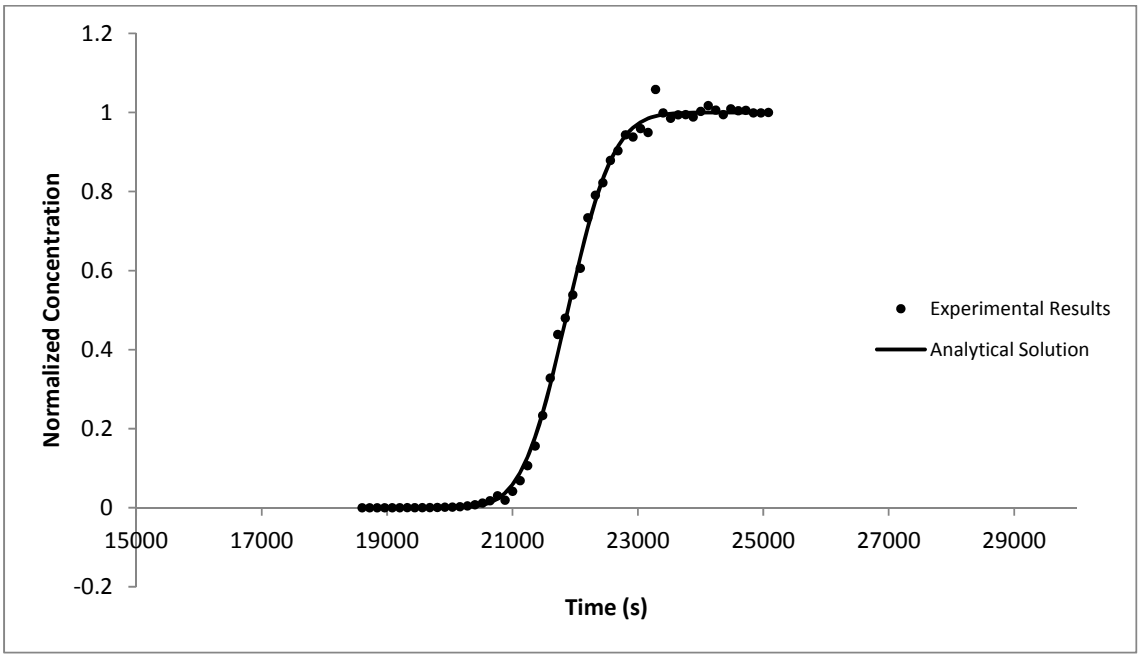

Figure 8.1. Comparison of the NaCl breakthrough curve obtained in the mixture Experiment 28 with the analytical solution (Q=1.0 ml/min, α_{as}=0.17 mm)

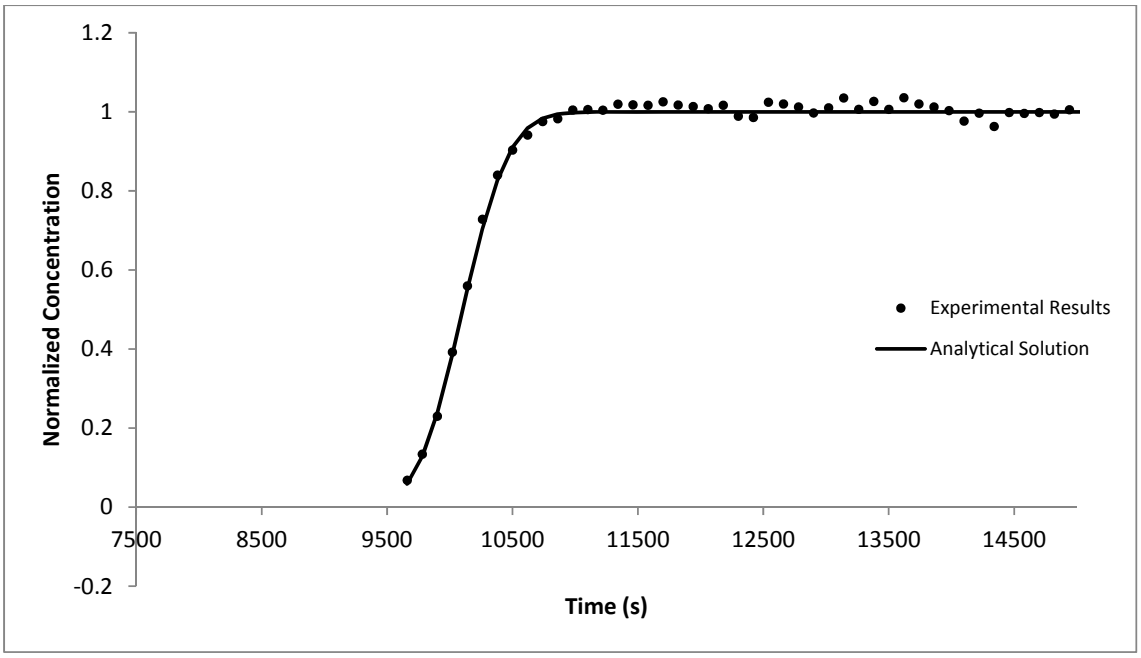

Figure 8.2. Comparison of the NaCl breakthrough curve obtained in the mixture Experiment 29 with the analytical solution (Q=2.0 ml/min, α_{as}=0.23 mm)

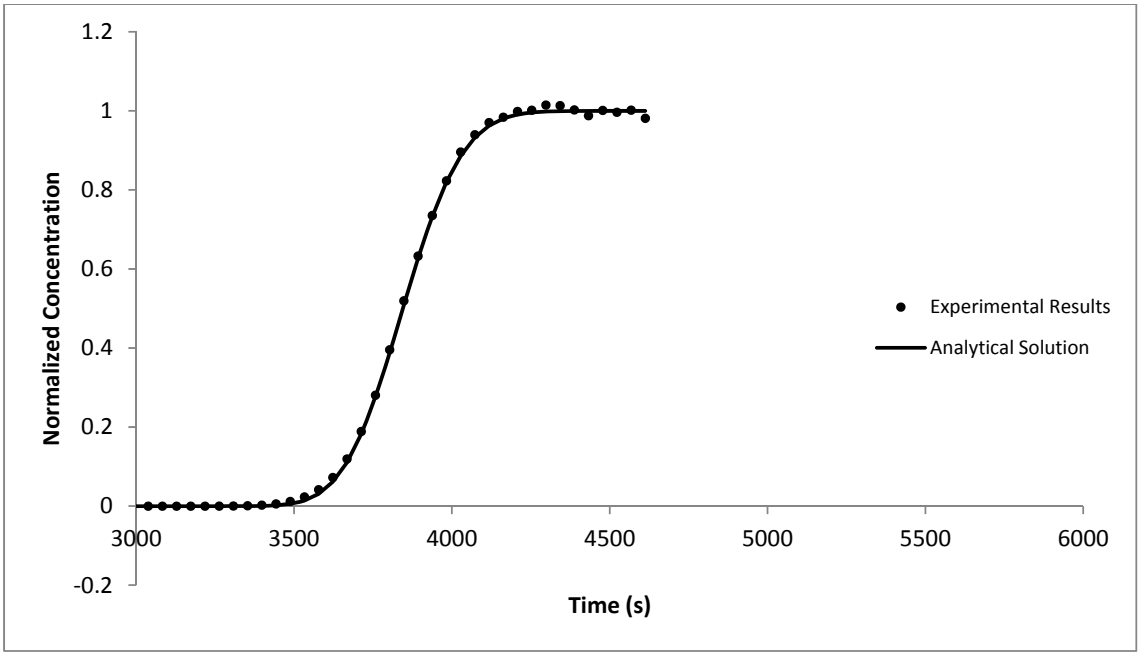

Figure 8.3. Comparison of the NaCl breakthrough curve obtained in the mixture Experiment 30 with the analytical solution (Q=5.0 ml/min, α_{as}=0.44 mm)

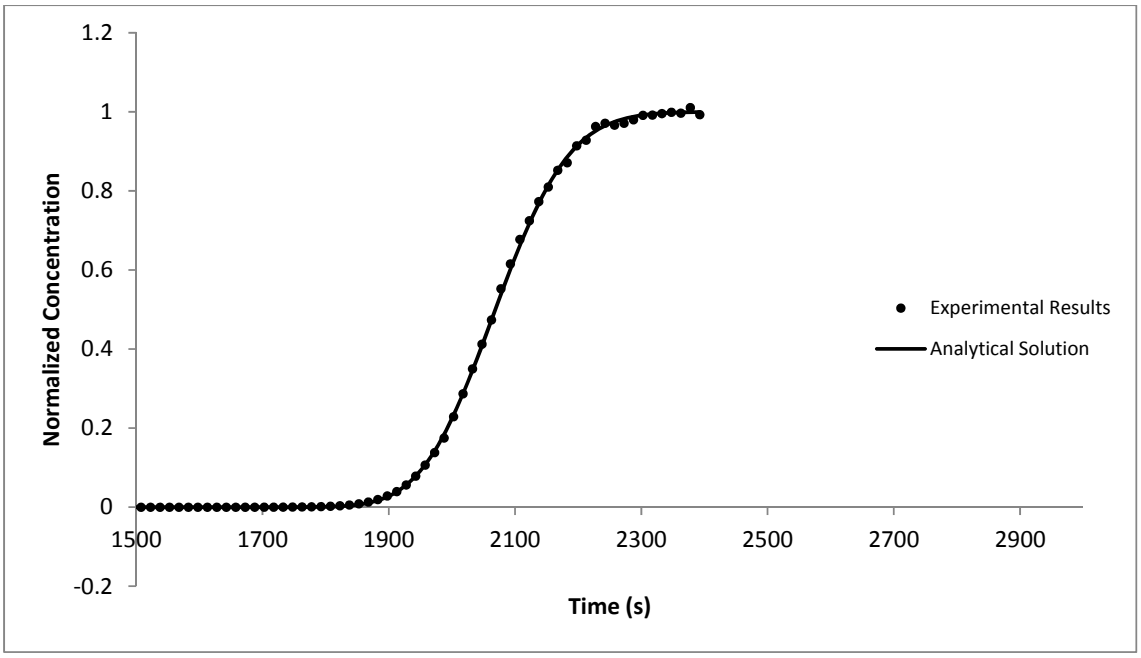

Figure 8.4. Comparison of the NaCl breakthrough curve obtained in the mixture Experiment 31 with the analytical solution (Q=10.0 ml/min, α_{as}=0.59 mm)

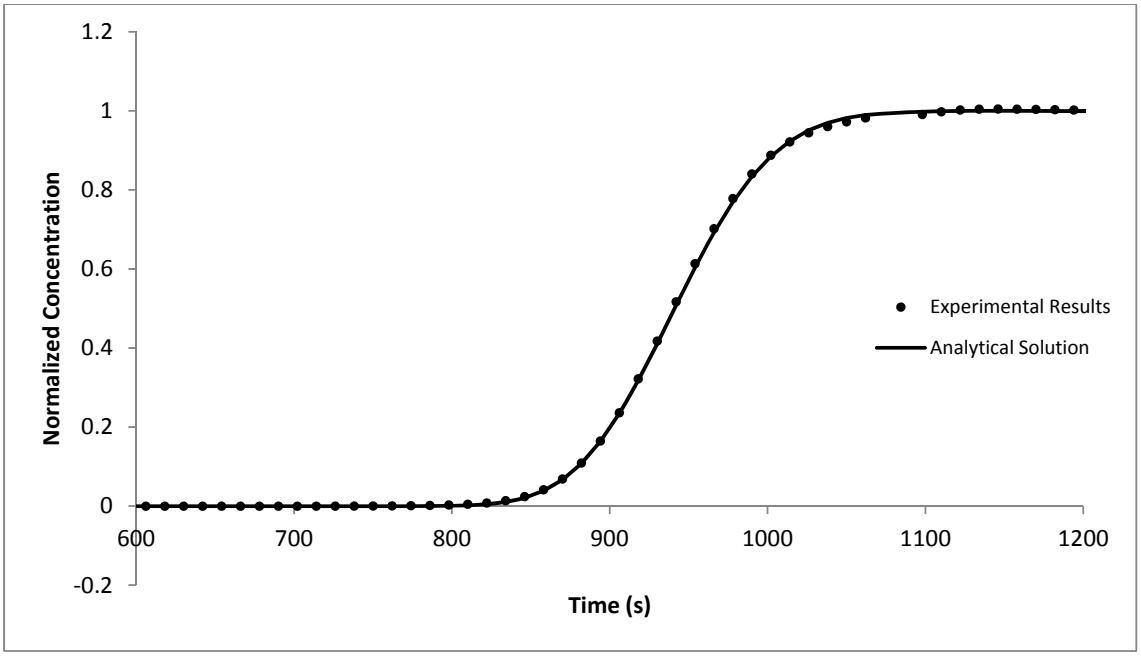

Figure 8.5. Comparison of the NaCl breakthrough curve obtained in the mixture Experiment 32 with the analytical solution (Q=25.0 ml/min, α_{as}=0.82 mm)

Figure 8.6 presents a scatter plot of apparent dispersivities observed for NaCl component in experiments 28 through 32 versus average linear velocity. Figure 8.7 presents a scatter plot of corresponding dispersion coefficients. As expected, observed trends were similar to those observed in brine experiments. Apparent dispersivities show an increase with increase in flow rate as suggested by the modified Fick's Law and contradicting with the original Fick's Law. Since dispersivities are not independent of the flow rate and the mechanical mixing term in the dispersion coefficient is defined as the product of the velocity and the dispersivity, the trend of increase in dispersion coefficient vs. average linear velocity plot is thought to be non-linear.

Figure 8.8 compares dispersion coefficients observed in mixture experiments for NaCl component with those observed in experiments 9 through 13. In other words it compares brine component of mixture experiments conducted in glass bead packed column to the tracer experiments with the same packing. It can be seen that, NaCl dispersion coefficients are lower than corresponding tracer dispersion coefficients although porous medium and the velocities were the same.

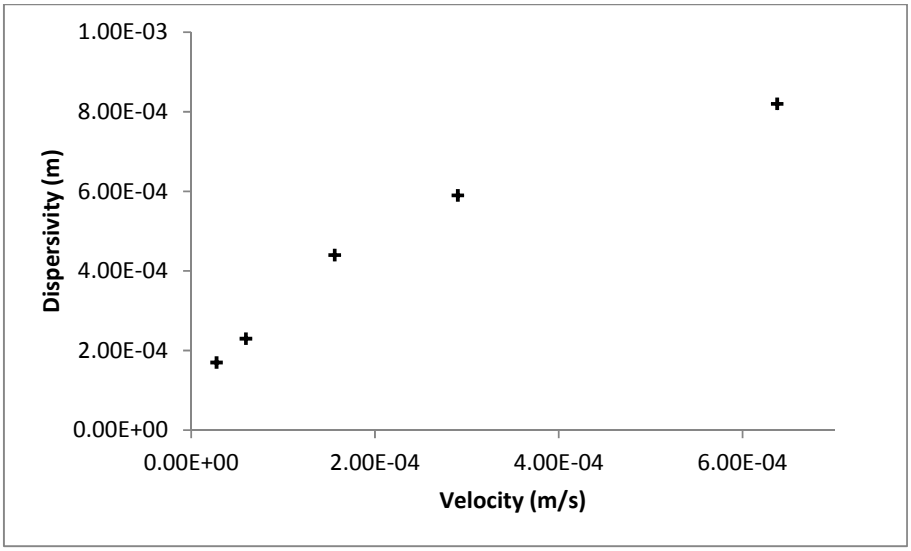

Figure 8.6. Apparent dispersivities for NaCl vs average linear velocity
(Experiments 28-32, $C_{displacing}$=2 M)

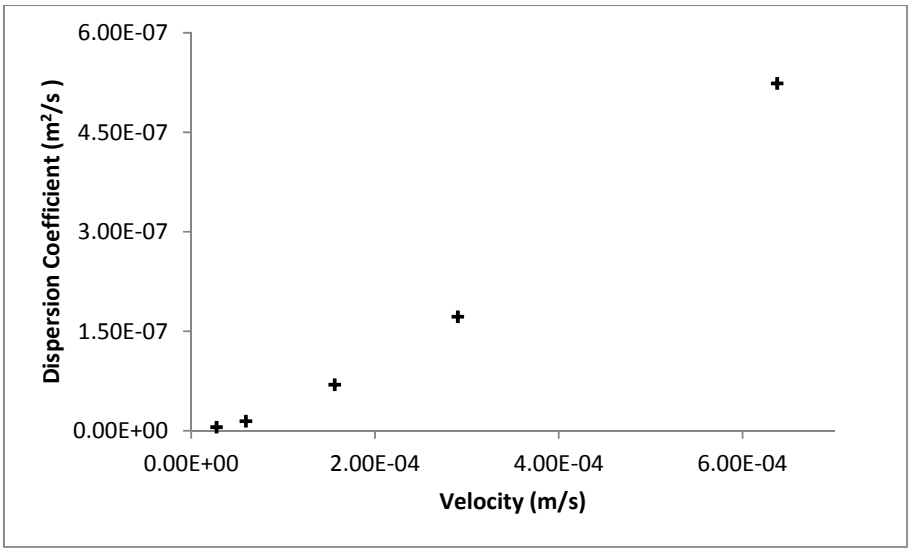

Figure 8.7. Dispersion coefficients observed for NaCl vs average linear velocity (Experiments 28-32, $C_{displacing}$=2 M)

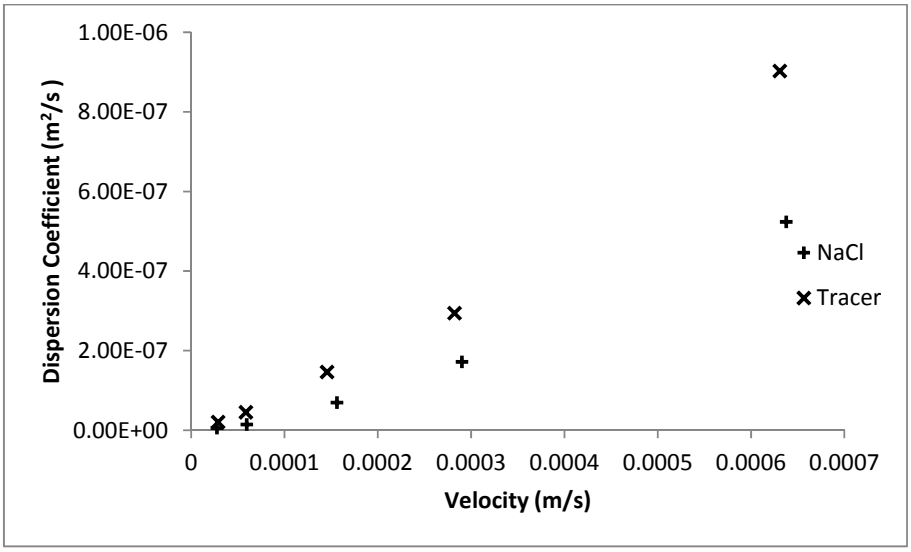

Figure 8.8. Comparison of NaCl dispersion coefficients observed in mixture experiments to those observed in corresponding tracer experiments

8.3. Evaluation of the Non-Linearity Coefficient

In order to test the non-linear theory, a set of numerical simulations were conducted for each mixture experiment using the dispersivity value obtained from the corresponding glass bead tracer experiment. All simulations in each set had the same flow and transport parameters, except the non-linearity parameter, β. Figure 8.9 through Figure 8.13 compare experimental curves to numerical curves. For each experiment the numerical curve that fits the experimental curve was determined and its β value was assigned as the non-linearity parameter for the velocity of the experiment. No exact matches were observed because β values had to be chosen arbitrarily before performing simulations, and moreover there were slight differences between the shapes of experimental and simulated breakthrough curves. As a result, the simulated curve that was closer to the experimental curve was taken as an approximate result, or a value was projected using the two closest curves. The β values thus obtained are shown as a function of specific discharges in Figure 8.14.

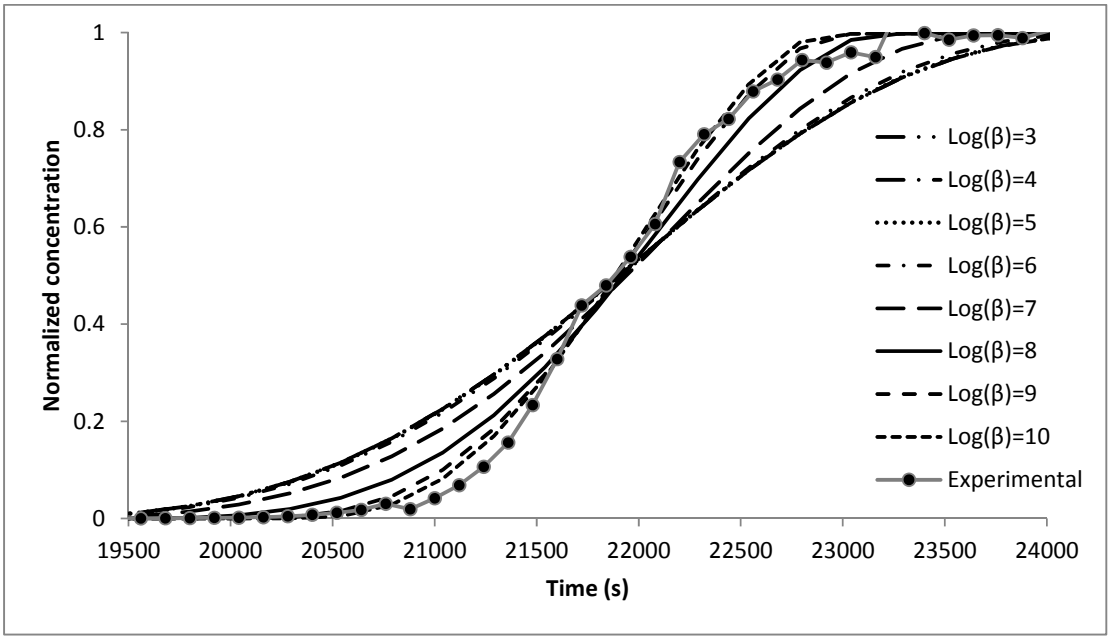

Figure 8.9. Comparison of the NaCl breakthrough curve from Experiment 28 with the numerical solution with different β (Q=1.0 ml/min, α_{ns}=0.69 mm)

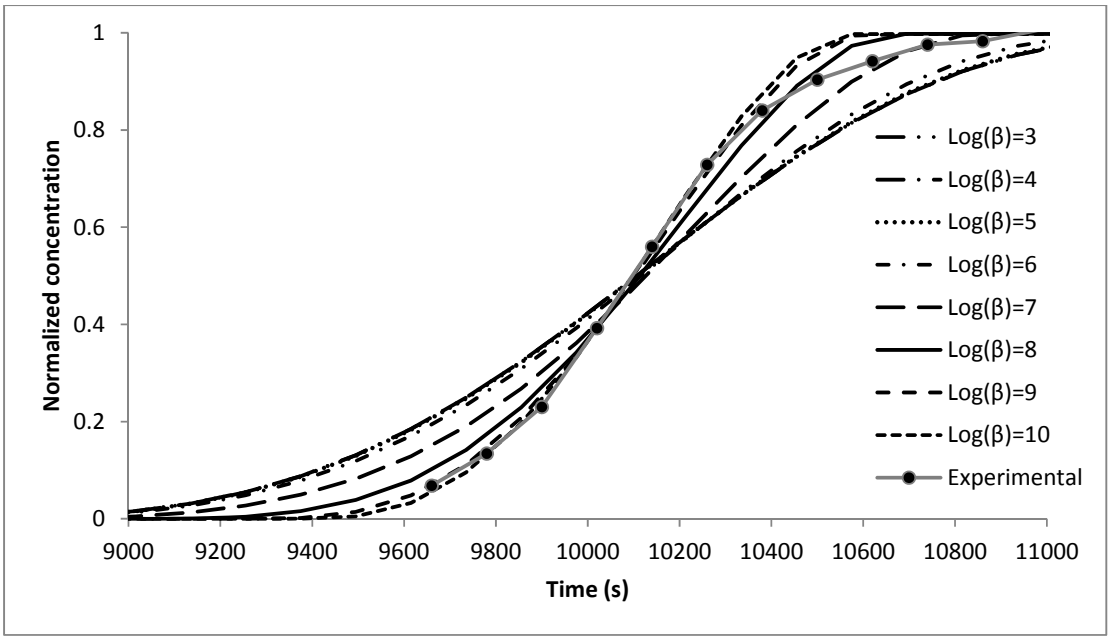

Figure 8.10. Comparison of the NaCl breakthrough curve from Experiment 29 with the numerical solution with different β (Q=2.0 ml/min α_{ns}=0.76 mm)

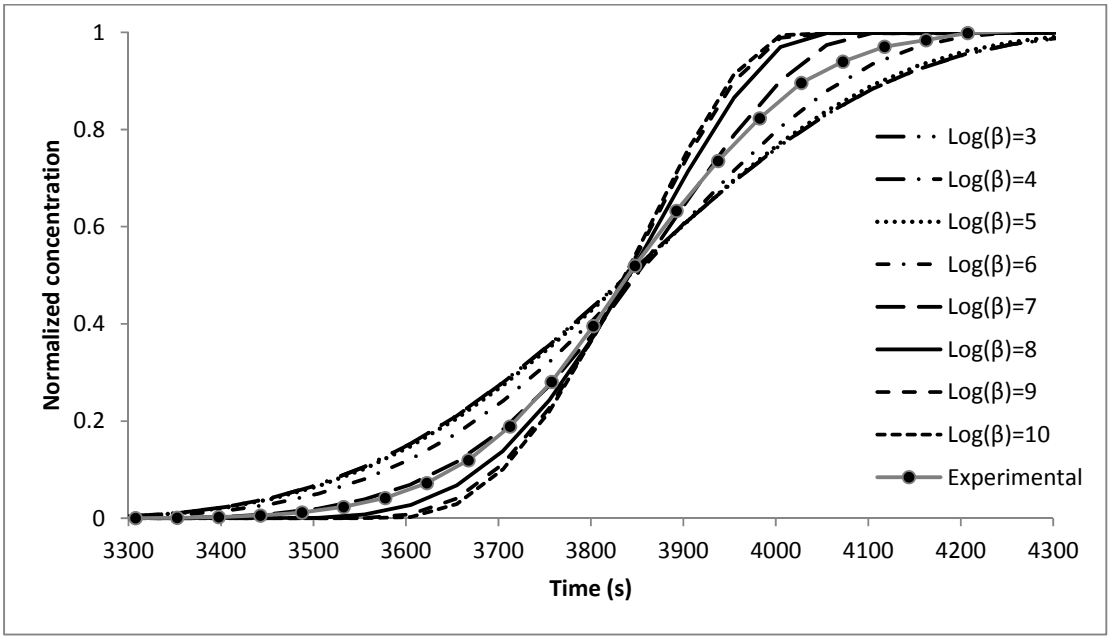

Figure 8.11. Comparison of the NaCl breakthrough curve from Experiment 30 with the numerical solution with different β (Q=5.0 ml/min α_{ns}=1.00 mm)

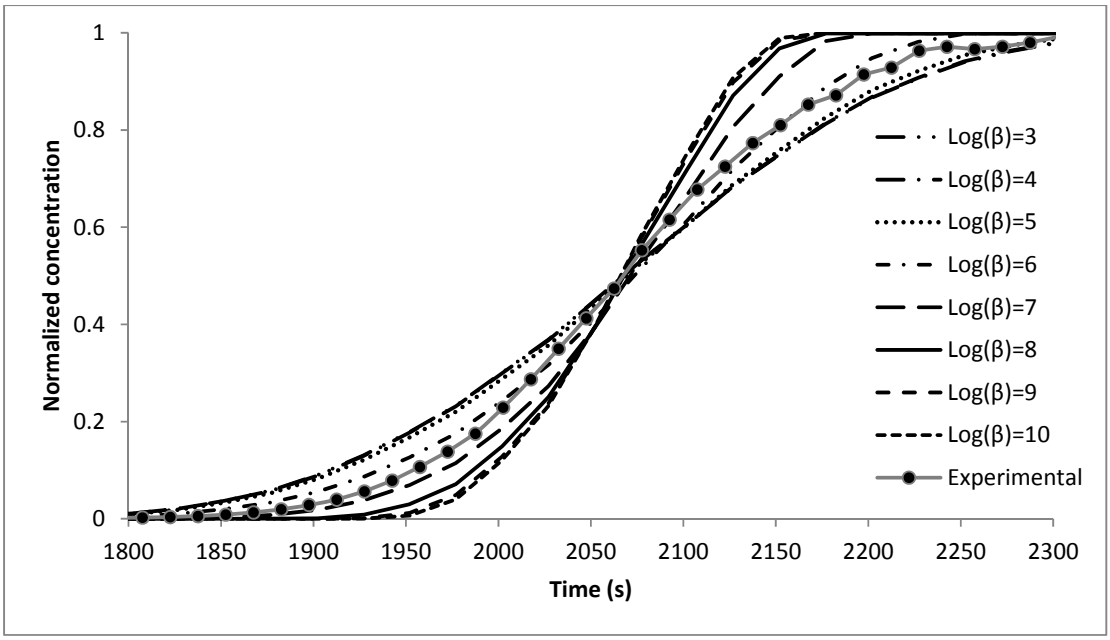

Figure 8.12. Comparison of the NaCl breakthrough curve from Experiment 31 with the numerical solution with different β (Q=10.0 ml/min α_{ns}=1.04 mm)

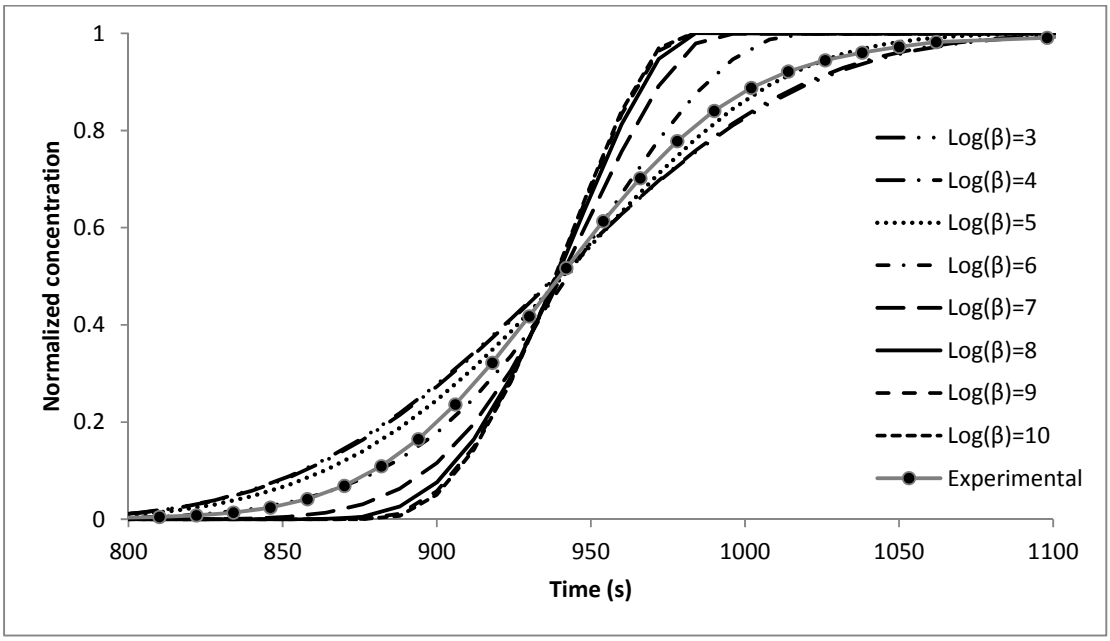

Figure 8.13. Comparison of the NaCl breakthrough curve from Experiment 32 with the numerical solution with different β (Q=25.0 ml/min α_{ns}=1.43 mm)

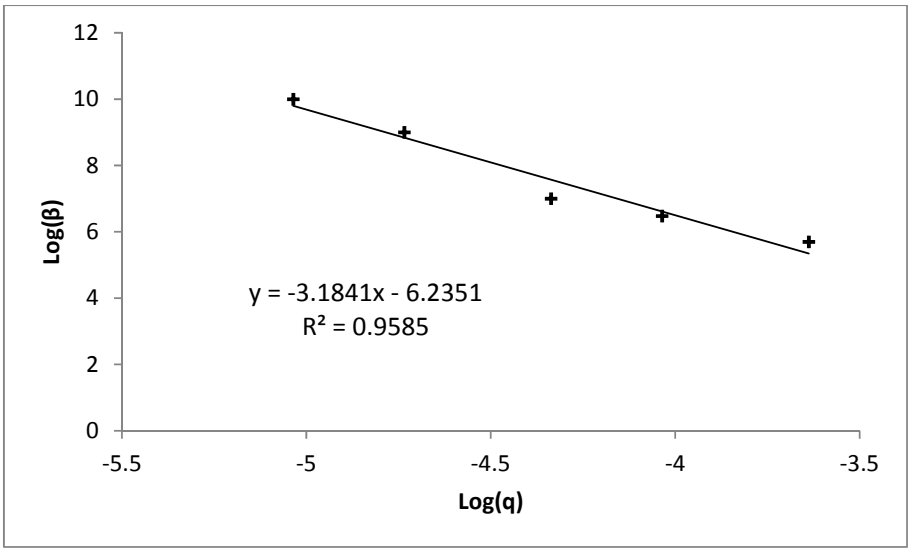

Figure 8.14. Base 10 logarithm of observed β values vs base 10 logarithms of specific discharges

A relationship between the non-linearity coefficient, β, and specific discharge, q, was obtained using the approximate β values obtained by curve fitting. The relationship thus obtained was $\beta=10^{-6.2}/q^{3.2}$, for 4.6×10^{-6} m/s < q < 2.4×10^{-4} m/s which is a typical range for natural groundwater velocities. Using the same non-linear expression for Fick's Law, Schotting et al. (1999) reported $\beta=10^{-1.9}/q^{1.76}$. However, it should be noted that, Schotting et al. provided their relationship for 9.0×10^{-5} m/s < q < 3.0×10^{-3} m/s, which only encompasses the highest two values employed in this study. The difference between β values calculated using the two relationships reduces to less than 10% for the highest flow rate (25 ml/min, Experiment 32) and becomes insignificant for a range that covers most of the range provided by Schotting et al.

8.4. Low Concentration Component

The potassium bromide, KBr, added to the contaminant mixture at 10^{-2} M is the low concentration component of the contaminant mixture. In the previous section, it was shown that the high concentration component behaves similar to brine. However, the behavior of the high concentration component does not necessarily set an example for the low concentration component since dispersive flux is classically defined as a function of the

concentration gradient for each component. As the non-linear dispersion theory reduces to the linear Fick's Law as the dispersive flux becomes smaller, the behavior of the low concentration component is of special concern.

A preliminary comparison of KBr breakthrough curves from experiments 28 through 32 with corresponding tracer breakthrough curves revealed that low concentration contaminants transported with concentrated solutions also deviate from Fickian behavior. Further comparison with corresponding brine experiments suggested that they behave similar to brines. Figure 8.15 through Figure 8.19 show KBr breakthrough curves ($C_{displacing}=10^{-2}$ M) and their best-fitting analytical solutions. Apparent dispersivities of best-fit analytical solutions are plotted versus average linear velocity in Figure 8.20.

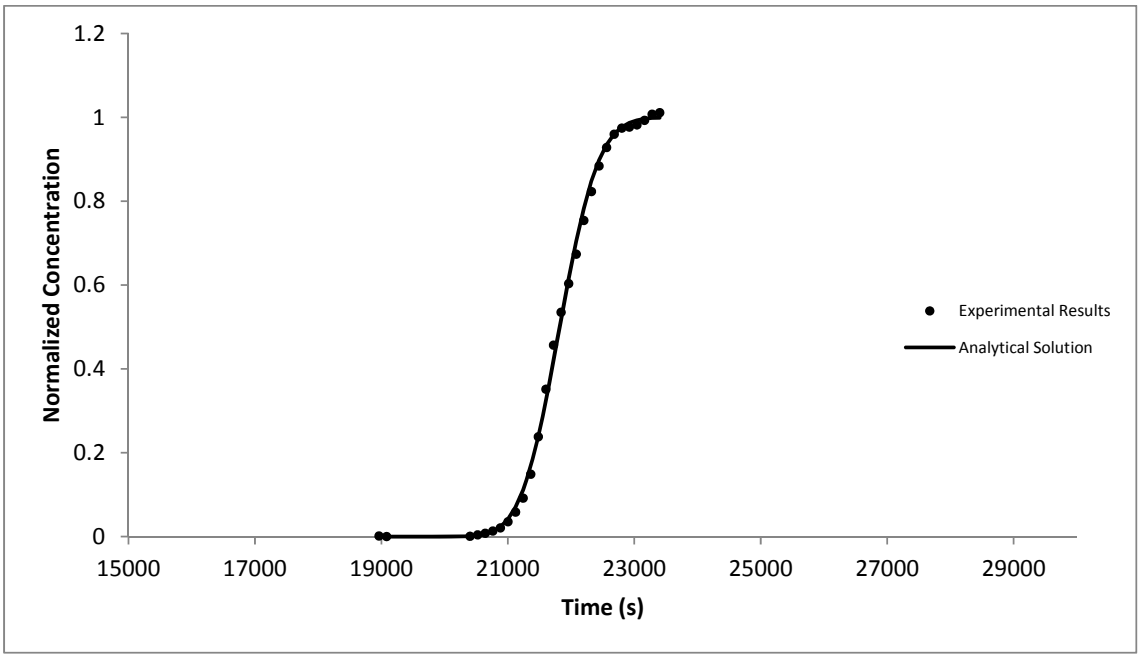

Figure 8.15. Comparison of the KBr breakthrough curve from the Experiment 28 with the analytical solution (Q=1.0 ml/min, α_{as}=0.11 mm)

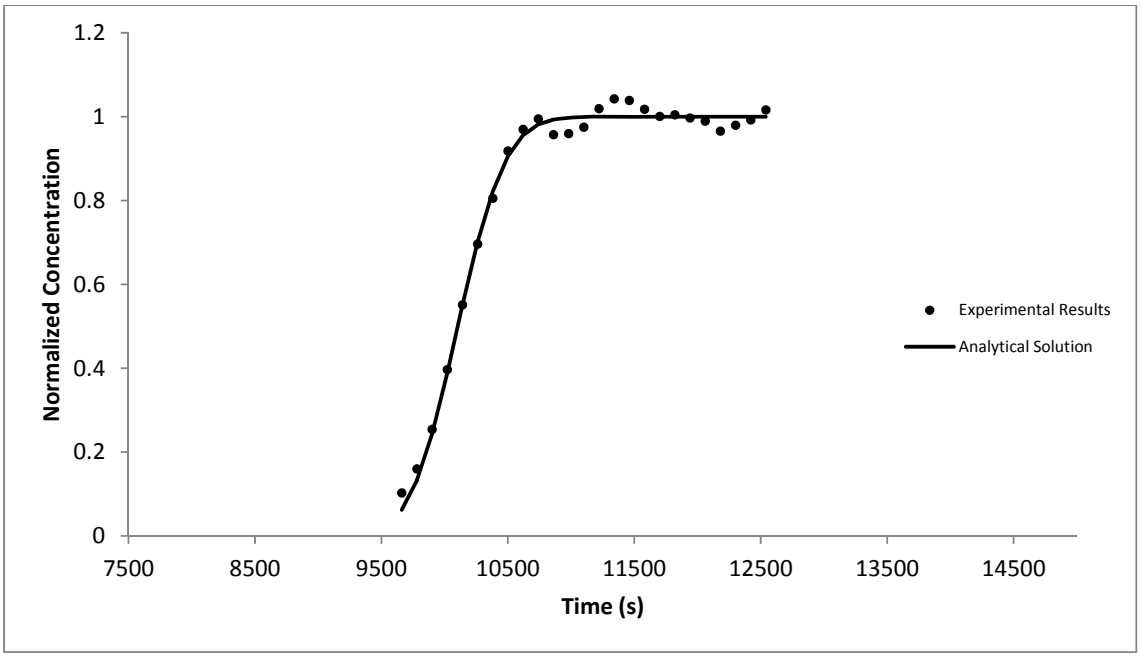

Figure 8.16. Comparison of the KBr breakthrough curve from the Experiment 29 with the analytical solution (Q=2.0 ml/min, α_{as}=0.24 mm)

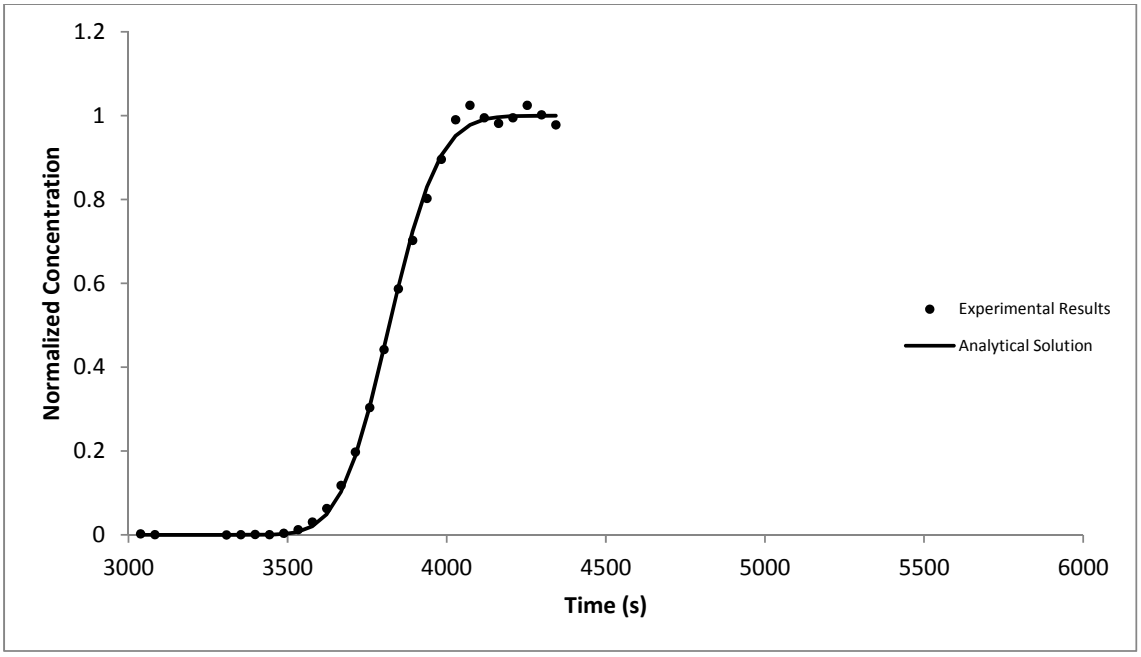

Figure 8.17. Comparison of the KBr breakthrough curve from the Experiment 30 with the analytical solution (Q=5.0 ml/min, α_{as}=0.30 mm)

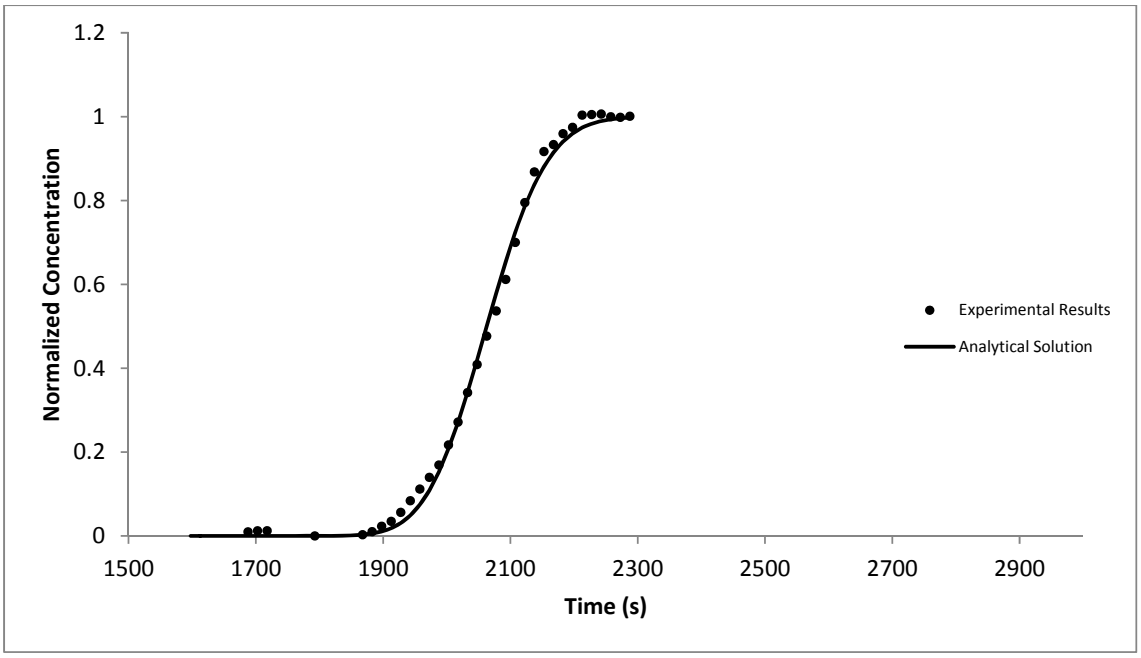

Figure 8.18. Comparison of the KBr breakthrough curve from the Experiment 31 with the analytical solution (Q=10 ml/min, α_{as}=0.39 mm)

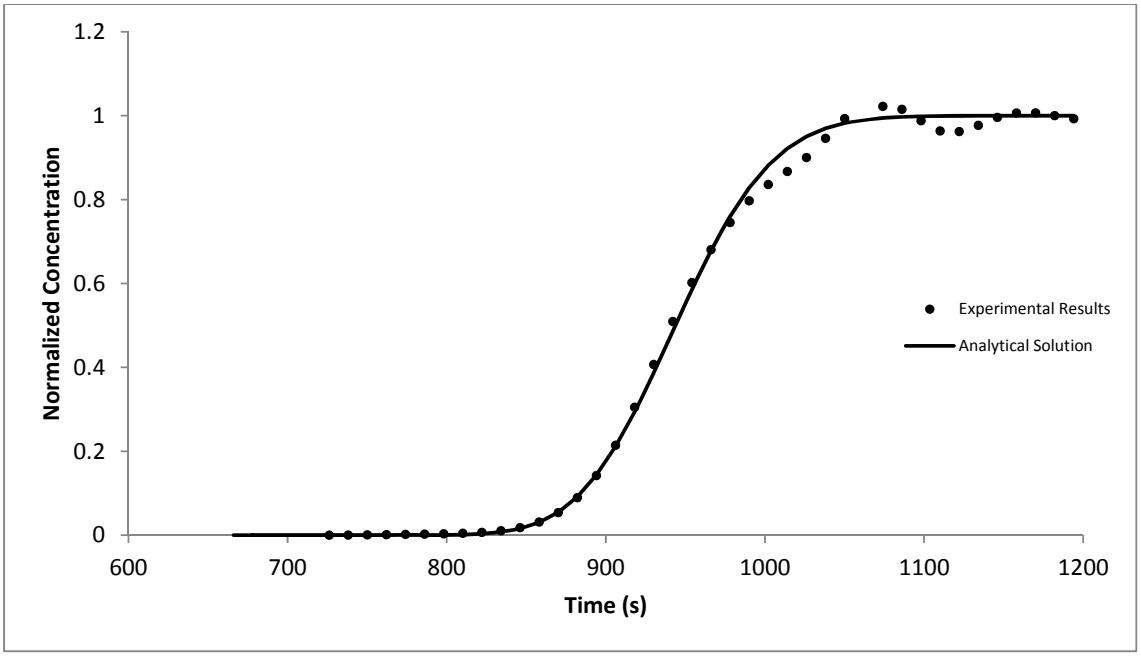

Figure 8.19. Comparison of the KBr breakthrough curve from the Experiment 32 with the analytical solution (Q=25 ml/min, α_{as}=0.77 mm)

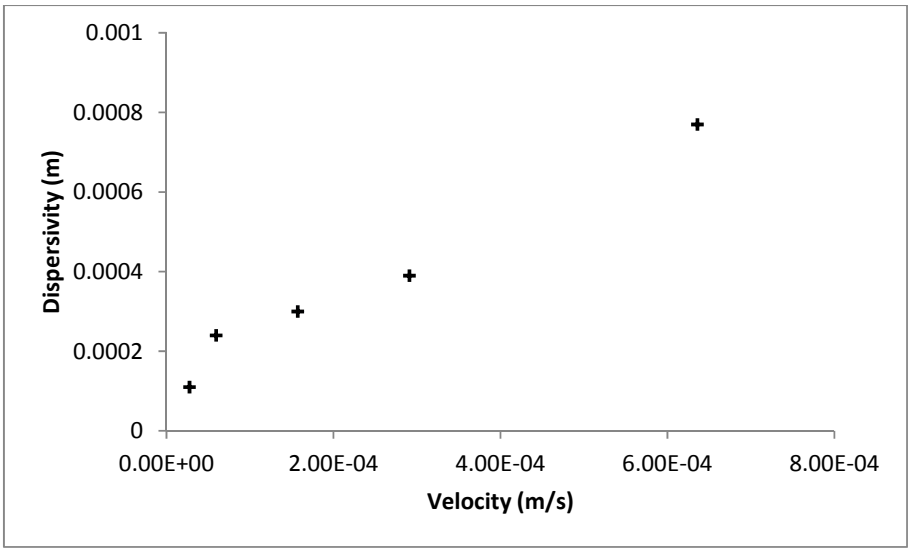

Figure 8.20. Apparent dispersivities of KBr vs average linear velocity
(Experiments 28-32, $C_{displacing}=10^{-2}$ M)

Figure 8.21 presents a scatter plot of KBr dispersion coefficients observed in mixture experiments 28 through 32 versus average linear velocity. The plot shows a non-linear trend of increase in dispersion coefficients with increase in flow rate.

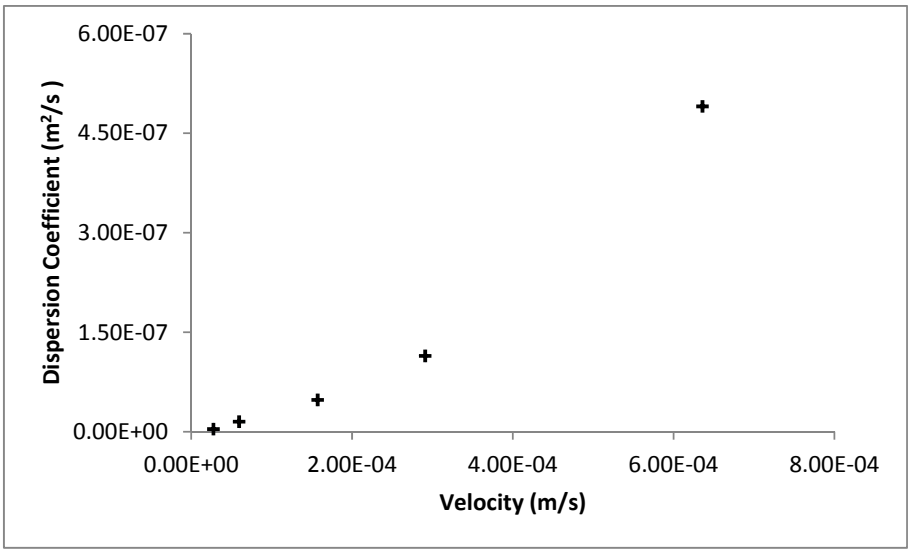

Figure 8.21. Dispersion coefficients of KBr vs average linear velocity
(Experiments 28-32, $C_{displacing}=10^{-2}$ M)

Figure 8.22 compares dispersion coefficients observed in mixture experiments for KBr with those observed in experiments 9 through 13. In other words it compares low concentration component of mixture experiments conducted in glass bead packed column to the tracer experiments with the same packing.

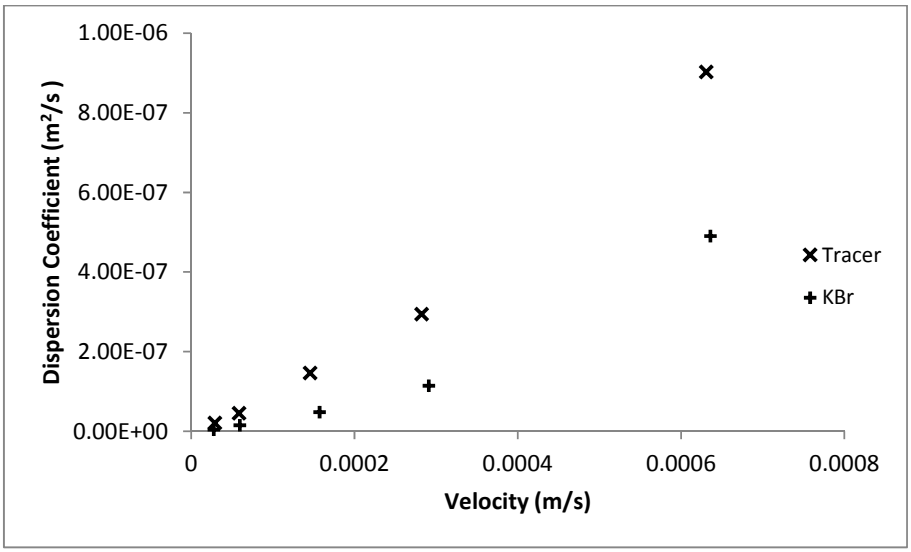

Figure 8.22. Comparison of KBr dispersion coefficients observed in mixture experiments to those observed in corresponding tracer experiments

Figure 8.8 and Figure 8.22 suggest that both high concentration and low concentration components of contaminant mixtures that cause significant density differences in the groundwater densities, behave in the same manner as brine.

9. NON-FICKIAN DISPERSION IN HETEROGENEOUS FIELDS

In previous chapters, the validity of Fick's Law and the alternative approaches for the modeling of hydrodynamic dispersion were discussed. Experimental evidence for deviation from the Fickian relationship was presented and a numerical analysis method for alternative theories was developed. On the other hand, all physical and mathematical models are subject to some simplifying assumptions that should be taken into account when using the modeling results out in the field. Simplifications are necessary for developing manageable models for the cost of accuracy. Most assumptions are made in the definition of the properties of the groundwater and the porous medium.

One example of simplifying assumption made in the physical model used for the experimental investigations was uniformity in the distribution of hydrogeological parameters that affect the flow whereas this homogeneity generally cannot be expected to exist in the field. Parallel to the laboratory experiments, numerical simulations described so far were also based on the assumption of homogeneous flow parameters, namely hydraulic conductivity. In order to account for the effect of heterogeneity in the distribution of hydraulic conductivity, Monte Carlo simulations were done. Monte Carlo simulations are a commonly used modeling approach that accounts for the impact of heterogeneity and uncertainty in the definition of input parameters on model predictions. This chapter describes these simulations and presents their results.

In most natural subsurface formations, the hydraulic conductivity is highly heterogeneous with complex patterns of spatial variability (e.g., Dagan, 1986). However, this variability is typically not fully reflected in models because the data needed for defining all the details of the field are not available and processing such large amounts of data is computationally inefficient. This lack of information ends up as uncertainty in the definition of input parameters which translates into uncertainty in model predictions. A common way for quantifying uncertainty in model predictions is the use of stochastic methods (Gelhar, 1993; Rubin, 2003).

Another aspect of heterogeneity that has to be taken into account in the context of hydrodynamic dispersion is that one component of hydrodynamic dispersion is the macrodispersion as mentioned in previous chapters. Macrodispersion is the spreading of the contamination due to preferential paths formed by the existence of layers of relatively higher hydraulic conductivities. As a consequence, dispersivities obtained for a medium, where large scale heterogeneities were absent, can not be used as a measure of dispersion in realistic hydrogeological settings even when a similar porous medium is in question (Dagan, 1994).

One simplifying assumption which is commonly used in modeling groundwater flow and contaminant transport is representing the hydraulic conductivity field by an apparent hydraulic conductivity. An apparent value is the observed value within the sensibility constraints of the measuring technique used. In general the apparent value reflects the effects of many elements that influence the observed value. In the determination of hydraulic conductivities in the field this is may represent some spatial average of point conductivities along the path where the apparent hydraulic conductivity was measured.

9.1. Monte-Carlo Simulations

Although a given real hydraulic conductivity field produces a single apparent hydraulic conductivity, there is no unique distribution of hydraulic conductivities to be found given an apparent value. For any apparent hydraulic conductivity value used in simulations based on homogeneous distributions, there are many heterogeneous distributions possible. One way of quantifying the uncertainty in the model predictions is to make Monte Carlo simulations.

Equiprobable values of the input parameters are repeatedly generated and each is used in the model simulations. The resultant model predictions are then statistically analyzed to assess the impact of heterogeneity. Monte Carlo methods rely on creating random realizations of possible distributions of the model input parameters and then computing model results based on them. Basically a Monte Carlo simulation is performed by defining the domain of possible inputs; generating possible input sets satisfying the statistical criteria of the domain and performing a deterministic computation using each input set.

Then the individual results are summarized into a single result using statistical techniques. In the context of this study, Monte Carlo simulations involve definition of the apparent hydraulic conductivity together with its ensemble statistical parameters, generating hydraulic conductivity fields based on these parameters and then making numerical model simulations using the generated hydraulic conductivity fields.

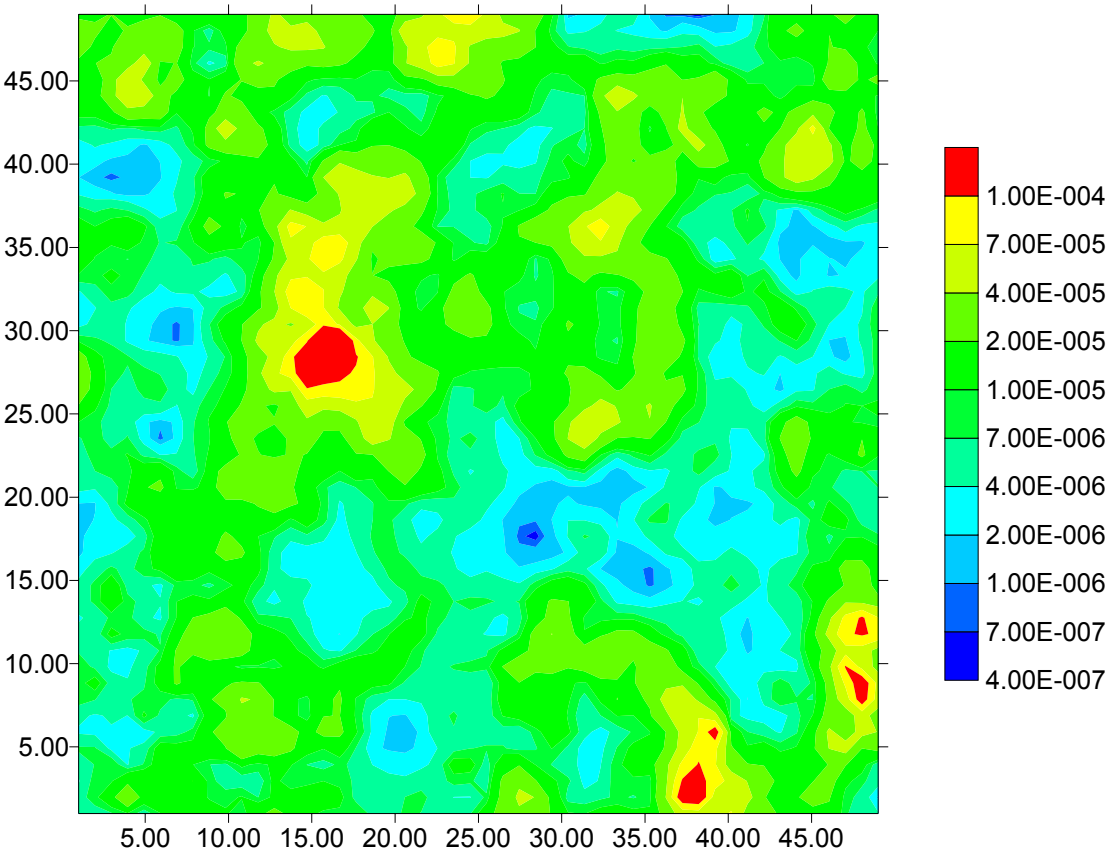

Figure 9.1. Example of the generated hydraulic conductivity field used in Monte Carlo Simulations

In order to investigate the effect of high concentration gradients on hydrodynamic dispersion in the presence of heterogeneity, Monte Carlo simulations involving 100 realizations of a 50 by 50 cells, vertical hydraulic conductivity field, were conducted. The developed numerical model was then used to simulate stable, upward transport in these hypothetical, two dimensional, heterogeneous domains. No flow boundaries conditions were imposed on the left and right-hand sides of the domain, while prescribed head

conditions were imposed on the upper and lower boundaries. The synthetic hydraulic conductivity fields were generated using a Gaussian random spatial function with exponential variogram (ln-K variance =1, integral scale = 5 length units). An example of the generated spatially-variable hydraulic conductivity fields is shown in Figure 9.1. In total 100 such fields were generated, all based on the same statistical parameters. Each hydraulic conductivity field was used for simulation of the advective dispersive transport twice, once using a Fickian dispersion model and once with the non-Fickian model.

9.2. Simulation Results

Each Monte Carlo simulation set is composed of 100 separate simulations conducted using the numerical model. As a result, each set contains 100 separate breakthrough curves. Since it is not feasible to analyze so many breakthrough curves individually, statistical techniques will be used in the analysis of the results. Specifically, the results of the Monte Carlo analysis will be presented in terms of:

- Ensemble mean and standard deviation of the concentration as a function of time at an observation point located at 35 length units downstream of the injection point,

- Zeroth, first, and second temporal moments of the concentration at the observation point. The zeroth and first order time moment are defined as:

$$m_n = \int_{\tau_1}^{\tau_2} t^n C(t) dt \tag{9.1}$$

where $C(t)$ is the normalized simulated concentration at the observation point, t is time and n=0 and 1 respectively. τ_1 and τ_2 are the start and end of the mixing zone defined to be between 0.01 and 0.99 C_0. The second-order central time moment is defined as:

$$m_2 = \int_{\tau_1}^{\tau_2} (t - m_1)^2 C(t) dt \tag{9.2}$$

Time-moments will be presented in terms of cumulative distribution functions (CDF).

Figure 9.2 shows the difference of the means of the concentrations observed at an observation point for Fickian and the non-Fickian sets. The arrival of the contamination to the observation point is delayed in the non-Fickian case. This observation suggests that less dispersion occurred when the dispersion model was non-Fickian, provided that the concentration gradient was high enough to cause deviation from Fickian behavior.

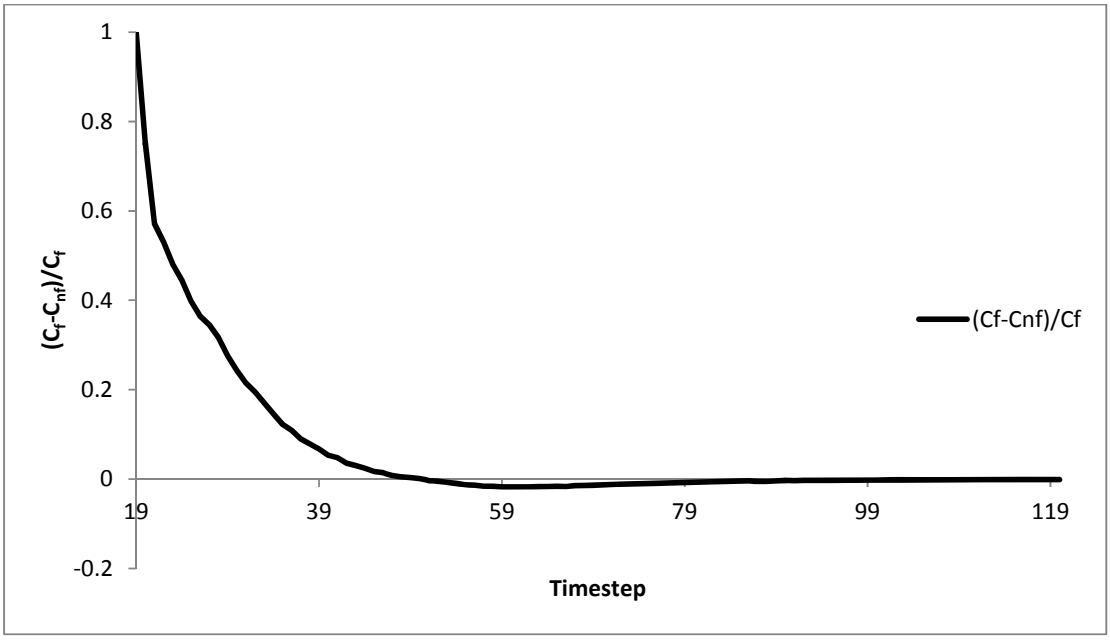

Figure 9.2. Relative difference of the means of the two sets (Fickian and non Fickian) as a function of time

Figure 9.3 compares the standard deviations of the simulated concentrations using the Fickian and the non-Fickian models as a function of time at the observation point. In each case, the standard deviation is computed from the 100 Monte Carlo simulations. The standard deviation reflects the uncertainty in the definition of the hydraulic conductivity. It can be seen in Figure 9.3 that the standard deviation was slightly changed by the non-Fickian behavior, which means that high concentration transport tends to affect the apparent impact of heterogeneity.

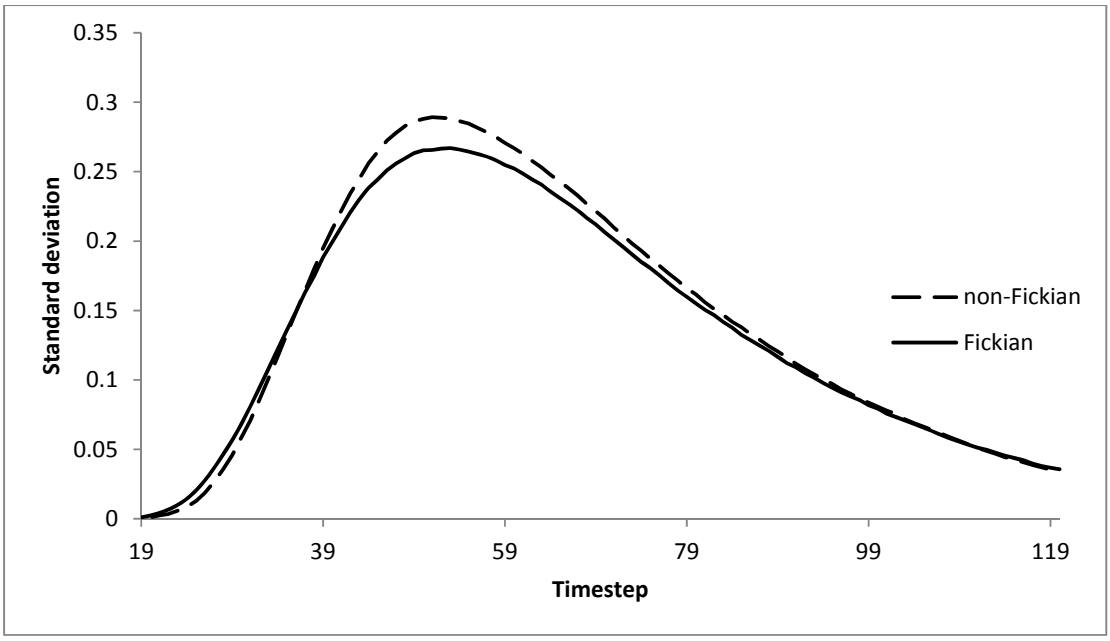

Figure 9.3. Relative difference of the standard deviations of the two sets (Fickian and non Fickian) as a function of time

Figure 9.4 compares the cumulative distribution functions of 0^{th} moments of Fickian and non-Fickian simulated concentrations. The zero moment (n=0, in Equation 9.1) is the measure of the mass in the mixing zone. For any given value of the 0^{th} moment, the probability of being lower than this value is higher for the non-Fickian set. Therefore, there is less mass in the mixing zone when the dispersion model is non-Fickian and concentration differences are high enough to effect dispersion. Having less mass in the mixing zone can especially have an impact on the reactive transport scenarios where most of the reactions occur in the mixing zone.

Figure 9.5 compares cumulative distribution functions of 1^{st} moments of Fickian and non-Fickian simulated concentration. The first moment (n=1, in Equation 9.1) is a measure of the average arrival time of the concentration. For any given value of the 1^{st} moment, the probability of being lower than this value is higher for the non-Fickian set. This means that the travel time in the mixing zone is shorter when the dispersion model is non-Fickian and concentration differences are high enough to effect dispersion.

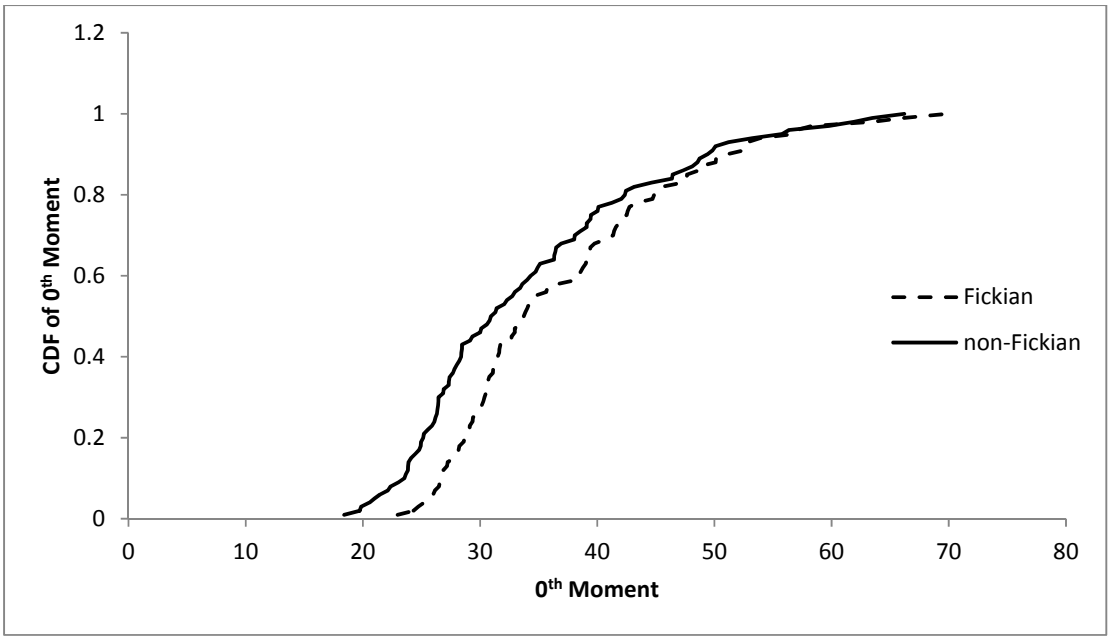

Figure 9.4. Cumulative distribution function of 0^{th} moments of the two sets (Fickian and non Fickian) as a function of time

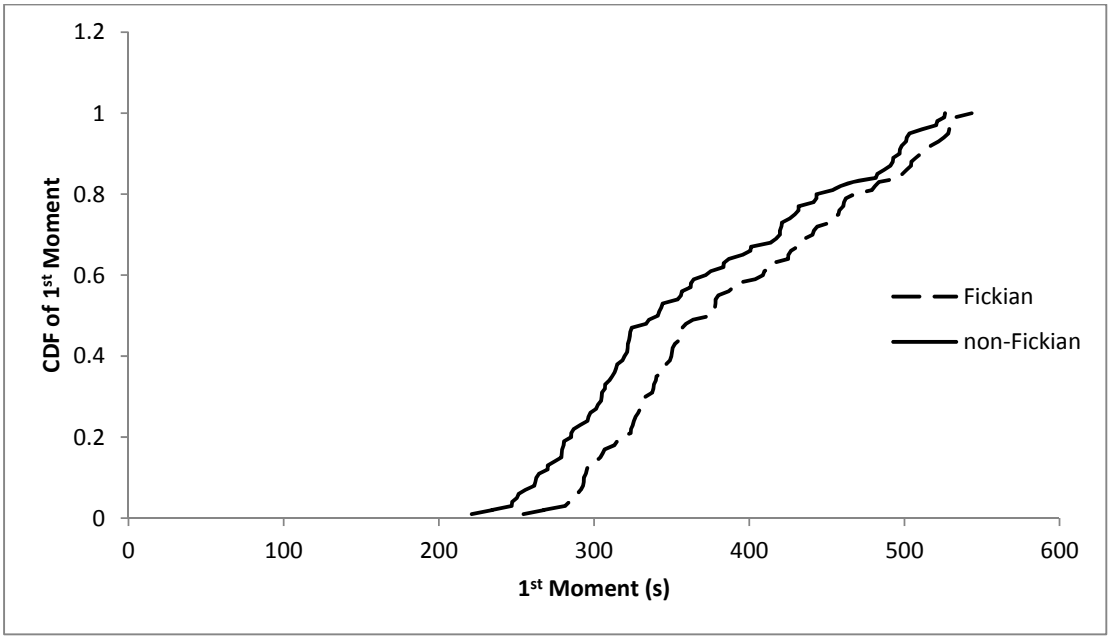

Figure 9.5. Cumulative distribution function of 1^{st} moments of the two sets (Fickian and non Fickian) as a function of time

Figure 9.6 compares cumulative distribution functions of 2nd moments of the Fickian and non-Fickian simulations. The second moment (Equation 9.2) is a measure of the spread of the concentration around the mean. This value reflects the dispersion in the simulated concentration due to Fickian/non-Fickian transport and the heterogeneity of the hydraulic conductivity field. For any given value of the 2nd moment, the probability of being lower than this value is higher for the non-Fickian set. This indicates that assuming Fickian transport when it is actually non-Fickian may lead to the over-estimation of the apparent dispersion due to heterogeneity.

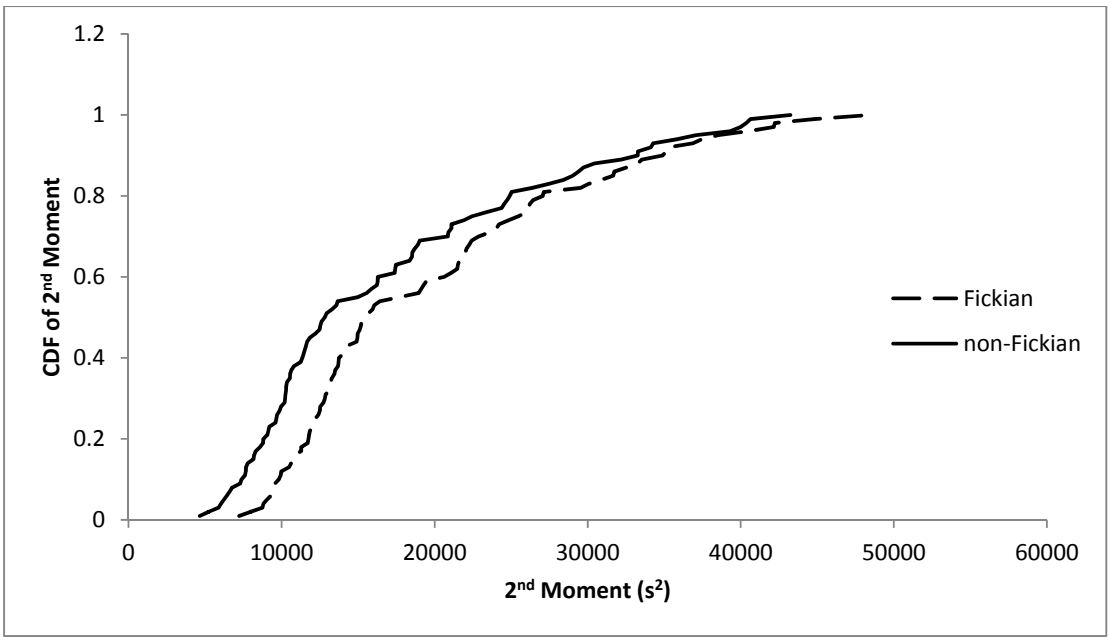

Figure 9.6. Cumulative distribution function of 2nd moments of the two sets (Fickian and non Fickian) as a function of time

Overall, this simple hypothetical example demonstrates the need to use an accurate dispersion model. Using Monte Carlo simulations with heterogeneous domains, the non-Fickian dispersion due to HCG resulted in less mass in the mixing zone (particularly significant for reactive transport modeling), delayed arrival time, and lower apparent dispersion.

10. CONCLUSIONS AND FUTURE RESEARCH

Although experimental evidence, including this study, suggests that the dispersive flux of contaminant transport in porous media is not a linear function of concentration difference, it has been customary to contaminant hydrogeologists to adopt a Fickian type equation to represent hydrodynamic dispersion term in groundwater transport equation. In recent years, efforts have been directly to define and quantify the "non-Fickian" effect on dispersive behavior, particularly due to consideration of salt formations as final repositories for high-level radioactive wastes.

Both experimental and modeling studies published to date had limitations in their scope. Experimental studies involved mostly homogeneous porous media and single species transport, whereas most modeling efforts focused on defining dispersion parameters as function of concentration gradients or velocities. However, in order to fully understand the dispersive behavior under high concentration gradient conditions and to make confident predictions of transport in realistic hydrogeological settings there is still need for more research and a transport model which can account for the effect of concentration gradients and velocity for conditions similar to those encountered in the field

In order to gain further insight into this phenomenon, experiments of miscible displacement were conducted for a range of concentration differences and velocities as well as multiple contaminants. The experiments were conducted using a water-saturated vertical column filled with either sand or glass beads. A non-linear dispersion model from the literature, which allows for predicting dispersion behavior starting with basic transport parameters, was calibrated based on the observed experimental results and incorporated into a computer code developed for numerically solving partial differential equations governing groundwater flow and contaminant transport in porous media. The developed model was used to simulate a hypothetical groundwater contamination problem with high density differences, in a heterogeneous hydrogeological setting to investigate mutual effects of high concentration gradient conditions and porous medium heterogeneity. The following sections summarize the main findings and conclusions of each component followed by recommendations for future research.

The first part of the experimental component of the study involved tracer tests. The aim of conducting tracer tests is to investigate the validity of the Fick's Law in transport problems where density differences are relatively small as well as to test the reliability of the experimental setup and determine the basic transport parameters for use in the analysis of both low and high concentration gradient dispersion conditions. The following observations are made.

- Predictions of hydrodynamic dispersion under low concentration gradient conditions can be modeled using a Fickian type equation, within acceptable error margins. However, apparent dispersivities show a slight dependence on velocity, contradicting with the Fickian definition of the parameter.
- The apparent dispersivities observed are around 4.9×10^{-4} m for the sand filled column and 9.9×10^{-4} for the coarser glass bead filled column, which are roughly 1/1000 and 1.5/1000 of the travel distance, respectively.

The second part of the experimental component included both brine experiments with varying concentration differences and brine experiments with varying flow rates. Brine experiments were conducted in order to investigate the validity of both the linear and non-linear dispersion theories. Additionally, dispersion parameters needed to account for the effect of under high concentration gradient conditions were determined for flow and transport conditions beyond those already investigated in published studies. The conclusions drawn from the results of brine experiments, particularly in their relation to the findings from the tracer experiments, are listed below.

- A decrease in dispersive flux was clearly observed with increase in concentration difference, for similar flow conditions and same experimental setup.
- The apparent dispersivities decreased by a factor of four as the displacing concentration increased from 10^{-3} M to 1 M, while the resident concentration was maintained equal to zero.
- The dispersive flux was also found to decrease with decrease in flow rates for the same high concentration difference.

- Apparent dispersivities observed in brine experiments were up to 20 times lower than the apparent dispersivities observed in the tracer experiments, depending on the flow rate.
- A regression equation was developed to account for the deviation from Fickian behavior, for the range of velocities considered in the experiments and for the non-linear dispersion model proposed by Hassanizadeh and Leijnse (1995).

Although a dispersion model was chosen for modeling contaminant transport under high concentration gradient conditions and validated for realistic groundwater flow rates, no data exists for the dispersive behavior of a low concentration contaminant transported together with a high concentration contaminant, such as brine. To study the effect of large density differences on the dispersive transport of a dilute solute, mixture experiments were conducted. Mixture experiments indicated to the following conclusions.

- Both the high and low concentration contaminants in a high density mixture behave similar to single species brine.
- The deviation from Fick's Law is not necessarily caused by the concentration of the contaminant in question but by the total concentration of all dissolved species.
- In mathematical model, vertical dispersion of all solute components of a high density mixture may be represented using the non-linear theory and the empirical relationship constituted using results of single-species brine experiments.

The non-Fickian dispersion model, validated and calibrated using experimental results, was developed into a computer program which numerically solves the governing non-linear partial differential equations describing density-dependent groundwater flow and contaminant transport. Monte-Carlo simulations were made using the developed program in order to quantify the effect of high concentration gradients on hydrodynamic dispersion in heterogeneous hydrogeological settings. Time moment analysis of the results showed that non-Fickian dispersive behavior caused by high concentration gradients has the following consequences on the transport of contaminants.

- Less contaminant mass resides in the mixing zone. The decrease in the volume of groundwater with transition concentrations may especially have an effect on reactive transport problems where highest reaction rates are observed in the mixing zone.
- Dispersive fluxes observed in the transport of fluids with densities significantly differing from the density of ambient groundwater may be lower than dispersive fluxes that would be observed in tracer tests. Reduction in the apparent values of dispersivity may result in incorrect model predictions.
- Arrival of contaminants may be delayed in heterogeneous hydrogeological settings when high concentration gradients exist. The increase in the arrival times may cause misinterpretation of aquifer parameters.

In summary, laboratory experiments confirmed that large density differences cause deviations from the commonly accepted Fickian behavior for all dissolved species in the dispersive transport of contaminants in porous media, and simulations made using the alternative non-Fickian model suggested that this deviation may have significant effects on the interpretation of the transport data and on the remediation efforts. However, more effort is needed to further enhance our knowledge in the transport of contaminants where high concentration gradients exist.

- Experimental studies with a larger range of concentration gradients and/or other solutes will clarify the dependence of deviation from Fickian behavior on the concentration differences and allow for better estimation of dispersivity values.
- Experiments using real mixtures, such as landfill leachates or NAPL flusing effluents, will improve applicability of the results to real environmental problems.
- Brine experiments with a larger range of velocities, particularly, for very low velocities were molecular diffusion becomes the dominant transport process, will increase the confidence and applicability of the relationship that defines the coefficient of high concentration gradient effect, β, as a function of Darcy velocity. The experiments with lower velocities where diffusion is the main

transport (low Peclet numbers) will show how diffusion is affected by density differences.

- Experiments in two- or three-dimensional physical models, where there is less constraints on the flow pattern will allow for more realistic determination of dispersion parameters and their variations with flow and transport conditions. Multi-dimensional experimental setups will also allow for designing heterogeneous physical models which may be used for determining combined effects non-Fickian behavior and heterogeneity.
- Two-dimensional experimental setups may also be specially designed for horizontal flow where the transverse dispersivity, aligned with the vertical direction may be observed.
- High concentration tracer tests conducted in the field will also include the effects of large scale heterogeneities of natural subsurface systems.
- More non-Fickian transport model simulations including the seawater intrusion problem, transport in the vicinity of a salt dome, groundwater remediation through injection of fluids with large contrasts in densities may be performed to assess the impact of high concentration gradients on model predictions.

REFERENCES

Anderson, M. P., 1984. Movement of Contaminants in Groundwater: Groundwater Transport– Advection and Dispersion. In National Research Council, Groundwater Contamination, National Academy Press.

Anderson, S. J., 1997. An experimental investigation of high concentration displacements in saturated porous media. Ph.D. thesis, The University of Western Australia.

Ataie-Ashtiani, B., Hosseini, S. A., 2005. Error analysis of finite difference methods for two-dimensional advection–dispersion–reaction equation. Advances in Water Resources, 28, 793–806.

Bear, J., 1961a. Some Experiments in Dispersion. Journal of Geophysical Research, 66, 8, 2455-2467.

Bear, J., 1961b. On the Tensor Form of Dispersion in Porous Media. Journal of Geophysical Research, 66, 4, 1185-1197.

Bear, J., 1972. Dynamics of fluids in porous media. American Elsevier Publishing Co.

Bear, J., 1979. Hydraulics of groundwater. McGraw-Hill.

Ben Salah, M. D., 1965. Influence des contrastes de viscosité et de densité sur le déplacement en milieu poreux de deux fluides miscibles. Revue de l'Institut Français du Pétrole, 20, 1237-1255.

Boehme, J. et al., 1985. Grundwasserbewegung im Deckgebirge über dem Salzstock Gorleben, Datenermittlung, Interpretation und Modellrechnungen. Report KWA 5107/3, Federal Institute for Geosciences and Natural Resources, Hannover.

Bouhroum, A., 1985. Beitrag zur Verdrängung mischbarer Flüssigkeiten in porösen Medien unter Berücksichtigung der Dichte - und Viskosität - Unterschiede. Genehmigte Dissertation von der Fakultät für Bergbau, Hüttenwesen und Maschinenwesen der Technischen Universität Clausthal.

Bouhroum, A., 1988. Einfluss der Viskosität - und Dichteunterschiede zweier mischbarer Flüssigkeiten auf den Koeffizienten der longitudinalen hydrodynamischen Dispersion. Teil I Viskositatsunterschiede. Deutsche Gewasserkundliche Mitteilungen, 32, 144-154.

Bouhroum, A., 1989. Einfluss der Viskosität - und Dichteunterschiede zweier mischbarer Flüssigkeiten auf den Koeffizienten der longitudinalen hydrodynamischen Dispersion. Teil II Dichteunterschiede. Deutsche Gewasserkundliche Mitteilungen, 33, 9-13.

Brigham, W. E., Reed, P. W., and Dew, J. N., 1961. Experiments on mixing during miscible displacements in porous media. Society of Petroleum Engineers Journal, 1, 1-8.

Cussler, E., 2007. Diffusion - Mass Transfer in Fluid Systems 3rd ed., Cambridge University Press.

Dagan, G., 1982. Analysis of flow through heterogeneous random aquifers. 2. Unsteady flow in confined formations, Water Resources Research 18(5), 1571–1585.

Dagan, G., 1984. Solute transport in heterogeneous porous formations. Journal of Fluid Mechanics, 145, 151-177.

Dagan, G., 1986. Statistical Theory of Groundwater Flow and Transport: Pore to Laboratory, Laboratory to Formation, and Formation to Regional Scale, Water Resources Research, 22, 120-134.

Dagan, G., 1994. The significance of heterogeneity of evolving scales to transport in porous formations, Water Resources Research 30(12), 3327–3336.

Dagan, G., and Neuman, S.P., Editors, 1997. Subsurface Flow and Transport: A Stochastic Approach, Cambridge University Press.

Darcy, H., 1856. Les Fontaines Publiques de la Ville de Dijon, Dalmont, Paris.

De Jong, G. D. J., and Bossen, M. J., 1961. Discussion of paper by J. Bear, On the tensor form of dispersion, Journal of Geophysical Research, 10, 66, 3623-3624.

Domenico, P. A., Schwartz, F. W., 1990. Physical and Chemical Hydrogeology, Second Edition, John Wiley & Sons, Inc., New York.

Fick, A., 1855. Poggendorff's Annel. Physik. 94, 59.

Frape, S. K., Fritz, P., and McNutt, R. H., 1984. Water-rock interaction and chemistry of groundwaters from the Canadian Shield. Geochemica et Cosmochimica Acta, 48, 1617-1627.

Freeze, R. A., Cherry, J. A., 1979. Groundwater, Prentice-Hall.

Fried, J. J., 1975. Groundwater Pollution, American Elsevier Publishing Company, Inc., New York.

Gelhar, L. W. and Axness, C. L., 1983. Three dimensional stochastic analysis of macrodispersion in aquifers. Water Resources Research, 19, 1, 161-180.

Gelhar, L. W., and Axness C. L., 1981. Stochastic analysis of macrodispersion in three-dimensionally heterogeneous aquifers. Geophysical Research Center, Hydrology Research Program. Rep. No. H8. New Mexico Inst. Of Mining and Technology, Socorro, New Mexico.

Gelhar, L. W., Gutjahr, A. L., and Naff, R. L., 1979. Stochastic analysis of macrodispersion in a stratified aquifer, Water Resources Research, 15, 1387- 1397.

Gelhar, L. W., 1993, Stochastic Subsurface Hydrology, Prentice Hall.

Guo, W. and Langevin, C. D., 2002. User's guide to SEAWAT: A computer program for simulation of three-dimensional variable-density ground-water flow: U.S. Geological Survey Open-File Report 01-434, 79 p.

Harbaugh, A. W., Banta, E. R., Hill, M.C., McDonald, M.G., 2000. MODFLOW-2000, The U.S. Geological Survey modular ground-water model–User Guide to modularization concepts and the ground-water flow process: U.S. Geological Survey, Reston, VA.

Hassanizadeh, S. M., 1986a. Derivation of basic equations of mass transport in porous media, Part 1. Macroscopic balance laws. Advances in Water Resources, Vol. 9, 196-206.

Hassanizadeh, S. M., 1986b. Derivation of basic equations of mass transport in porous media, Part 2. Generalized Darcy's and Fick's laws. Advances in Water Resources, Vol. 9, 207-222.

Hassanizadeh, S. M., Leijnse, A., De Vries, W. J. and Stapper, R. A. M., 1990. Experimental study of brine transport in porous media, Report 728514005, RIVM, Bilthoven, The Netherlands.

Hassanizadeh, S. M., Leijnse, T, 1995. A non-linear theory of high concentration gradient dispersion in porous media. Advances in Water Resources; 18, 203-215.

Hill, S., 1952. Channeling in packed columns. Chemical Engineering Science, 1, 6, 247-253.

Jiao, C. Y., 2001. Miscible displacements in porous media with variation of fluid density and viscosity. PhD Thesis, University of Karlsruhe, Germany.

Jiao, C. Y. and Hötzl, H., 2004. An experimental study of miscible displacements in porous media with variation of fluid density and viscosity. Transport in Porous Media, 54, 125-144.

Johannsen, K., Kinzelbach, W., Oswald, S., and Wittum, G., 2002. The saltpool benchmark problem - numerical simulation of saltwater upconing in a porous medium. Advances in Water Resources, 25, 3, 335-345.

Kempers, L. J. T. M. and Haas, H., 1994. The dispersion zone between fluids with different density and viscosity in a heterogeneous porous medium. Journal of Fluid Mechanics, 267, 299-324.

Kempers, L. J. T. M., 1991. Dispersive mixing in stable and unstable miscible displacements. PhD Thesis, Delft University of Technology, the Netherlands.

Kolditz, O., Ratke, R., Diersch, H.J. and Zielke, W., 1998. Coupled groundwater flow and transport: 1. Verification of density variable flow and transport models. Advances in Water Resources, 21, 27-46.

Kretz, V., Berest, P., Hulin, J. P., and Salin, D., 2003. An experimental study of the effects of density and viscosity contrasts on macrodispersion in porous media. Water Resources Research, 39, 2, 1032-1040.

Krupp, H. K. and Elrick, D. E., 1969. Density effects in miscible displacement experiments. Soil Science, 107, 5, 372-380.

Lambe, T. W. and Whitman, R. V., 1969. Soil Mechanics, John Wiley and Sons, New York.

Langevin, C. D., Shoemaker, W. B., and Guo, W., 2003. "MODFLOW-2000, the USGS modular groundwater model—Documentation of the SEAWAT 2000 version with variable-density flow process (VDF) and the integrated MT3DMS transport process (IMT)." USGS Open File Rep. 03-426.

Leroy, C., Hulin, J. P., and Lenormand, R., 1992. Tracer dispersion in stratified porous media: influence of transverse dispersion and gravity. Journal of Contaminant Hydrology, 11, 51-68.

Lewis J., and Sjöstrom, J., 2010. Optimizing the experimental design of soil columns in saturated and unsaturated transport experiments. Journal of Contaminant Hydrology, 115, 1-13.

Mannhardt, K., and Nasreldin, H. A., 1994. A review of one-dimensional convection-dispersion models and their applications to miscible displacement in porous media. In Situ, 18, 277–345.

Matheron, G., and de Marsily, G., 1980. Is transport in porous media always diffusive? Water Resources Research, 16, 901-917.

Moser, H., 1995. Einfluß der Salzkonzentration auf die hydrodynamische Dispersion im porösen Medium. Technical University of Berlin, Germany

Nikolaevskii, V. N., 1959. Convective diffusion in porous media. J. Appl. Math. Mech. (P. M. M.), 6, 23, 1042-1050.

Ogata, A., Banks, R.B., 1961. A solution of the differential equation of longitudinal dispersion in porous media. U. S. Geological Survey Professional Papers 411-A

Oldenburg, C. M., Pruess, K., 1995. Dispersive Transport Dynamics in a Strongly Coupled Groundwater-Brine Flow System. Water Resources Research, 31, 2, 289-302.

Oswald S., 1998. Dichteströmungen in porösen Medien: Dreidimensionale Experimente und Modellierung. PhD Thesis, Institut für Hydromechanik und Wasserwirtschaft, ETH Zürich.

Pfannkuch, H.O., 1963. Contribution a l'étude des déplacements de fluides miscibles dans un milieu poreux. Revue de l'Institut Français du Pétrole, 18, 215-270.

Pinder, G. F. and Cooper, H. H. Jr., 1970. A Numerical technique for calculating the transient position of the saltwater front. Water Resources Research, 6(3), 875-882.

Roxburg, I. S., 1987. Geology of High-Level Nuclear Waste Disposal. Chapman and Hall, London.

Rubin, Y., 2003. Applied Stochastic Hydrogeology, Oxford University Press, New York

Sander, W. and Herbert, H. J., 1985. NaCl crystallization at the MgCl2/NaCl solution boundary - a possible natural barrier to the transport of radionuclides. Mineralogical Magazine, 49, 265-270.

Scheidegger, A. E., 1954. Statistical hydrodynamics in porous media. Journal of Applied Physics, 25(8), 994-1001.

Scheidegger, A. E., 1960. The Physics of flow through Porous Media. Revised edition, University of Toronto Press.

Schotting, R. J., Moser, H., Hassanizadeh, S. M., 1999. High-concentration gradient dispersion in porous media: experiments, analysis and approximations. Advances in Water Resources; 22, 655-680.

Schwartz, F. W., 1977. Macroscopic Dispersion in Porous Media: The Controlling Factors. Water Resources Research, 13(4): 743-752.

Slichter, C. S., 1905. Field measurements of the rate of underground water. U. S. Geological Survey Water Supply Papers, 140, 9-85.

Slobod, R. L. and Howlett, W. E., 1964. The effects of gravity segregation in laboratory studies of miscible displacement in vertical unconsolidated porous media. Society of Petroleum Engineers Journal, 4, 1-8.

Smith, L., and Schwartz, F. W., 1980. Mass Transport, 1. A Stochastic Analysis of Macroscopic Dispersion. Water Resources Research, 16(2), 303-313.

Sohn, H. Y., Moreland, C., 1968. The effect of particle size distribution on packing density. Canadian Journal of Chemical Engineering, 46:162-7.

Spitz, K., Dispersion in Porösen Medien: Einfluss von Inhomogenität und Dichteunterschieden. Mitteilungen Heft 60, Institut für Wasserbau, Universität Stuttgart, 1985.

Starr, J. L. and Parlange, J., 1976. Solute dispersion in saturated soil columns. Soil Science, 121, 6, 364-380.

Stheeman, H. A., 1963. Petroleum development in the Netherlands, with special reference to the origin, subsurface migration and geological history of the country's oil and gas resources. Verhandelingen van het Koninklijk Nederlands Geologisch Mijnbouwkundig Genootschap: Geologische Serie, 21, 57-95.

Sudicky, E. A., and Cherry, J. A., 1979. Field observations of tracer dispersion under natural flow conditions in an unconfined sandy aquifer. Water Pollution Research Journal of Canada, 14, 1-17

Taylor, G. I., 1921. Diffusion by continuous movements. Proceedings London Mathematical Society, 2 (20), 196-212.

Taylor, G. I., 1953. The dispersion of soluble matter in solvent flowing slowly through a pipe. Proceedings of the Royal Society of London. Series A., 219, 189-203.

Visser, W. A., 1974. Waste disposal and underground waters. Geologie en Mijnbouw, 53, 249-256.

Voss, C. I., Provost, A. M., 2003. SUTRA, A model for saturated-unsaturated, variable-density ground-water flow with solute or energy transport: U.S. Geological Survey Water-Resources Investigations Report 02-4231, U.S. Geological Survey, Reston, Virginia.

Wang, H. F. and M. P. Anderson, 1982. Introduction to groundwater modeling: Finite difference and finite element methods. Freeman and Co, 237 pp.

Wentworth, C.K., 1922. A scale of grade and class terms for clastic sediments. The Journal of Geology, 30, 377–392.

Watson, S. J., Barry, D. A., Schotting, R. J., and Hassanizadeh, S. M., 2002b. On the validity of Darcy's law for stable high-concentration displacements in granular porous media. Transport in Porous Media, 47, 149-167.

Watson, S. J., Barry, D. A., Schotting, R. J., and Hassanizadeh, S. M., 2002a. Validation of classical density-dependent solute transport theory for stable, high-concentration gradient brine displacements in coarse and medium sands. Advances in Water Resources, 25, 611-635.

Zheng, C., Wang, P.P., 1999. MT3DMS: A modular three-dimensional multispecies transport model for simulation of advection, dispersion, and chemical reactions of contaminants in groundwater systems; documentation and user's guide, Contract Report SERDP-99-1, U.S. Army Engineer Research and Development Center, Vicksburg, MS.

Zeynel, A., 2002. Ana tahliye kanalındaki ağır metallerin Tuz Gölü'ne etkisi. MSc Thesis, Mühendislik ve Fen Bilimleri Enstitüsü, Gebze Yüksek Teknoloji Enstitüsü, İstanbul.

APPENDIX A: ANALYSIS OF SAND USED FOR PACKING

siltaş
SİLİS KUMLARI SAN. ve TİC. A.Ş.
Mrk.Tel: (216) 335 70 00-09 - Faks: 335 71 57
Fab1.Tel: (216) 732 83 72 - Faks: 732 85 00
Fab2.Tel: (216) 731 35 98-99 - Faks: 731 35 88

Döküm Kumu Numune Kalite Kontrol Raporu

Ürün Adı	60/70 AFS
Rapor No	KKG 02
Üretim/Parti No	KKC06A6
Müşteri	BOĞAZİÇİ ÜNİVERSİTESİ
Vasıta Plaka No	
Fabrika Çıkış Tarihi	05.07.2006

Sıra No	Muayene ve Deneyler	İlgili Standartlar
1	Elek Analizi	TS 5426 / 5425

elek göz açıklığı (mm)	elek üstü a (gr)	elek üstü b (%)	elek altı c (%)	elek üstü küm	elek altı küm.
		0,00	0,00	0,00	100,00
1,400	0,000	0,00	0,00	0,00	100,00
1,000	0,000	0,00	0,00	0,00	100,00
0,710	0,000	0,00	0,00	0,00	100,00
0,500	0,000	0,00	0,66	0,00	100,00
0,355	0,330	0,66	14,13	0,66	99,34
0,250	7,060	14,13	51,62	14,79	85,21
0,180	25,790	51,62	31,93	66,41	33,59
0,125	15,950	31,93	1,58	98,34	1,66
0,090	0,790	1,58	0,08	99,92	0,08
0,063	0,040	0,08	0,00	100,00	0,00
0,020	0,000	0,00	0,00	100,00	0,00
Toplam	49,96	100,00	100,00		

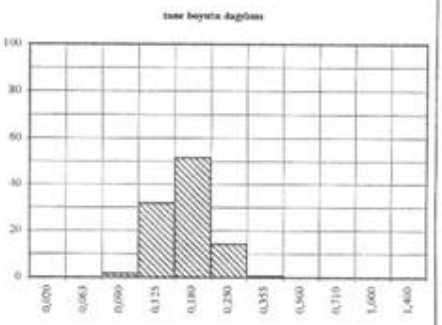

Tane Boyutu		Sonuçlar
	AFS	65,42
	Mikron	203,95

2 Teorik Özgül Yüzey (cm^2/g)		115,97

3 Dağılım Katsayısı ($S_o=Q_1/Q_3$)		1,41
	Q_1 (mm)	0,24
	Q_3 (mm)	0,17

4 Ortalama Tane Büyük. (Mk-M50)		0,20	50
	2/3 Mk	0,14	5
	4/3 Mk	0,27	89
	Homojenlik Derecesi %		84

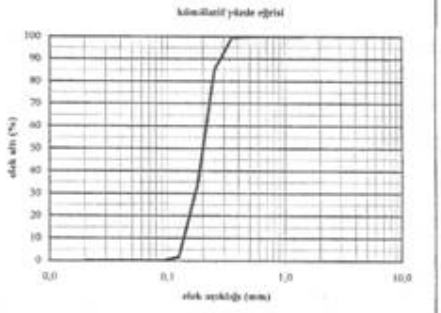

Sıra No	Muayene ve Deneyler		İlgili Standartlar	Sınır değerler	Sonuçlar 1.Num	Sonuçlar 2.Num	Numune İçindir.
5	Görle Muayene		TS 5426		OK		
6	Bileşim		TS 2979				
		SiO_2 %			98,6		
		Fe_2O_3 %			0,23		
		CaO + MgO %			0,02+0,00		
		Na_2O + KO %			0,07+0,11		
		Al_2O_3 %			0,54		
7	Kızdırma Kaybı %		TS 2980		0,25		
8	Sinterleşme Sıcaklığı °C		TS 5426		>1500		Müşteri Şartnâme No:
9	Kil %		TS 5426				Yayın Tarihi:
10	Rutubet %		TS 3084				

Deneyi Yapan				Onay			
K.K.Teknisyeni	İmza	Tarih	Saat	K.G.Müdürü	İmza	Tarih	Saat
R.YÖRÜK		05/07/06	16:40	T.YILDIZ		05/07/06	16:42

APPENDIX B: LIST OF FORTRAN PROGRAM

```
Implicit double precision (a-h,o-z)
  Parameter(nz0=101,ny0=3,nt0=400)

Dimension dz(nz0),dy(ny0),dt(nt0)
Dimension conc1(nz0,ny0),conc2(nz0,ny0),conc3(nz0,ny0)
  Dimension rho1(nz0,ny0),rho3(nz0,ny0)
Dimension omega1(nz0,ny0),omega3(nz0,ny0)
Dimension h1(nz0,ny0),h2(nz0,ny0),h3(nz0,ny0)
Dimension qz1(nz0,ny0),qz3(nz0,ny0)
Dimension qy1(nz0,ny0),qy3(nz0,ny0)
Dimension dispcoz1(nz0,ny0),dispcoy1(nz0,ny0)
Dimension dispcoz3(nz0,ny0),dispcoy3(nz0,ny0)
Dimension dispfluz1(nz0,ny0),dispfluy1(nz0,ny0)
Dimension dispfluz3(nz0,ny0),dispfluy3(nz0,ny0)
Dimension hyc(nz0,ny0)

C     OPEN DATA FILES
   Open(3,file="hydrcond.in",status="unknown")
   Open(4,file="initial.out",status="unknown")
   Open(5,file="qz.out",status="unknown")
   Open(6,file="qy.out",status="unknown")
   Open(7,file="dispcoz.out",status="unknown")
   Open(8,file="dispcoy.out",status="unknown")
   Open(9,file="rho.out",status="unknown")
   Open(10,file="conc.out",status="unknown")
   Open(11,file="normconc.out",status="unknown")
    Open(12,file="converge.out",status="unknown")
    Open(13,file="kare.out",status="unknown")
    Open(14,file="prmtr.in",status="unknown")
```

```
C     FINISHED OPENING DATA FILES



C     READ MODELING PARAMETERS
c     Dispersion model index: 1. non-Fickian 2. Fickian
      read(14,*)idispersion
c     Non-Fickian formulation index: 1. Square root 2. Division
      read(14,*)inonfickian
c     Heterogeneity index: 1. Homogeneous 2. Heterogeneous
      read(14,*)iheterogeneity
c     Weighting index: 1. Central 2. Upstream 3. TVD
      read(14,*)iweighting
c     Transport condition index: 1. None 2. <concs
      read(14,*)itcondition
c     Steady state (constant density) flow index: 1. Steady state 2. Transient
      read(14,*)istdflow
c     The number of timesteps after which selected values will be written to output files
      read(14,*)intervalout
C     FINISHED READING MODELING PARAMETERS



C     TIME AND SPACE DISCRETIZATION
c     Timestep length (s)
      read(14,*)dt0
c     Cell height and width (m)
      read(14,*)dz0
     read(14,*)dy0
c     Grid dimensions      in z
      do 50 i=1,nz0
      dz(i)=dz0
50    continue
c     Grid dimensions      in y
```

```
      do 51 j=1,ny0
      dy(j)=dy0
51    continue
c     Timestep lengths
      do 55 n=1,nt0
      dt(n)=dt0
55    continue
C     DISCRETIZATION FINISHED


C     READ GLOBAL CONSTANTS
c     Coefficient that relates density to mass fraction (0.6923 in Schotting et al 1999)
      read(14,*)gamma
c     Specific density of water (kg/m3)
      read(14,*)rho0
c     FINISHED READING GLOBAL CONSTANTS


c     READ PROBLEM SPECIFIC CONSTANTS
c     Dispersivity (m) in z direction (0.001 in Schotting et al 1999 for L=130 cm)
      read(14,*)alphaz
c     Dispersivity (m) in y direction (0.001??? in Schotting et al 1999 for L=130 cm)
      read(14,*)alphay
c     Brine density (kg/m3) (1063.7 kg/m3 in Schotting et al 1999 for constant density
difference experiments)
      read(14,*)rhos
c     Background salt density (kg/m3)
      read(14,*)rhobg
c     Convergence criteria: Tolerances and maximum iteration numbers
c     tolf and niterf for head; tolt and nitert for concentration
      read(14,*)tolf
     read(14,*)tolt
      read(14,*)niterf
```

```
      read(14,*)nitert
c     flow rate (m3/s)
      read(14,*)flowrate
c     Area of the column (m2)
      read(14,*)colarea
c     Initial head in the lowest row (m)
      read(14,*)head0
c     Constant/Effective hydraulic conductivity  (m/s)
      read(14,*)hyc0
c     Porosity (~0.39 in Schotting et al 1999 for eff. particle d=0.47 mm)
      read(14,*)porosity
c     Effective Molecular diffusion coefficient (m2/s)
      read(14,*)diff0
c     Cell number of observation point (vertical)
      read(14,*)obs
c     FINISHED READING PROBLEM SPECIFIC CONSTANTS


c     CALCULATE OTHER CONSTANTS
c     Brine mass fraction (kg/kg) (Calculated from brine density)
      omegas=log(rhos/rho0)/gamma
c     Brine concentration (kg/m3) (Calculated from brine density)
      concs= rhos*omegas
c     Background salt mass fraction (kg/kg) (Calculated from background salt density)
      omegabg=log(rhobg/rho0)/gamma
c     Background salt concentration (kg/m3) (Calculated from background salt density)
      concbg= rhobg*omegabg
c     Specific discharge (m/s) (0.00054 m/s in Schotting et al 1999 for constant q
experiments- Table 5)
      q0=flowrate/colarea
c     Hydraulic gradient
      hydgrad=q0*dz0/hyc0
c     High concentration gradient coefficient (Schotting et al 1999)
```

```
      beta=0.0125/((q0)**1.76)
c     FINISHED CALCULATING OTHER CONSTANTS


c     ASSIGN CELL VALUES
c     Hydraulic conductivities
     do 57 j=1,ny0
     do 58 i=1,nz0
     if(iheterogeneity.eq.1)then
      hyc(i,j)=hyc0
      elseif(iheterogeneity.eq.2)then
      read(3,8)(hyc(i,j),i=1,nz0)
      hyc(i,j)=1e-05*hyc(i,j)
      endif
58    continue
57    continue

c     Heads (M/L3)
     do 60 j=1,ny0
      do 59 i=1,nz0
     h1(i,j)=head0-hydgrad*(i-1)
59    continue
60    continue

c     Densities (kg/m3)
     do 62 j=1,ny0
      do 61 i=1,nz0
      rho1(i,j)=rhobg
      rho3(i,j)=rho1(i,j)
61    continue
62    continue

c     Concentrations (M/L3)
```

```
      do 64 j=1,ny0
       do 63 i=1,nz0
       conc1(i,j)=concbg
       conc3(i,j)=conc1(i,j)
63     continue
64     continue

c      Lower/Upper boundary cells (h1, rho13, conc13)
      do 70 j=1,ny0
       h1(1,j)=head0
      rho1(1,j)=rhos
      conc1(1,j)=concs
      rho3(1,j)=rhos
      conc3(1,j)=concs

       h1(nz0,j)=head0-q0*float(nz0-1)*dz0/hyc(nz0,j)
      rho1(nz0,j)=rhobg
      conc1(nz0,j)=concbg
      rho3(nz0,j)=rhobg
      conc3(nz0,j)=concbg
70     continue
c      FINISHED ASSIGNING CELL VALUES


c          CALCULATE HEADS (STEADY STATE AND CONSTANT DENSITY)
      AND VELOCITIES
c      Initial heads
      do 110 nif=1,niterf
      do 120 j=2,ny0-1
      do 130 i=2,nz0-1
      h1(i,j)= +(hyc(i,j)+hyc(i,j+1))*h1(i,j+1)
       &       +(hyc(i,j)+hyc(i,j-1))*h1(i,j-1)
       &       +(hyc(i,j)+hyc(i+1,j))*h1(i+1,j)
```

```
     &       +(hyc(i,j)+hyc(i-1,j))*h1(i-1,j)

    h1(i,j)= h1(i,j)/(4.*hyc(i,j)
    &       +hyc(i,j+1)+hyc(i,j-1)+hyc(i+1,j)+hyc(i-1,j))
130   continue
120   continue

c     update left/right boundaries
      do 135 i=2,nz0-1
    h1(i,1)=h1(i,2)
    h1(i,ny0)=h1(i,ny0-1)
135   continue

c     calculate difference and update last iteration value
    diff1=0.
    do 140 j=1,ny0
    do 150 i=1,nz0
      if (nif.eq.1) then
      h2(i,j)=h1(i,j)
    goto 110
    else
    if(diff1.le.abs(h1(i,j)-h2(i,j)))diff1=abs(h1(i,j)-h2(i,j))
      h2(i,j)=h1(i,j)
    endif
150   continue
140   continue
    if(diff1.le.tolf) then
    write(12,*)n,nif,diff1,'flow'
    goto 151
    endif
110   continue

c     update last iteration value
```

```
151   do 155 j=1,ny0
      do 156 i=1,nz0
        h3(i,j)=h1(i,j)
156   continue
155   continue

c     calculate velocities
        do 160 j=2,ny0
      do 170 i=2,nz0
        qz1(i,j)=-(hyc(i,j)+hyc(i-1,j))/2*(h1(i,j)-h1(i-1,j))/dz(i)
        qy1(i,j)=-(hyc(i,j)+hyc(i,j-1))/2*(h1(i,j)-h1(i,j-1))/dy(j)
170   continue
160   continue
c     FINISHED CALCULATING HEADS AND VELOCITIES


c     WRITE INITIAL CELL VALUES INTO "initialh.out"
        write(4,*)'h1'
        do 1000 j=1,ny0
      write(4,4)(h1(i,j),i=1,nz0)
1000  continue
        write(4,*)'qz1'
        do 1001 j=1,ny0
      write(4,4)(qz1(i,j),i=1,nz0)
1001  continue
        write(4,*)'qy1'
        do 1002 j=1,ny0
      write(4,4)(qy1(i,j),i=1,nz0)
1002  continue
        write(4,*)'rho1'
        do 1003 j=1,ny0
      write(4,4)(rho1(i,j),i=1,nz0)
1003  continue
```

```
      write(4,*)'conc1'
      do 1004 j=1,ny0
     write(4,4)(conc1(i,j),i=1,nz0)
1004  continue
      write(4,*)'hyc'
      do 1005 j=1,ny0
     write(4,4)(hyc(i,j),i=1,nz0)
1005  continue
c     FINISHED WRITING INITIAL CELL VALUES


c     WRITE STARTING PARAMETERS INTO "normconc.out"
      if(idispersion.eq.2)then
     write(11,*)'Fickian dispersion model'
      elseif(idispersion.eq.1)then
        if(inonfickian.eq.1)then
      write(11,*)'non-Fickian dispersion model (sqrt)'
        elseif(inonfickian.eq.2)then
      write(11,*)'non-Fickian dispersion model (division)'
      endif
     endif
      if(iweighting.eq.2)then
     write(11,*)'Upstream weighting'
      elseif(iweighting.eq.1)then
     write(11,*)'Central weighting'
      elseif(iweighting.eq.3)then
     write(11,*)'total variation diminishing'
     endif
      if(istdflow.eq.2)then
     write(11,*)'Density driven flow'
      elseif(istdflow.eq.1)then
     write(11,*)'Staedy state flow'
     endif
```

```
      if(iheterogeneity.eq.2)then
     write(11,*)'Heterogeneous hydraulic conductivity field'
      elseif(iheterogeneity.eq.1)then
     write(11,*)'Homogeneous hydraulic conductivity field'
     endif
      if(itcondition.eq.2)then
     write(11,*)'Concentration cannot exceed brine concentration'
      elseif(itcondition.eq.1)then
     write(11,*)'No conditions were applied on concentration'
     endif
      write(11,*)'number of cells in z     = ',nz0
      write(11,*)'number of cells in y     = ',ny0
      write(11,*)'cell height              = ',dz0
      write(11,*)'cell width               = ',dy0
      write(11,*)'number of timestep       = ',nt0
      write(11,*)'timestep length          = ',dt0
      write(11,*)'Write every', intervalout, ' timesteps'
      write(11,*)'dispersivity in z        = ',alphaz
      write(11,*)'dispersivity in y        = ',alphay
      write(11,*)'flow rate                = ',flowrate
      write(11,*)'initial spec. disch.     = ',q0
      write(11,*)'Constant hyd. cond.      =', hyc0
      write(11,*)'beta (non-fickian)       = ',beta
      write(11,*)'brine density            = ',rhos
      write(11,*)'background density       = ',rhobg
      write(11,*)'Flow tolerance           = ',tolf
      write(11,*)'Transport tolerance      = ',tolt
      write(11,*)'max # flow iteration     = ',niterf
      write(11,*)'max # tran. iteration    = ',nitert
c     FINISHED WRITING STARTING PARAMETERS


c     TIME LOOP STARTS HERE
```

```
      do 200 n=1,nt0

c     SOLVE FLOW EQUATION  [n]
      do 210 nif=1,niterf
c     calculate heads      [n,nif]
      do 220 j=2,ny0-1
      do 230 i=2,nz0-1
      h3(i,j)= (rho3(i,j)+rho3(i,j+1))*(hyc(i,j)+hyc(i,j+1))*h3(i,j+1)
     &      +(rho3(i,j)+rho3(i,j-1))*(hyc(i,j)+hyc(i,j-1))*h3(i,j-1)
     &      +(rho3(i,j)+rho3(i+1,j))*(hyc(i,j)+hyc(i+1,j))*h3(i+1,j)
     &      +(rho3(i,j)+rho3(i-1,j))*(hyc(i,j)+hyc(i-1,j))*h3(i-1,j)

     &      +(rho1(i,j)+rho1(i,j+1))*(hyc(i,j)+hyc(i,j+1))*h1(i,j+1)
     &      +(rho1(i,j)+rho1(i,j-1))*(hyc(i,j)+hyc(i,j-1))*h1(i,j-1)
     &      +(rho1(i,j)+rho1(i+1,j))*(hyc(i,j)+hyc(i+1,j))*h1(i+1,j)
     &      +(rho1(i,j)+rho1(i-1,j))*(hyc(i,j)+hyc(i-1,j))*h1(i-1,j)

     &      -(rho1(i,j)+rho1(i,j+1))*(hyc(i,j)+hyc(i,j+1))*h1(i,j)
     &      -(rho1(i,j)+rho1(i,j-1))*(hyc(i,j)+hyc(i,j-1))*h1(i,j)
     &      -(rho1(i,j)+rho1(i+1,j))*(hyc(i,j)+hyc(i+1,j))*h1(i,j)
     &      -(rho1(i,j)+rho1(i-1,j))*(hyc(i,j)+hyc(i-1,j))*h1(i,j)

     &      -8*porosity*dz(i)*dz(i)*(rho3(i,j)-rho1(i,j))/dt(n)

      h3(i,j)= h3(i,j)/((rho3(i,j)+rho3(i,j+1))*(hyc(i,j)+hyc(i,j+1))
     &      +(rho3(i,j)+rho3(i,j-1))*(hyc(i,j)+hyc(i,j-1))
     &      +(rho3(i,j)+rho3(i+1,j))*(hyc(i,j)+hyc(i+1,j))
     &      +(rho3(i,j)+rho3(i-1,j))*(hyc(i,j)+hyc(i-1,j)))
230   continue
220   continue

c     update left/right boundaries   [n,nif]
      do 235 i=2,nz0-1
```

```
   h3(i,1)=h3(i,2)
   h3(i,ny0)=h3(i,ny0-1)
235   continue


c     calculate difference and update last iteration value  [n,nif]
   diff1=0.
   do 240 j=1,ny0
   do 250 i=1,nz0
    if (nif.eq.1) then
    h2(i,j)=h3(i,j)
   goto 210
   else
   if(diff1.le.abs(h3(i,j)-h2(i,j)))diff1=abs(h3(i,j)-h2(i,j))
    h2(i,j)=h3(i,j)
   endif
250   continue
240   continue
   if(diff1.le.tolf) then
   write(12,*)n,nif,diff1,'flow'
   goto 211
   endif
210   continue
c  write(*,*)'flow iterations finished', n

c     Calculate Flow Rates   [n]
211         do 260 j=2,ny0
   do 270 i=2,nz0
   qz3(i,j)=-(hyc(i,j)+hyc(i-1,j))/2*(h3(i,j)-h3(i-1,j))/dy(j)
   qy3(i,j)=-(hyc(i,j)+hyc(i,j-1))/2*(h3(i,j)-h3(i,j-1))/dz(i)
    if(istdflow.eq.1)then
   qz3(i,j)=qz1(i,j)
   qy3(i,j)=qy1(i,j)
```

```
   endif
270   continue
260   continue

c  write(*,*)'flow rates calculated', n

c     calculate dispersion coefficients  [n]
     do 280 j=2,ny0
    do 290 i=2,nz0
     dispcoz1(i,j)=diff0+1./porosity*(alphaz*qz1(i,j)+alphay*qy1(i,j))
     dispcoy1(i,j)=diff0+1./porosity*(alphaz*qy1(i,j)+alphay*qz1(i,j))
     dispcoz3(i,j)=diff0+1./porosity*(alphaz*qz3(i,j)+alphay*qy3(i,j))
     dispcoy3(i,j)=diff0+1./porosity*(alphaz*qy3(i,j)+alphay*qz3(i,j))
290   continue
280   continue
c     FINISHED SOLVING FLOW EQUATION   [n]

c     SOLVE TRANSPORT       EQUATION  [n]
    do 310 nit=1,nitert

c     calculate the dispersive flux at the cell interfaces   [n,nit]
    do 320 j=2,ny0
    do 330 i=2,nz0




c     new write statement 11.01.10 delete after finding why nf doesn't run
     kare=1.-4*beta*porosity*dispcoz3(i,j)*(conc3(i,j)-conc3(i-1,j))
    &          /dz(i)
    if(i.eq.2)then
    if(j.eq.2)then
c      write(13,3)n, nit, i, j, dispcoz3(i,j), conc3(i,j), conc3(i-1,j)
c      write(13,*)n, nit, conc3(i,j)
```

```
      endif
      endif
c     new write statement 11.01.10 delete after finding why nf doesn't run


      if(idispersion.eq.1) then
      if(inonfickian.eq.1) then
      dispfluz1(i,j)=(-1.+(1.-4*beta*porosity*dispcoz1(i,j)*(conc1(i,j)
     &-conc1(i-1,j))/dz(i))**0.5)/2./beta
      dispfluz3(i,j)=(-1.+(1.-4*beta*porosity*dispcoz3(i,j)*(conc3(i,j)
     &-conc3(i-1,j))/dz(i))**0.5)/2./beta
      elseif(inonfickian.eq.2) then
      dispfluz1(i,j)=-porosity*dispcoz1(i,j)*(conc1(i,j)
     &  -conc1(i-1,j))/dz(i)
       dispfluz1(i,j)=dispfluz1(i,j)/(1+beta*dispfluz1(i,j))
      dispfluz3(i,j)=-porosity*dispcoz3(i,j)*(conc3(i,j)
     &  -conc3(i-1,j))/dz(i)
       dispfluz3(i,j)=dispfluz3(i,j)/(1+beta*dispfluz1(i,j))
      endif
       endif

      if(idispersion.eq.2) then
      dispfluz1(i,j)=-porosity*dispcoz1(i,j)*(conc1(i,j)
     &  -conc1(i-1,j))/dz(i)
      dispfluz3(i,j)=-porosity*dispcoz3(i,j)*(conc3(i,j)
     &  -conc3(i-1,j))/dz(i)
      endif

      dispfluy1(i,j)=-porosity*dispcoy1(i,j)*(conc1(i,j)
     &-conc1(i,j-1))/dy(j)
      dispfluy3(i,j)=-porosity*dispcoy3(i,j)*(conc3(i,j)
     &-conc3(i,j-1))/dy(j)
      dispfluy3(i,j)=0.
```

```
      dispfluy1(i,j)=0.
  330 continue
  320 continue
c  write(*,*)'dispersive fluxes calculated', n


c     calculate new concentration values at each cell (in terms conc3 and conc1, q3 and
q1, dispfluy 3 and dispfluy1 and dispfluz 3 and dispfluz1)  [n,nit]
      do 340 j=2,ny0-1
      do 350 i=2,nz0-1
      if (iweighting.eq.1) then
c     central in space weighting
      advz3=dt(n)/(4.*porosity*dz(i))*
      &(qz3(i+1,j)*(conc3(i+1,j)+conc3(i,j))-
      & qz3(i,j)*(conc3(i,j)+conc3(i-1,j)))

      advz1=dt(n)/(4.*porosity*dz(i))*
      &(qz1(i+1,j)*(conc1(i+1,j)+conc1(i,j))-
      & qz1(i,j)*(conc1(i,j)+conc1(i-1,j)))

      advy3=dt(n)/(4.*porosity*dz(i))*
      &(qy3(i,j+1)*(conc3(i,j+1)+conc3(i,j))-
      & qy3(i,j)*(conc3(i,j)+conc3(i,j-1)))

      advy1=dt(n)/(4.*porosity*dz(i))*
      &(qy1(i,j+1)*(conc1(i,j+1)+conc1(i,j))-
      & qy1(i,j)*(conc1(i,j)+conc1(i,j-1)))
       elseif (iweighting.eq.2) then
c     upstream weighting
      advz3=dt(n)/(4.*porosity*dz(i))*
      &(qz3(i+1,j)*(conc3(i,j)+conc3(i,j))-
      & qz3(i,j)*(conc3(i-1,j)+conc3(i-1,j)))
```

```
      advz1=dt(n)/(4.*porosity*dz(i))*
     &(qz1(i+1,j)*(conc1(i,j)+conc1(i,j))-
     & qz1(i,j)*(conc1(i-1,j)+conc1(i-1,j)))

      advy3=dt(n)/(4.*porosity*dz(i))*
     &(qy3(i,j+1)*(conc3(i,j)+conc3(i,j))-
     & qy3(i,j)*(conc3(i,j-1)+conc3(i,j-1)))

      advy1=dt(n)/(4.*porosity*dz(i))*
     &(qy1(i,j+1)*(conc1(i,j)+conc1(i,j))-
     & qy1(i,j)*(conc1(i,j-1)+conc1(i,j-1)))

      elseif (iweighting.eq.3) then
c     Total variation diminishing
      if(i.eq.2)then
      advz3=dt(n)/(4.*porosity*dz(i))*
     &(qz3(i+1,j)*(conc3(i+1,j)+conc3(i,j))-
     & qz3(i,j)*(conc3(i,j)+conc3(i-1,j)))

      advz1=dt(n)/(4.*porosity*dz(i))*
     &(qz1(i+1,j)*(conc1(i+1,j)+conc1(i,j))-
     & qz1(i,j)*(conc1(i,j)+conc1(i-1,j)))
      else
       c_r=qz3(i,j)*dt(n)/dz(i)/porosity
      c_i_up=(conc3(i,j)+conc3(i-1,j))/2.-
     &       c_r*(conc3(i,j)-conc3(i-1,j))/2.-
     &    (1.-c_r*c_r)*(conc3(i,j)-2.*conc3(i-1,j)+conc3(i-2,j))/6.
      c_i_down=(conc3(i+1,j)+conc3(i,j))/2.-
     &       c_r*(conc3(i+1,j)-conc3(i,j))/2.-
     &    (1.-c_r*c_r)*(conc3(i+1,j)-2.*conc3(i,j)+conc3(i-1,j))/6.
      advz3=dt(n)/(2.*porosity*dz(i))*
     &(qz3(i+1,j)*(c_i_down)-qz3(i,j)*(c_i_up))
```

```
c_r=qz1(i,j)*dt(n)/dz(i)/porosity
c_i_up=(conc1(i,j)+conc1(i-1,j))/2.-
 &       c_r*(conc1(i,j)-conc1(i-1,j))/2.-
 &    (1.-c_r*c_r)*(conc1(i,j)-2.*conc1(i-1,j)+conc1(i-2,j))/6.
c_i_down=(conc1(i+1,j)+conc1(i,j))/2.-
 &       c_r*(conc1(i+1,j)-conc1(i,j))/2.-
 &    (1.-c_r*c_r)*(conc1(i+1,j)-2.*conc1(i,j)+conc1(i-1,j))/6.
advz1=dt(n)/(2.*porosity*dz(i))*
&(qz1(i+1,j)*(c_i_down)-qz1(i,j)*(c_i_up))
endif

advy3=dt(n)/(4.*porosity*dz(i))*
&(qy3(i,j+1)*(conc3(i,j+1)+conc3(i,j))-
& qy3(i,j)*(conc3(i,j)+conc3(i,j-1)))

advy1=dt(n)/(4.*porosity*dz(i))*
&(qy1(i,j+1)*(conc1(i,j+1)+conc1(i,j))-
& qy1(i,j)*(conc1(i,j)+conc1(i,j-1)))
endif

 dispz1=dt(n)/(2.*porosity*dz(i))*
&(dispfluz1(i+1,j)-dispfluz1(i,j))

 dispz3=dt(n)/(2.*porosity*dz(i))*
 &(dispfluz3(i+1,j)-dispfluz3(i,j))

 dispy1=dt(n)/(2.*porosity*dz(i))*
 &(dispfluy1(i,j+1)-dispfluy1(i,j))

 dispy3=dt(n)/(2.*porosity*dz(i))*
 &(dispfluy3(i,j+1)-dispfluy3(i,j))

 conc3(i,j)=conc1(i,j)-advz3-advz1-advy3-advy1
```

```
     &                -dispz1-dispy1-dispz3-dispy3

    if(itcondition.eq.2)then
     if(conc3(i,j).gt.conc3(i-1,j))conc3(i,j)=conc3(i-1,j)
    endif

350   continue
340   continue
c   write(*,*)'concentrations calculated', n



c     update left/right boundaries [n,nit]
      do 355 i=2,nz0-1
      conc3(i,1)=conc3(i,2)
      conc3(i,ny0)=conc3(i,ny0-1)
355   continue

c     update top boundaries  [n,nit]
      do 356 j=1,ny0
      conc3(nz0,j)=conc3(nz0-1,j)
356   continue



c     calculate difference and update last iteration value  [n,nit]
      diff2=0.
      do 360 j=1,ny0
      do 370 i=1,nz0
      if (nit.eq.1) then
      conc2(i,j)=conc3(i,j)
      goto 310
      else
      if(diff2.le.abs(conc3(i,j)-conc2(i,j)))
     & diff2=abs(conc3(i,j)-conc2(i,j))
```

```
c     NEW UPDATE STATEMENT
      conc2(i,j)=conc3(i,j)
      endif
370   continue
360   continue
      if(diff2.le.tolt) then
      write(12,*)n,nit,diff2, 'transport'
      goto 371
      endif
310   continue
371   write(*,*)'transport iterations finished', n, nit
      write(13,*)n, nit


c  update all parameters for next time step  [n]
      do 400 i=1,nz0
      do 410 j=1,ny0
      h1(i,j)=h3(i,j)
      conc1(i,j)=conc3(i,j)
c     calculate omega and rho, but first check for negative conc values [n]
      if(conc3(i,j).lt.1.0e-10)then
      omega3(i,j)=0
      rho3(i,j)=rho0
      else
      omega3(i,j)=1./2./gamma*(-1.+dsqrt(1.+4.*gamma*conc3(i,j)/rho0))
      rho3(i,j)=conc3(i,j)/omega3(i,j)
      endif
      omega1(i,j)=omega3(i,j)
      rho1(i,j)=rho3(i,j)
c     update flow rate and dispersion coef.  [n]
      qz1(i,j)=qz3(i,j)
      qy1(i,j)=qy3(i,j)
      dispcoz1(i,j)=diff0+1./porosity*(alphaz*qz1(i,j)+alphay*qy1(i,j))
```

```
      dispcoy1(i,j)=diff0+1./porosity*(alphaz*qy1(i,j)+alphay*qz1(i,j))

410   continue
400   continue


c     print output (qz1,qy1,rho1,conc1)  [n]
500   if(n/intervalout*intervalout.eq.n)then
      write(5,*)n
      write(6,*)n
      write(9,*)n
      write(10,*)n
      write(7,*)n
      write(8,*)n
      write(11,*)n
      do 611 j=2,ny0-1
      write(5,4)(qz1(i,j),i=1,nz0)
      write(6,4)(qy1(i,j),i=1,nz0)
      write(9,4)(rho1(i,j),i=1,nz0)
      write(10,4)(conc1(i,j),i=1,nz0)
      write(7,4)(dispcoz1(i,j),i=1,nz0)
      write(8,4)(dispcoy1(i,j),i=1,nz0)
      write(11,4)(rho1(i,j)*omega1(i,j)/rhos/omegas,i=1,nz0)
611   continue
      endif

      write(10,*)conc1(1,2),conc1(obs,2)

2       format(i5,201e12.5)
3       format(4i5,3e12.5)
4       format(201e12.5)
8       format(10f10.6)
```

```
c     go to next time step
200   continue
c     TIME LOOP ENDS HERE


      stop
      end
```